Cities from Space:

Influence of Rural to Urban Gradients on Remote Sensing of Urban Heat Island

Submitted by

Paras Sidiqui

A thesis submitted in fulfilment of the requirements for the degree of

Doctor of Philosophy

School of Life Sciences, Faculty of Science

University of Technology Sydney

Australia

July 2019

Certificate of original authorship

I certify that the work in this thesis has not previously been submitted for a degree nor has it been submitted as part of requirements for a degree except as fully acknowledged within the text.

I also certify that the thesis has been written by me. Any help that I have received in my research work and the preparation of the thesis itself has been acknowledged. In addition, I certify that all information sources and literature used are indicated in the thesis. This research is supported by the Australian Government Research Training Program.

Production Note:
Signature removed prior to publication.

Signature of Student

16-07-2019

Acknowledgements

I am grateful to God for everything. I would also like to express my very great appreciation to my research supervisor, Distinguished Prof. Alfredo Huete, for his patient guidance, enthusiastic encouragement, valuable suggestions and useful critiques during the planning and development of this PhD work. His willingness to give his time so generously has been very much appreciated.

I want to extend thanks to Dr Rakhesh Devedas and Dr Xualang Ma for their valued comments and suggestions during the early years of my PhD. I am also grateful to Dr Ha & Dr Q. Xie for their constructive comments and suggestions, particularly at student meeting sessions. I am very much appreciative to Dr Zar chi, for her helpful feedback, I appreciate it very much.

I am very much grateful to staffs in IT support, administrative staff members of the School of Life Sciences, Graduate Research School and Faculty of Science at UTS. I appreciate the help for all these years.

I am very much thankful to my friends for their motivation and support, to name, Mehwish Shafi Khan, Adnan Aziz, Ncog, Steve (Sicong Gao), Esther (Qinggaozi Zhu), Buddhi, Zunyi, Chris, Wenjie, Yuxia, Song, and Leandro. I am very much grateful to my friend Dr Salma Anwer, being a friend she always kept me motivated. I would also like to thank Prof. Khalid Anis; he was a father figure in my life, always motivated me and believed in me. I am also grateful to Dr Said Rehman, a very kind-hearted person; he was my boss at my old workplace, I can’t thank enough for his support and guidance.

Finally, I would like to thank my family for their support and understanding throughout my candidature, particularly my parents and my husband. My father always wanted me to do a PhD; it was his dream, he worked very hard for it, he gave me the best education. But now when I am close to fulfilling his dream, he is a patient of dementia/Alzheimer, and he does not remember anything, even doesn’t recognise me, but in the real sense, I am fulfilling his dream. My mother, she supported me throughout my life, and she always stood by my side, I can't thank enough for her support and love. My husband always encouraged me. In fact, he was real support particularly during my PhD as my parents were not here with me all this time, but he was here. He motivated me and believed in me; I am very much grateful to God for blessing me with a life partner like him, he was more of strength.

This PhD thesis research was supported by UTS Doctoral Scholarship, UTS President’s Scholarship and partially by ARC Discovery Scholarship. I am very much grateful to the University of Technology Sydney for providing me with the opportunity to study at UTS and conduct the subject research work.

Table of Contents

List of Figures

List of Tables

Abstract

The Urban Heat Island (UHI) effect occurs when urban areas have higher surface/ air temperature differences relative to surrounding rural reference areas. Most of the studies carried out in past are limited to a certain time in a year or a day, and lack a long term analysis. Moreover, the research potential of satellites and its modern tools remain largely untapped.

The overall goal of this thesis is to investigate and characterise the UHI in selected Australian cities with satellite data sets, particularly the Moderate Resolution Imaging Spectro-radiometer (MODIS). To achieve these objectives, (1) I, firstly investigated the inter-annual and seasonal characteristics of diurnal land surface temperature (LST) and UHI across urban and rural areas from 2003- to 2017; (2) then I assessed the long-term trends (significant/non-significant) in UHI and LST and their interactions/dependencies with its drivers/indicators (greenness, albedo); (3) furthermore I examined the phenology patterns for greenness and urban greenness deficit in relationship with the diurnal, seasonal, inter-annual characteristics in UHI; (4) lastly, I examined an extreme heat wave event in Sydney and its influence on UHI utilising the geostationary Himawari-8 satellite.

The temporal analysis on seasonal and inter-annual variations of UHI revealed maximum intensities in the daytime period for both the cities of Melbourne and Sydney. Melbourne and Sydney experienced the highest daytime UHI in the austral 'spring' and austral 'summer' season respectively. A nighttime UHI was present in both cities in the 'summer' season. Inter-annual trends in UHI revealed a significant increasing trend in daytime UHI (p-value < 0.01) for both selected cities despite no significant trends in daytime urban LST in both cities. The increasing UHI trends were primarily attributed to increasing greenness and declining temperatures in the rural zones surrounding both

cities. We found the choice of a rural reference class, whether forest, pasture, or mixed, significantly altered computed UHI values. Greenness and urban green deficit (UGD) showed an inverse relationship with daytime UHI, whereas albedo and delta albedo (urban minus rural albedo) did not show any correlation with UHI. During the extreme heatwave event, the UHI was seen to be more widespread and dominant in the city for a longer time than for an average day, while the intensity remained more or less similar.

This thesis highlights the value of remote sensing techniques (e.g. MODIS and Himawari-08 satellites) as essential tools for improved assessments and management of urban landscapes in selected Australian cities.

Chapter 1: Introduction

1.1 General research background

Humans always change the environments that they live in. The growing expanse of cities has now reached a stage where more than 50 per cent of the world population lives in cities, and this proportion continues to grow (DESA, 2012). While living in these urban centres offers numerous lifestyle opportunities, there are inevitable changes in the natural environment as a result of urbanisation. One such environmental change is in the urban climate and in particular, the formation of the Urban Heat Island. The Urban Heat Island (UHI) is a phenomenon where metropolitan areas show higher temperatures than the surrounding rural landscapes (Fig.1.1). The replacement of naturally vegetated surfaces with hard, impervious infrastructure alters the processes of radiative and energy exchange at the land surface, causing the formation of distinct urban climates. These impervious urban built-up surfaces have high heat capacities and low thermal inertia, and therefore these can retain high amounts of thermal energy compared to rural areas.

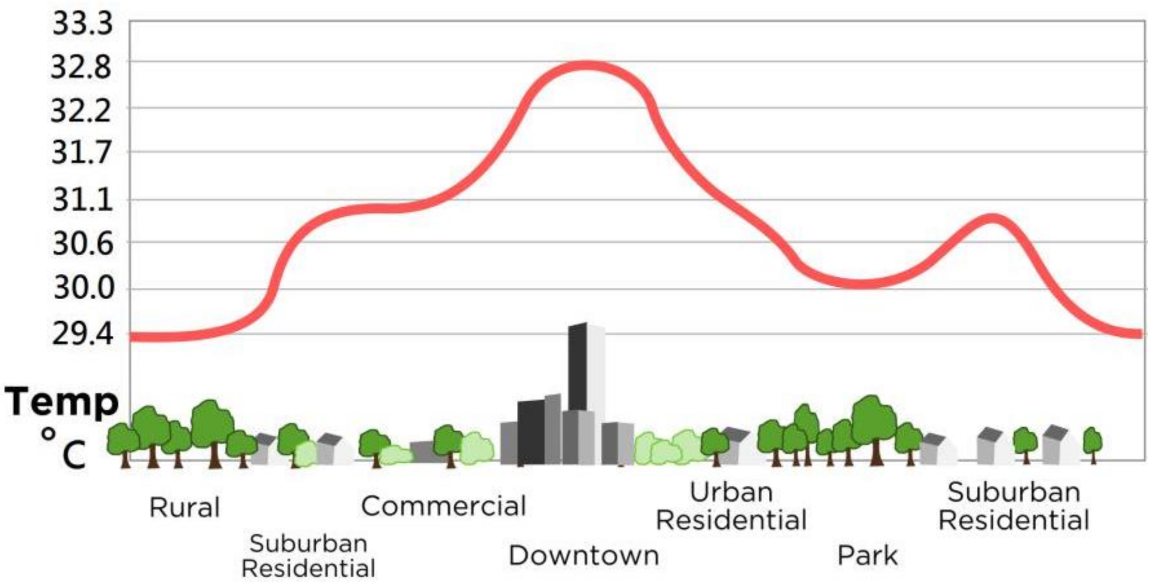

Figure 1.1. A generalised description of the UHI (modified from http://www.pmsilicone.com/urban -heat-island-effect/ cited on 15//02/2016)

The detrimental effects of the UHI significantly reduce both the sustainability and liveability of cities through increases in air pollution, greenhouse gas emissions and minimise human comfort, making it harder for people to cool down. Since urban residents are not only contributors to – but also the victims of – UHIs. Hence, urban inhabitants are exposed to a feedback loop with adverse impacts on their health and productivity. In addition to it, as more energy and water are consumed, mainly during summer time in those areas where the air conditioning/refrigerator needs are high, even more, waste heat and air pollution are generated.

In the context of climate change, elevated urban temperatures can stretch the adaptive capacity of urban residents to respond to extreme heat. Increases in temperature from the UHI, in combination with heat waves, can lead to many heat-related illnesses and mortality. For example, during the heat wave of summer 2003 in Europe, about 35,000 to 50,000 people died due to heat-related illnesses (Mirzaei and Haghighat, 2010). According to one more study, during the heat wave of 1993 in Philadelphia, USA, heat-related mortality was concentrated in areas with higher UHI intensity levels only (Johnson and Wilson, 2009).

As a result of global warming, mean temperatures across Australia are projected to increase, but extreme temperatures (heat waves) are also projected to change, with heat waves becoming more frequent, more intense, and longer lasting (Cleugh et al., 2011). In Australia, studies have shown that, the UHI is evident in Melbourne (Victoria), as well as across Victoria State's rural cities and towns. Some studies conducted automobile transects across Melbourne and towns in rural Victoria (Torok et al., 2001). In Melbourne, a transect across the city at 9 pm on the 25th August 1992 revealed a maximum observed UHI intensity of 7.1 °C between the CBD and rural areas, with smaller peaks in the industrial areas and the medium density terrace housing in the inner northern suburbs

(Torok et al., 2001). In Victoria, a heat wave in January 2009 was linked to 374 excess deaths (DHS, 2009).

The conventional approach to UHI monitoring and mapping uses data collection from permanent meteorological stations. The data collected at meteorological stations in cities may not represent urban weather conditions since most of the stations are established for forecasting synoptic situations at places where the elements of the weather are not disturbed by urban structures or human activities and thus the data may be misleading (Lee et al., 1993). Satellite data, on the other hand, provides the synoptic view with great details. Remote sensing and GIS techniques offer ample opportunities to monitor, map and inform the situation for better management and planning. Remote sensing and GIS approaches may provide new dimensions to study and understand UHI in more efficient ways.

Examining the UHI is vital for understanding its impacts on climatic patterns. Furthermore, understanding the thermal response of individual land covers within a city is equally valuable, as radiative transfer varies significantly over space due to the diversity of urban land covers and their respective physical properties. Moreover the interplay between land use - land cover and UHIs needs much more research. In the following subsections, I have provided a brief review of literature with main emphasis on the land use modifications in urban environments, their resulting impacts on the urban heat island, and remote sensing & GIS applications.

1.1.1. Urbanisation and Landscape Change

According to the reports published by United Nations Department of Economic and Social Affairs/Population Division, in 1950, approximately 30 per cent of the global population lived in urban areas, and by 2000 this figure had increased to 47 per cent, and it is projected to rise to 68 per cent by 2050 (UN DESA, 2018). This process of urbanisation is very advanced in much of the developed world, where at least 75 per cent of the population now live in urban areas, a figure projected to rise to 83 per cent by 2030 (UN DESA, 2018).

Urbanisation is one of the most profound examples of human modification of the Earth's surface (Weng et al., 2011). This process can be described as either a change in the absolute area of urban space or the pace at which non-urban land is converted to urban uses (Rainis et al., 2003; Ruslan et al., 2003). Urbanisation causes land surface and atmospheric changes that may affect local climate, hydrology, and biogeochemical cycles by altering temperature, wind, humidity, and rainfall (Argüeso et al., 2014; Stefanov and Netzband, 2005; Voogt and Oke, 2003). Local environmental changes, such as heat islands in the hearts of cities, are brought about by changes in exchange of heat and moisture between the land surface and lower atmosphere (Weng et al., 2011; Weng et al., 2014). Urbanisation affects its local environment through several distinct but coupled mechanisms. The most significant impact is expressed by a reduction in the fraction of vegetation and the subsequent inhibition of photosynthetic activity and plant's water transpiration and interception losses (Zhou and Shepherd 2010). Further, increase in impervious surface area in the urban landscape alters the partitioning of surface runoff and water infiltration into the ground and changes the soil moisture content and water table location which in turn may contribute to the local climate modifications (Jiang and Zhang, 2007; Bounoua and Zhang, 2015).

1.1.1.1 Impervious Surfaces

Impervious surfaces are defined as those surfaces which water cannot infiltrate; these are primarily associated with transportation (streets, highways, parking lots and footpaths) and buildings in urban areas. Expansion of impervious surfaces increases water runoff and is a primary determinant of stormwater runoff volumes, water quality of lakes and streams, and stream habitat quality in urbanised areas (Yuan and Bauer, 2007). Surface materials can be classified as impervious and pervious depending on their response to energy and water flow (Rashed and Jürgens, 2010). In an urban region, a central business district (CBD), a residential area or a city park, each will have different moisture regimes, runoff rates, moisture storage capacity, and evapotranspiration depending on their characteristics. The areal extent and spatial occurrence of impervious surfaces in urban areas significantly influence the urban environment by altering heat fluxes within the urban canopy and boundary layers. Therefore, mapping (detecting, monitoring, and analysing) and estimating impervious surface are valuable when studying urban environments and their climates (Coutts and Beringer, 2007; Weng et al., 2011; Weng et al., 2014). Measuring or mapping imperviousness in an urban environment may be possible using the V-I-S model. The vegetation-impervious surface-soil (V-I-S) model was proposed by Ridd (1995) for characterising urban environments. This model assumes that urban land cover is a linear combination of three biophysical components: vegetation, impervious surface, and soil.

1.1.1.2 Reduced Vegetation in Urban Areas

Urban areas are developed at the cost of changes in the local landscape. Buildings, roads and other infrastructure replace open land and vegetation. Vegetation and open land lowers the surface temperature by reducing air temperature through evapotranspiration (Oke et al., 1979, Taha et al., 1997). Vegetation provides permeable and moist surfaces that reduce the runoff. Highly developed urban areas are characterised by 75-100 per cent impervious surfaces (Fig.1.2) and have less surface moisture available for evapotranspiration compared with that of natural ground cover, which has less than 10 per cent impervious cover (Gao and Niu, 2015). This difference contributes to higher surface and air temperatures in urban areas.

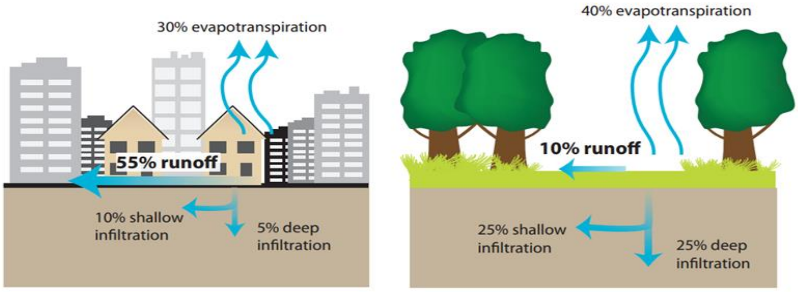

Figure 1.2. Built up areas have less evapotranspiration and more runoff (left); while vegetated areas have more evapotranspiration and less runoff (modified from Gao and Niu, 2015).

1.1.1.3 Albedo

Albedo is the reflectivity of Earth's surfaces, as measured by the amount of the sun's energy that a surface is capable of reflecting (as opposed to absorbing). The albedo or reflection coefficient is the diffuse reflectivity or reflecting power of a surface (Ramírez and Muñoz 2012). It is generally defined as the ratio of reflected radiation to incident radiation on a surface. A surface that absorbs all of the incoming radiations has an albedo of 0 (black surface), whereas a perfect reflector has an albedo of 1 (white surface) (Kotak and Gul, 2015; Ramírez and Muñoz 2012). Lighter colour surfaces have a higher albedo and reflect a more significant percentage of the sun's incoming energy than darker surfaces. Urban areas have low albedo surface materials, such as roofing and paving (asphalt roads, brick buildings, etc.), that act to absorb more radiation than those in rural settings (Oke et al., 1982). Dense distributions of buildings can also reduce albedo due to multiple internal reflections resulting from the urban canopy geometry (Jin and Dickinson, 2005).

1.1.2 Urban Thermal Climate Change

Alteration of the landscape through urbanisation causes the transformation of the radiative, thermal, moisture, and aerodynamic characteristics of the earth's surface (Weng et al., 2003). Hence, this impacts the exchange of heat and moisture between land surface and lower atmosphere, creates the UHI phenomenon, and influences local, mesoscale, and even larger scale climate (Imhoff et al., 2010).

1.1.2.1 Characteristics of Urban Heat Island (UHI) Effect

The best-documented example of anthropogenic climate modification is the UHI effect. UHI is defined as having higher temperatures (air /surface) in the built environment of cities than in the surrounding rural areas (Bonafoni and Anniballe, 2015; Gray and Finster 1999; Roth and Oke, 1989). Fig.1.3 further clarifies the same in the form of a flow diagram which depicts urbanisation causing decreased vegetation, decreased albedo, and increased impervious infrastructure. Hence, this, in turn, leads to reduced evaporative cooling, increased heat absorption and radiant and waste heat production resulting in a UHI. UHI is highly dependent on regional climate, time of day, seasonality, and urban land cover and surrounding land cover type. UHI impacts not only local and regional climate, but also water resources, air quality, human health, biodiversity and ecosystem functioning (Platt and Rowntree, 1994).

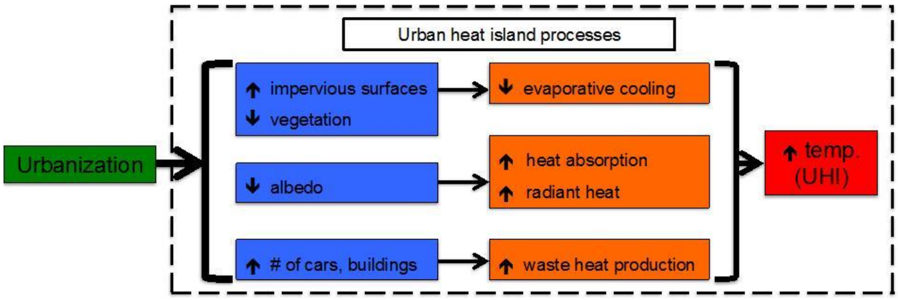

Figure 1.3. A flow chart showing urbanisation changing local climate and causing an UHI birth (https://bloomington.in.gov/media/media/image/jpeg/12924.jpg cited on 02/09/2015).

1.1.2.2 Types of UHI Effect

1.1.2.2.1 Canopy and boundary layer heat islands

By definition, the urban canopy layer extends upwards from the ground surface to approximately mean building height, with the urban boundary layer, is located above the canopy layer. The Canopy layer heat island (CLHI) and the boundary layer heat island (BLHI) are atmospheric heat islands since they denote warming of the atmosphere. Atmospheric urban heat islands are larger during day time and are normally measured by in situ sensors of air temperature (Roth and Oke, 1989).

1.1.2.2.2 Surface urban heat island

The Surface urban heat island (SUHI) is defined as the relative warmth of urban surfaces compared with surrounding rural areas. It is known that the surface UHIs are more substantial during the daytime (Oke et al., 1982). Daytime surface temperatures of dry ground are usually warmer than of the adjacent temperature of the air, and that is why SUHI are more evident on satellite images (Yuan and Bauer, 2007).

1.1.2.3 Daily and Seasonal Considerations

1.1.2.3.1 Nighttime vs daytime

The literature on UHI studies showed that the effect was found to be dominant at nighttime in metropolitan areas. For example, a study carried out by Wilby (2003) showed that UHI in London was most active near the centre of the city during nighttime, condition to calm weather. Few more studies reported intense UHI particularly at nighttime (Fung and Lam, 2009; Wilby et al., 2003). Similarly, the surface temperature measurements also indicated nighttime UHI to be dominant near metropolitan areas (Azevedo and Chapman, 2016; Bonafoni and Anniballe, 2015; Bounoua and Zhang, 2015; Sharifi and Lehmann, 2014; Streutker et al., 2003; Voogt and Oke 2003; Zhao and Lee, 2014; Zhou and Zhao, 2015). These studies demonstrated that urban zones relative to rural zones were at higher air/surface temperature particularly during the night. The nighttime presence of SUHI/CLHI is justified by the fact that built surfaces such as buildings, roads, car parks, etc., in urban areas have high thermal inertia, that causes the buildings, streets and other built-up surfaces to release the solar heating back to the atmosphere very slowly relative to non-built surfaces. Hence, this causes urban areas to remain at a relatively higher temperature even after sunset as compared to rural areas.

On the other hand, few other studies found that the effect to be present in the daytime as well. For instance, Kolokotroni and Giridharan (2008) carried out their study for London and found that the UHI was present at daytime with an intensity of 1.1°C, weaker than the nighttime UHI in London. Similarly, few more studies on air temperature reported the presence of daytime UHI along with nighttime UHI near city centres (Azevedo and Chapman, 2016; Bonafoni and Anniballe, 2015; Kłysik and Fortuniak, 1999). Similarly, the analysis based on surface temperature also reported similar results with daytime UHIs present in metropolitan areas along with nighttime UHIs (Ramamurthy and Li, 2017, Wang and Du, 2018). However, the studies which utilised surface temperature data, observed UHI intensities to be stronger during daytime in comparison to nighttime UHI intensity (Azevedo and Chapman, 2016; Bonafoni and Anniballe, 2015; Bounoua and Zhang, 2015; Kolokotroni and Giridharan 2008; Sidiqui and Huete, 2016; Zhao et al. 2014; Zhou et al. 2015). Hence, it can be argued from the above literature review that the UHI can be present at different times of the day, before and after sunset or midnight or even during the daytime, and this may be mainly defined by the thermal balance in the specific urban and rural zones (Skoulika et al., 2014). These studies also point towards specific diurnal characteristics of UHI which still need to be explored to understand the UHI characteristics more efficiently.

1.1.2.3.2 Seasonality of UHI (winter vs summer)

Apart from the daytime and nighttime variations in UHI intensity, there are distinct seasonal patterns as well in the UHI spatial and temporal patterns; studies found that UHI was intense during summer seasons and few other studies observed it to be dominant in autumn or winter. Zhao (2010) found that UHI was strongest in summer in Nanjing, China. Similarly, Zhou and Shepherd (2010) observed similar seasonality for Atlanta, USA. On the other hand, Liu and Ji (2007) found that the UHI intensity for Beijing, China was strongest in winter. They further showed that UHI reached its maximum during the dry season of winter and spring and its minimum during the humid summer period (Liu and Ji, 2007). Another study revealed that, in Ulan Bator, Mongolia, the daily maximum UHI intensity during the winter period was 6.4 Kelvin, while the weakest one occurred during the summer season, 2.5K (Ganbat and Han, 2013). Therefore, not only the patterns but also the processes themselves change over time.

1.1.2.4 UHI and its Driving Factors

Seasonal UHI intensity may vary with any change in the seasonal variation of relative humidity, clouds, soil moisture change; vapour pressure and day length (Runnalls and Oke, 2000; Lehmann and Sharifi, 2014). Studies carried out for Seoul, Korea, showed that the land use land cover (LULC) in the city had a significant influence on the seasonality of the UHI (Kim and Baik, 2005). In another study, it was seen that the LULC in rural zones can also have particular impacts on UHI behaviour, for example, a study on Phoenix, the city in desert, showed that the city developed a heat sink, whereas for Salt Lake City there was heat island (Bounoua and Zhang, 2015). A heat sink can be defined as urban temperatures become cooler than surrounding rural areas. It is also certain from studies that LULC responds to land surface temperature in different ways during different times of day and season; depending upon local climate (arid, semi-arid to humid), urban morphology and structures, elevation, slope, population density and proximity to ocean (Grimm and Faeth, 2008; Zhou and Chen, 2011; Zhou and Chen, 2013). Furthermore, weather can also affect the intensity of UHI, as precipitation increases the thermal admittance in rural areas and decreases the corresponding cooling rates compared with the cooling rates in urban areas. Hence, rain, cloudiness or wind speed may reduce the intensity of UHI (Zhou and Shepherd, 2010). Studies also showed that urban greenness can play a vital role in diminishing the UHI effect. In addition to it, the vegetation cover and agriculture activities in urban to rural transition zones can also play an essential role in driving the seasonality of UHI in cities.

1.1.2.5 Mitigation Strategies for UHI

There are two main UHI reduction strategies: the first one is, to increase surface reflectivity (i.e. high albedo). Hence, this would be beneficial in reducing the radiation absorption of urban surfaces. Reflective surfaces result from light coloured or white paint on the surface of given construction material or from cover the construction material surface with a white membrane. The second strategy to mitigate UHI is to increase vegetation cover to maximise the multiple vegetation benefits in controlling the temperature rises. Both techniques have been applied mostly to roofs and pavements. Cool roofs can be highly efficient in commercial and residential zones, where significant energy demand for cooling can be lessened by reducing the heat gain to buildings (Mills et al., 1997). However white surfaces may be cheaper to install at first, but need to be periodically repainted, or they get dirty and fail to reflect light well. Another strategy is roof greening that is to employee layer of roof-friendly soils and plants on the rooftops of buildings in the city to reduce the rate of absorption in the summer. However, a few researchers argue that the locally applied roof greening may not influence the air temperatures inside the building canyons. The air cooled by roof greening may disperse into the above roof flow rather than be entrained into the street canyon. Only for perpendicular or oblique winds, or under low wind conditions, the cooled rooftop air may get entrained into the street canyon and result in noticeable air temperature reductions (Gromke and Blocken, 2015).

1.1.2.6 Measuring and Monitoring UHI

Traditional ways in which UHI are measured, include station pairs or the use of transects. By station pairs, we mean the meteorological stations in urban and rural regions. Most of the methods use meteorological observatory data to analyse air temperature gradients in urban and peri-urban regions monitoring Canopy Layer Heat Island (CLHI) and Boundary Heat Island (BHI) (Bornstein and Lin, 2000; Gedzelman and Austin, 2003; Jin and Shepherd 2005; Zhou and Dickinson, 2011). However, the data collected at meteorological stations in cities may not be suitable for representing urban weather conditions, since most stations are established for synoptic forecasting at places where the parameters of the weather are not disturbed by urban structures or human activities (Lee et al., 1993). Urban climatologists also tend to use numerical modelling techniques.

1.2 Geospatial Techniques for Mapping Urban Landscape Dynamics

Geospatial data analysis techniques such as remote sensing and Geographic Information System (GIS) provide useful and feasible opportunities for mapping and regional monitoring on a synoptic scale. The digital format can offer additional benefits, such as convenient scale conversion, aggregation and disaggregation, ready access to statistics and attributes, and ready integration with other GIS data (Ridd et al., 1995).

1.2.1 Remote Sensing

Remote sensing relates to the activities of recording/observing/perceiving (sensing) objects or events at distant places. Hence, the remote sensing sensors are not in direct contact with the objects being monitored or observed. These sensors record the information about objects via electromagnetic radiations. The output of a remote sensing sensor is usually an image representing the scene being scanned or observed. These images are then further analysed to extract useful information. Remote sensing usually defined as the technology of recording information about the earth (land, ocean and atmosphere) using sensors onboard airborne or spaceborne platforms. The spaceborne platforms are classified as satellites or space stations whereas the airborne sensors are unmanned areal vehicles (UAVs), helicopters, airplanes or balloons.

The space-borne sensors look through a layer of atmosphere separating the sensors from the Earth's surface. Hence, it becomes necessary to understand the effects of the atmosphere on the electromagnetic energy being reached at satellite sensors via the atmosphere from the Earth surface.

The atmospheric interference with electromagnetic signals may cause particular wavelengths in the electromagnetic range to be absorbed or blocked by the atmosphere. The available wavelengths in the electromagnetic spectrum for remote sensing sensors are limited to the atmospheric transmission windows. Hence, the remote sensing sensors are built to function within one or more of the atmospheric windows (Richards and John, 1999). The microwave region, some region in the infrared range, the entire visible and part of the near ultraviolet range are in these atmospheric windows where the electromagnetic radiations are not blocked by the atmosphere and can be utilised to record the information from earth surface via sensors boarded on satellites (Fig.1.4). Although the atmosphere is practically transparent to x-rays and gamma rays, these radiations are not generally used in remote sensing of the earth.

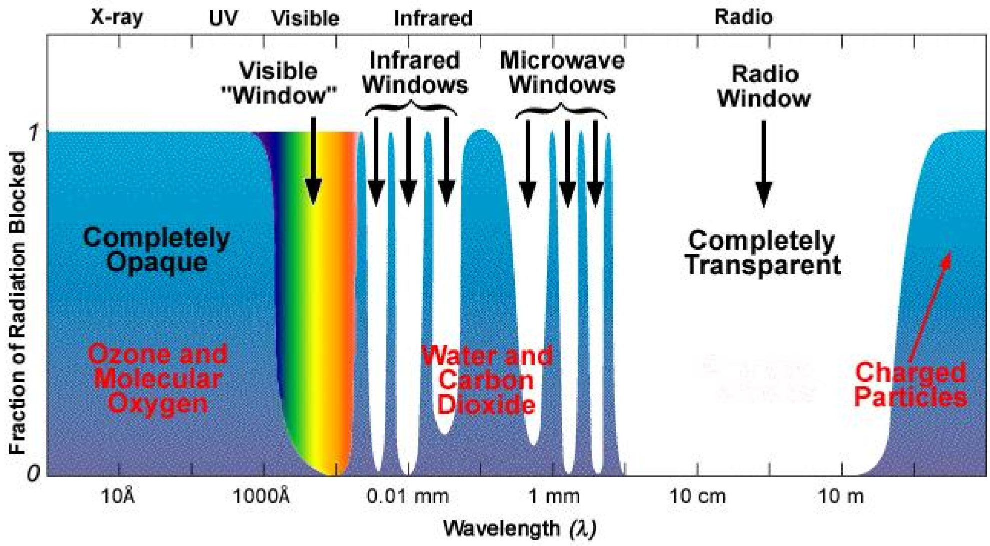

Figure 1.4. Shows fraction of radiations blocked and transmitted by atmosphere at various wavelengths in the electromagnetic spectral band. (Modified from https://christinatang1992.wordpress.com/tag/atmospheric-windows/ dated 01-02-2018)

1.2.2 Satellite data

During the past half century, remote sensing imagery has been acquired by both airborne and spaceborne sensors. These sensors record the information about land, ocean and atmosphere in multiple spectral bands of the electromagnetic spectrum ranging from visible to microwave wavelengths. The spatial resolution, or pixel size, may range from centimetres to kilometres, and temporal revisit periods may range from 15 minutes to weeks (Xie and Sha, 2008).

Table 1.1. Examples of satellite and sensor systems relevant to applications.

Satellite / Sensor	Archive Availability	Spatial Resolution at Nadir (multispectral)	Temporal Resolution at Equator	Applications
Open Source Data:				
NOAA / AVHRR series	1979	1.1 km	1 day	Monitoring surface temperature (Kidder and Wu 1987; Streutker 2002)
Landsat satellite series	1987	60 – 30 m 100 m	16 Days	Monitoring surface temperature changes; land cover mapping; albedo, greenness vegetation mapping (Aniello and Morgan, 1995; Odindi and Bangamwabo, 2015)
ASTER	1999	15 m / 90 m	16 Days	Monitoring surface temperature changes; land cover mapping (Chrysoulakis 2003; Zhu and Blumberg, 2002)
Aqua / Terra Satellites (MODIS)	2000	1 km	Four images per day	Monitoring surface temperature / air temperature; land cover mapping; material characteristics & albedo, greenness vegetation mapping
Sentinel series	2015	10 m	10 days	Land cover, change detection (Wang et al., 2016)
Himawari 8 / 9	2016	0.5 -2 km	15 min	Rainfall , sea surface temperature and atmospheric monitoring (Kurihara and Murakami, 2016; Yumimoto and Nagao, 2016)
Commercial Data:				
Ikonos QuickBird GeoEye-1	1999	3.2 – 1.24 m	On demand	Urban land cover classification, detecting urban features, mapping

WorldView (1,2,3,4)				urban greenness (Lu and Hetrick, 2010; Lu and Weng, 2009)
SPOT satellite series (5, 6, 7)	2002	10 – 6.0 m	26 Days	Land cover; land surface temperature (Durieux and Lagabrielle, 2008)

For land cover and use mapping across peri-urban areas, there are a range of fine spatial resolution sensors, such QuickBird (Grau and Hernández, 2008), SPOT, and Landsat, that enable fine detailed spatial mapping of surface conditions (Table.1.1). Table.1.1 lists some of the most commonly used satellite/sensors in urban/ peri-urban studies, along with satellite lifespan, spatial and temporal resolutions, and examples of relevant applications. These include the high temporal frequency (daily) satellites such as the Moderate Resolution Imaging Spectroradiometer (MODIS) and Advanced Very High-Resolution Radiometer (AVHRR).

Although some of these available satellite image datasets are commercial and expensive, in the last decade there has been an enormous increase in public and free satellite data availability, such as data from Aqua / Terra, Landsat, ASTER, Himawari and Sentinel-2. The MODIS sensor onboard Aqua / Terra offers multispectral data available from 2000 to present. Aqua has 1:30 am and 1:30 pm equatorial crossing times, while Terra crosses at 10:30 am and 10:30 pm. The data is highly suitable for macro scale mapping such as analysing diurnal land surface temperatures or vegetation cover change and so on. The MODIS data and derived MODIS products are available on NASA web page (https://urs.earthdata.nasa.gov/). "The MODIS data products are validated and calibrated globally by the MODIS land science team at NASA, that incorporates a number of validation methods to characterise and measure the uncertainty factor among its products (Justice and Vermote, 1998;)"Landsat data are at 30 m spatial resolution in the optical bands and 60 m in the thermal band with a temporal resolution of 16-days, and available from the USGS web site (http://www.earthexplorer.usgs.gov/). The Sentinel-2 mission is a land monitoring constellation of two satellites that offer high resolution optical imagery. MultiSpectral Instrument (MSI) on-board Sentinel-2 offers higher resolution optical imagery than Landsat series. Sentinel-2 data are available at European Space Agency (ESA) web site (https://scihub.copernicus.eu/).

1.2.3 Spectral Products / Indices Derived from Satellite Data

Remote sensing provides spectral information in a variety of ways that are useful to delineate and classify vegetation, built up infrastructure, soil, and water bodies. Spectral equations and algorithms can exploit this data to derive spectral indices that use unique combinations of spectral channels. Spectral indices are biophysical measures of the state, structure, and composition of the surface elements within a landscape. These indices are formed by adding, dividing, or multiplying individual spectral channels in a manner designed to enhance or reveal specific land surface properties, such as live vegetation, snow, woody vegetation, water, pigments, etc. Table.1.2. lists some of the more useful indices derived from satellite products that are widely used in satellite monitoring of urban/peri-urban land dynamics.

Table 1.2. Selected satellite products relevant for urban monitoring studies. Blue, Red, Near-infrared (NIR) and Short-wave infrared (SWIR) indicate surface reflectance values in those wavebands and BT represents satellite brightness temperature.

Spectral Index	Formula	Application
Normalised Difference Vegetation Index (NDVI)	$\frac{NIR - Red}{NIR + Red}$ (Rouse et al., 1974)	Enhances healthy, green vegetation

Enhanced Vegetation Index (EVI)	$G \times \frac{NIR - Red}{NIR + C1\ X\ Red + C2\ X\ Blue + L}$ *G = 2.5 , C1 = 6 , C2 = 7.5 and L = 1* (Huete et al., 2002)	Enhances vegetation / greenness. It uses the blue reflectance region to correct for soil background signals to reduce atmospheric influences, including aerosol scattering
Normalised Difference Built up Index (NDBI)	$\frac{SWIR - NIR}{SWIR - NIR}$ (Zha and Gao, 2003)	Enhances urban features
Modified Normalized Difference Water Index (MNDWI)	$\frac{Green - SWIR}{Green + SWIR}$ (Xu et al., 2006)	Enhances open water features while suppressing noise from built-up land, vegetation, and soil
Land Surface Temperature (LST)	$\frac{BT}{1 + \left(\lambda * \frac{BT}{c_2}\right) * \ln(e)}$ λ = *wavelength of emitted radiance,* c_2*=0.014388 m K* (Weng and Lu, 2004)	Measures surface temperature of land
Albedo	$\frac{Outgoing\ Shortwave\ Radiation}{Incoming\ Shortwave\ Radiation}$	Identifies surfaces and their properties

1.2.3.1 Land Use Land Cover (LULC) Classification:

A land cover map provides information about the coverage of forests, wetlands, impervious surfaces, vegetation and other landscapes. On the other hand, land use maps provide more information on land usage by landowners, such as commercial or residential urban usage, agriculture/livestock management activities, or fallow/ barren areas in peri-urban areas. More detailed information can be provided by land function maps, which integrate local information from landowners to develop maps based on land function.

Land use/land cover maps at various scales can be utilised to keep information current in peri-urban lands for better management and planning of agriculture activities.

Remote sensing and GIS data may be best utilised to produce up to date land use/land cover maps at various scales. A few approaches have been analysed by researchers, including multispectral classification (Atkinson et al., 2005; Dougherty et al., 2004), spectral mixture analysis (SMA) (Weng et al., 2001; Weng et al., 2002; Wu and Xu, 2005), and few others based on scale and application of data (Yang and Titus, 2003).

1.2.3.2 Vegetation Indices

Several vegetation indices (VIs) provide measures of canopy “greenness”, an integrative property of green leaf area, canopy structure, and leaf chlorophyll content (Veroustraete and Patyn, 1994). One of the most widely used VIs is the Normalised Difference Vegetation Index (NDVI) (Tucker (1979). NDVI have values that vary between -1 and +1. The Enhanced Vegetation Index (EVI) is an 'optimised' vegetation index designed to enhance the vegetation signal with better sensitivity in high biomass areas and improved vegetation mapping and monitoring through a de-coupling of the canopy background signal and a reduction in atmosphere influences (Huete et al. 1997). EVI is often used to monitor ecosystems over time and to assess phenology patterns in vegetation.

1.2.3.3 Land Surface Temperature

Satellite thermal channels are utilised to assess land surface temperatures. The thermal images measure and record ‘brightness temperature’, which is then processed to ‘land surface temperature (LST)’ values using separate measures or estimates of emissivity (Kalma and McVicar, 2008; Weng and Lu, 2004).

1.2.3.4 Validation

Remotely sensed data need to be validated against field observations. Many sources of data have been employed for validation. Validation data can be collected from field observations observed either from multiple locations (Studer et al., 2007) or at individual sites (Fisher and Mustard, 2007). Validation can also be based on data predicted by simulation models (Huete et al., 2012; Schwartz and Ahas, 2006).

1.3 Australian Perspective

1.3.1 Climate variability in Australia

According to the Australian Bureau of Statistics (ABS), Australia's urban or built environment encompasses about 2.4 million hectares or 0.3 per cent of the total land mass. Australia's population has urbanised considerably during the last century. At present, 89 per cent of the Australian population lives in urban areas, and this is predicted to rise to 93 per cent by 2050. Australia is highly urbanised - although sparsely populated - relative to other countries in the world (DESA, 2012). Approximately 67 per cent of the Australian population is located in the major cities of Sydney, Melbourne, Brisbane, Perth and Adelaide (Cleugh et al., 2011; ABS 2017).

In Australia, the surface temperatures have increased by 1ºC since 1910 (Grose, et al., 2015; BOM, 2017). The 11-year mean temperature for 2008–2018 was the record high approximately 0.77ºC above average (BOM, 2019). Warming remained modest in Australia during the early 20th century, with a slight drop from 1935 to 1950, and then it rapidly increased (Cleugh et al., 2011; BOM, 2019). Almost all of Australia has warmed over the 50 years since 1960 (Cleugh et al., 2011). Some regions have experienced a temperature rise of up to 2ºC over this time, while other areas have experienced little or no change (Cleugh et al., 2011). Overall, the frequency of extreme cold weather has decreased across most of Australia, while the frequency of warm weather has increased. The number of days with record hot temperatures has increased each decade over the past 50 years (Fig.1.5). It is further reported that the strongest trends in the frequency of hot days and warm nights have occurred in the north-east of the country since the mid-20th century, while the strongest declines in the frequency of cold days have occurred across the south (Cleugh et al., 2011).

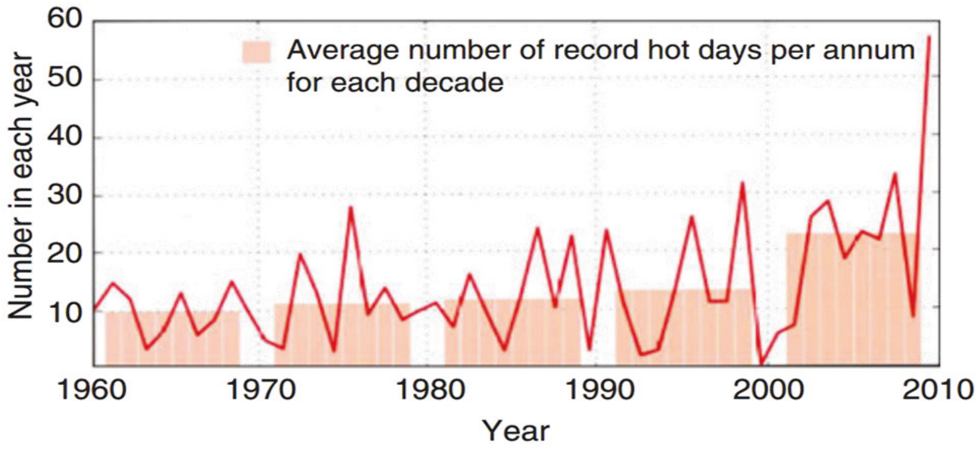

Figure 1.5. The Number of Record Hot Days for Each Year from 1960 to 2010 across Australia and the histogram further indicates the average number of hot days per year for each decade; modified from Cleugh (2011)

1.3.2 UHI in Australia

Australian cities are reported to be 5ºC hotter compared to surrounding areas due to the UHI effect that could eventually turn the cities into death traps. There are a small number of studies that have been carried out on UHI effect in Australian cities. However, these studies are limited to a certain time in a year or a day, and no long term analysis has been yet carried out for subject cities. For example, a study carried out for Adelaide, analysed air temperature data from ground-based temperature sensors (15 min interval diurnal cycle) and observed an intense urban canyon heat island effect (6 - 8°C) (Erell and Williamson, 2007). However, the study was carried out for particularly nighttime at canyon to suburban level, whereas UHI has its diurnal nature and particular seasonality that varies spatially and temporally (Schatz and Kucharik, 2014). Similarly other studies, which were carried out for Melbourne (Morris and Simmonds, 2000; Torok et al. 2001; Morris and Simmonds, 2001; Coutts and Beringer, 2007; Parker et al., 2013; Razzaghmanesh and Beecham, 2016; Suppiah and Whetton 2007; Tapper et al., 2012;) also reported the urban surface heat island using satellite image data and meteorological data at certain time in a year and particularly dealt with nighttime effect. Other studies also provided evidence of UHI for cities such as Camperdown, Colac, Hamilton (Torok et al., 2001), Hobart (Nunez and Oke, 1976) and Sydney (Adams and Smith, 2014; Sharifi & Lehmann 2014; Sharifi and Philipp, 2014). Over Sydney, some studies have used airborne thermal data focusing on the CBD area and revealed that roads and pavements were warmer as compared to roofs, despite the roofs remaining exposed to the sun for longer times. The airborne thermal data were helpful due to its higher spatial resolution but very expensive due to some flights required for each imagery, therefore limited to a certain time of year and day. These studies, to date, on UHIs have yet not considered the large picture such as diurnal patterns, seasonality of UHI, long term trends and its drivers / relationship with other indicators such as land use land cover in urban and rural areas, impervious surface area per cent, albedo, vegetation cover and its impacts on urban ecosystem health.

Moreover, the studies carried out in the past were limited to relatively smaller spatial extents due to the limited swath of airborne sensors or the limited number of stations in urban to rural zones. In addition to it, the studies also did not look at diurnal variations in LST and UHI variations across urban to rural zones. Moreover, studies in the literature analysed various UHI drivers and relationships with UHI over time and space such as radiation balance, weather parameters, urban LULC, vegetation/greenness cover in cities, population density, etc. to understand the UHI behaviour. Studies based in Australia also indicated presence of a strong nightime UHI in its selected cities (Jamei and Rajagopalan, 2019; Iping and Kidston-Lattari, 2019; Coutts and Harris; 2016; Sharifi and Philipp, 2014). However, much more details were ignored such as the importance of rural class as reference which can be dominated by different biomes, for example, vegetation or pasture lands which may have certain seasonal characteristics, deserts or forests which may not have any seasonal patterns. Hence, these settings may eventually affect the UHI amplitude in adjacent cities in a day and over a year. There is need of an extended study on UHI by examining the long-term analysis on diurnal and seasonal characteristics of UHI and cross-correlation of parameters such as vegetation cover, albedo, diurnal UHI intensity and impervious surface per cent to better understand the urban climates to a better extent.

1.4 Current issues and corresponding thesis objectives

It is certain from the literature review that UHI responds in different ways during different times of day and season. UHI indicators/drivers play an important role in driving UHI behaviour in space and time. I went through many studies in literature that have analysed few parameters and relationships of UHI over time and space with radiation balance, weather parameters, urban vegetation / greenness cover, population density and found that very few in literature have looked upon the fact that UHI can also be function of heterogeneity in land use land cover (LULC) in urban to rural transition zones. In addition to this, even in rural class, which is the combination of more than one LULC class, that could be ‘forest’, ‘pasture’, ‘desert’, or ‘mixed; can have different inter-annual response and these patterns can affect the intensity of UHI and seasonality/trends differently. The discussion is still unclear and needs more insight on understanding the patterns in the UHI and factors that drive its daytime/nighttime and seasonal variance. There is still a huge need of understanding the patterns and drivers that cause the effect to be dominant.

Moreover, most studies considered a particular time of year and day for monitoring the UHI behaviour, however, a long-term study is highly needed. Last, not the least, most of the studies completely ignored the effect of climate variance or climate extremes on existing UHIs in cities, which needs further insight. In addition to it, most of the studies in literature confined themselves at UHI intensity, and not looking at footprints or centre location of UHI in space and time.

The overall aims of this study were to analyse urban landscape processes and understand their relationships with drivers of UHI dynamics. In this thesis, I applied advanced geospatial data analysis techniques to understand, monitor and map historical and present urban landscape modifications and urban heat island (UHI) phenomena induced by land surface heterogeneity. I have confined my proposed work to scales associated with city / regional scales (1 - 10 km) by utilising MODIS data with a spatial resolution of 250m (band 1-2), 500m (band 3-7) to 1000 m (band 8-36) and Himawari-8 data with a spatial resolution of 2000 m. Remote sensing technology was assessed as to its capability of providing measurements of urban to rural conditions for heat island modelling, which is highly demanding using the traditional energy budget approaches. The urban climate information derived from remote sensing data and the data sets generated were of great value for civil and environmental applications and management of the impacts of urban-related activities on the natural environment. The correlation between urban land covers in space and time were analysed using remotely sensed data to identify the key indicators of UHIs and the vulnerability and resilience of the ecological areas.

1.4.1 Study Area

This study focusses on the two major cities in Australia that are Sydney and Melbourne. Sydney is home to over 5 million people, approximately more than 20 percent of total population of Australia. Melbourne is the capital city of Victoria state with a population of over 4.8 million, which is approximately 19.05% of the total population of Australia (ABS 2018). The Melbourne city ranks the second most populated state in Australia after Sydney and the most densely populated city in Australia with a population density of 453/km2 (Population Australia, 2018). Both cities are growing in population with time, such as Melbourne was reported to have largest growth of all capital cities in Australia with a change of 2.7% in population over 2016 to 2017. Similarly, Sydney faced a change of 2.0% rise in population over the one year (2016-2017). Sydney and Melbourne both cities are located in the southeast Australia; the climate is temperate with mild winters and summers being hot (Watson et al. 2006). Fig.1.6 shows the selected cities with their greater city boundaries comprising the municipal districts. The outskirts of the populated land extend to dryland agriculture, grasses and pastures along with the forest areas.

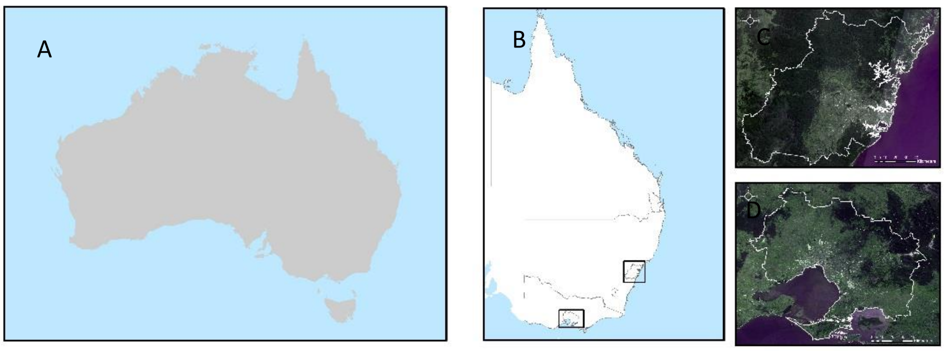

Figure 1.6. (a) Australia (b) East Australia showing Sydney and Melbourne (c) Greater Sydney Region boundary in white colour overlayed on mosaicked satellite image of Landsat dated 29 April and 15 August 2018 (d) Greater Melbourne region boundary in

white colour overlayed on mosaicked satellite image of Landsat dated 20 January and 16 May 2018.

1.4.2 Research Questions

Specifically, I attempted to answer the following research questions in my thesis:

(1) What are the diurnal and seasonal characteristics of UHI in selected Australian cities

(2) What are the long term trends in UHI?

(3) What are the drivers of UHI trends in selected Australian cities (Sydney and Melbourne)?

(4) How does the spatiotemporal dynamics in rural class impact the UHI dynamics as a reference?

(5) What is the role and influence of vegetation in rural and urban areas on UHI?

(6) What are the dynamics and impacts of extreme heat events on UHIs in cities (Case study Sydney)?

The answer to these questions and scientific knowledge acquired are significantly important for the quantitative analysis of the impacts of urbanisation on UHI, both spatially and temporally, and for developing mitigation/adaptation measures. The study will be helpful in understanding the role of indicators in driving daytime and nighttime UHI, its inter-annual seasonality and respective trends. These investigations will be beneficial to urban scientists and designers and policymakers to explore the best mitigation techniques in space and time. This thesis will expand knowledge of the thermal, greenness, and brightness behaviour of urban landscapes and the mechanisms of heat islands, greenness dynamics (phenology and extent) by quantifying their diurnal and seasonal characteristics for considered cities and by tracing the evolution of these variables through last two decades of historical satellite data.

1.4.3 Research Chapters

This thesis is presented as a collection of published and submitted journal articles/book chapter, each of which contributes to addressing the specific aims of this thesis. The papers are linked and integrated into the existing scientific literature by a general introduction chapter (Chapter 1), and the results are summarised and a conclusion is presented in my general discussion (Chapter 6).

Chapter 2: Spatial and Temporal Analysis of Surface Temperature in Urban – Peri Urban Surroundings for modelling and quantifying the Urban Heat Island Effect. The focus of this study is to characterise the inter-annual and seasonal characteristics of diurnal (night and daytime) LST and UHI across urban and neighbouring rural areas in selected cities across Australia. This chapter addresses the issues of variations in spatial and temporal patterns of LST for quantifying the evolution of the UHI formation. To carry out the subject study MODIS based land surface temperature (LST) data are acquired from 2003 to 2017 at diurnal, weekly, and monthly time scales and were processed accordingly. LULC data were obtained from the Australian Bureau of Statistics (ABS) to carry out the subject study.

The objectives of this chapter were as follows:

1. To analyse spatial and temporal variations in LST in urban to rural zones for modelling and quantifying the urban heat island formation

2. To examine the statistical significance of UHI day vs night

3. To evaluate seasonality and inter-annual variations in UHI

Chapter 3: UHI Time Series Trends and their Drivers. The focus of this study is to link the LST and UHI variability and seasonality to spatiotemporal dynamics in LULC classes of rural zones as UHI reference. The focus of this study is to assess long-term trends (significant/non-significant) in UHI and LST and their interactions/dependencies with its drivers / indicators (EVI, albedo, rains) over a period of fifteen years that is from 2003 to 2017.

The objectives of this chapter are as follows:

1. To report on any significant shifts in slope and trend over a period of fifteen years for LST, UHI, EVI, precipitation and albedo.
2. Exploring the impact of LULC heterogeneity in rural zones as reference on UHI dynamics and its indicators/drivers in space and time.

Chapter 4: Interactions of vegetation phenology with UHI. After analysing the diurnal and seasonal characteristics in UHI for selected cities and rural LULC impact on UHI, I processed phenology curves for greenness and urban greenness deficit to better understand the role of vegetation phenology and its impacts on UHI.

The objectives of this chapter are as follows:

1. To investigate the urban, peri-urban and rural interactions of vegetation phenology on UHI patterns and dynamics.
2. To determine whether vegetation patterns and phenological differences between urban and rural reference areas amplify or mitigate UHI.

Chapter 5: Influence of Heat Waves onto Urban Heat Island Effect. After analysing the diurnal, seasonal, inter-annual characteristics in UHI and their relationship with various indicators for selected cities, I analysed a heat wave event and its influence on UHI. For this, I processed Himawari-8 based LST data at hourly, daily, 03 day, 08 day and monthly time scale. For the heat wave event, I considered heat wave event in South east Australia that occured in February 2017. The selection of heat wave event was done on the availability of data sets.

The objectives of this chapter are as follows:

1. To analyse diurnal variations in UHI and quantify its intensity around the metropolitan area during a heat wave event using high temporal resolution data of Himawari-8

2. Analysing MODIS based observations to further detect the effect of heat wave on UHI and compare the results from MODIS with Himawari-8 data

Chapter 6: In this Chapter, I summarized my key findings and present my conclustion based on the analysis done. The overall aims of this study were to analyse urban landscape processes and understand their relationships as drivers of UHI dynamics in Australian cities (Sydney and Melbourne). Satellite remote sensing and in situ data sets were used to address thesis objectives based on combination of complementary materials. The current issues and corresponding objectives to address them in this thesis are listed below by chapters.

1.5 References

Adams, M.P. & Smith, P.L. 2014, 'A systematic approach to model the influence of the type and density of vegetation cover on urban heat using remote sensing', Landscape and Urban Planning, vol. 132, pp. 47-54.

Aniello, C., Morgan, K., Busbey, A. and Newland, L., 1995. Mapping micro-urban heat islands using Landsat TM and a GIS. Computers & Geosciences, 21(8), pp.965-969.

Australian Buereau of Statistics (ABS) website https://www.abs.gov.au/AUSSTATS/abs@.nsf/Lookup/3218.0Main+Features12017-18?OpenDocument cited on 16 July 2019

Atkinson, P.M. 2005, 'Sub-pixel target mapping from soft-classified, remotely sensed imagery', Photogrammetric Engineering & Remote Sensing, vol. 71, no. 7, pp. 839-46.

Argüeso, D., Evans, J.P., Fita, L. & Bormann, K.J. 2014, 'Temperature response to future urbanization and climate change', Climate dynamics, vol. 42, no. 7-8, pp. 2183-99.

Azevedo, J.A., Chapman, L. and Muller, C.L., 2016. Quantifying the daytime and night-time urban heat island in Birmingham, UK: A comparison of satellite derived land surface temperature and high resolution air temperature observations. Remote Sensing, 8(2), p.153.

Bonafoni, S., Anniballe, R. & Pichierri, M. 2015, 'Comparison between surface and canopy layer urban heat island using MODIS data', Urban Remote Sensing Event (JURSE), 2015 Joint, IEEE, pp. 1-4.

Bornstein, R. & Lin, Q. 2000, 'Urban heat islands and summertime convective thunderstorms in Atlanta: three case studies', Atmospheric Environment, vol. 34, no. 3, pp. 507-16.

Bounoua, L., Zhang, P., Mostovoy, G., Thome, K., Masek, J., Imhoff, M., Shepherd, M., Quattrochi, D., Santanello, J. & Silva, J. 2015, 'Impact of urbanization on US surface climate', Environmental Research Letters, vol. 10, no. 8, p. 084010.

Chrysoulakis, N., 2003. Estimation of the all-wave urban surface radiation balance by use of ASTER multispectral imagery and in situ spatial data. Journal of Geophysical Research: Atmospheres, 108(D18).

Cleugh, H., Smith, M.S., Battaglia, M. & Graham, P. 2011, Climate change: science and solutions for Australia, CSIRO.

Coutts, A.M., Beringer, J. & Tapper, N.J. 2007, 'Impact of increasing urban density on local climate: spatial and temporal variations in the surface energy balance in Melbourne, Australia', Journal of Applied Meteorology and Climatology, vol. 46, no. 4, pp. 477-93.

DESA, U., 2015. World population prospects: The 2015 revision, key findings and advance tables. United Nations Department of Economic and Social Affairs. Population Division working paper no. ESA/P/WP, 241.

DHS, J. 2009, 'Heatwave in Victoria: an assessment of health impacts. Victorian Government Department of Human Services', Victoria.

Dougherty, M., Dymond, R.L., Goetz, S.J., Jantz, C.A. & Goulet, N. 2004, 'Evaluation of impervious surface estimates in a rapidly urbanizing watershed', Photogrammetric Engineering & Remote Sensing, vol. 70, no. 11, pp. 1275-84.

Durieux, L., Lagabrielle, E. and Nelson, A., 2008. A method for monitoring building construction in urban sprawl areas using object-based analysis of Spot 5 images and existing GIS data. ISPRS Journal of Photogrammetry and Remote Sensing, 63(4), pp.399-408.

Fisher, J.I. & Mustard, J.F. 2007, 'Cross-scalar satellite phenology from ground, Landsat, and MODIS data', Remote Sensing of Environment, vol. 109, no. 3, pp. 261-73.

Fung, W.Y., Lam, K.S., Nichol, J. and Wong, M.S., 2009. Derivation of nighttime urban air temperatures using a satellite thermal image. Journal of Applied Meteorology and Climatology, 48(4), pp.863-872.

Ganbat, G., Han, J.-Y., Ryu, Y.-H. & Baik, J.-J. 2013, 'Characteristics of the urban heat island in a high-altitude metropolitan city, Ulaanbaatar, Mongolia', Asia-Pacific Journal of Atmospheric Sciences, vol. 49, no. 4, pp. 535-41.

Gao, P., Niu, X., Wang, B. & Zheng, Y. 2015, 'Land use changes and its driving forces in hilly ecological restoration area based on gis and rs of northern china', Scientific reports, vol. 5.

Gedzelman, S., Austin, S., Cermak, R., Stefano, N., Partridge, S., Quesenberry, S. & Robinson, D. 2003, 'Mesoscale aspects of the urban heat island around New York City', Theoretical and Applied Climatology, vol. 75, no. 1-2, pp. 29-42.

Grau, H.R., Hernández, M.E., Gutierrez, J., Gasparri, N.I., Casavecchia, M.C., Flores-Ivaldi, E.E. and Paolini, L., 2008. A peri-urban neotropical forest transition and its consequences for environmental services. Ecology and Society, 13(1).

Gray, K.A. & Finster, M.E. 1999, The urban heat island, photochemical smog, and Chicago: Local features of the problem and solution, Northwestern University, Department of Civil Engineering.

Grimm, N.B., Faeth, S.H., Golubiewski, N.E., Redman, C.L., Wu, J., Bai, X. & Briggs, J.M. 2008, 'Global change and the ecology of cities', science, vol. 319, no. 5864, pp. 756-60.

Gromke, C., Blocken, B., Janssen, W., Merema, B., van Hooff, T. & Timmermans, H. 2015, 'CFD analysis of transpirational cooling by vegetation: Case study for specific meteorological conditions during a heat wave in Arnhem, Netherlands', Building and Environment, vol. 83, pp. 11-26.

Huete, A.R. 2012, 'Vegetation indices, remote sensing and forest monitoring', Geography Compass, vol. 6, no. 9, pp. 513-32.

Huete, A., Didan, K., Miura, T., Rodriguez, E.P., Gao, X. and Ferreira, L.G., 2002. Overview of the radiometric and biophysical performance of the MODIS vegetation indices. Remote sensing of environment, 83(1-2), pp.195-213.

Huete, A., Liu, H., Batchily, K.v. & Van Leeuwen, W. 1997, 'A comparison of vegetation indices over a global set of TM images for EOS-MODIS', Remote sensing of environment, vol. 59, no. 3, pp. 440-51.

Imhoff, M.L., Zhang, P., Wolfe, R.E. & Bounoua, L. 2010, 'Remote sensing of the urban heat island effect across biomes in the continental USA', Remote Sensing of Environment, vol. 114, no. 3, pp. 504-13.

Jiang, X.Y., Zhang, C.L., Gao, H. and Miao, S., 2007. Impacts of urban albedo change on urban heat island in Beijing—a case study. Acta Meteorologica Sinica, 65(2), pp.301-307.

Jin, M., Dickinson, R.E. & Zhang, D. 2005, 'The footprint of urban areas on global climate as characterized by MODIS', Journal of Climate, vol. 18, no. 10, pp. 1551-65.

Jin, M. & Shepherd, J.M. 2005, 'Inclusion of urban landscape in a climate model: How can satellite data help?', Bulletin of the American Meteorological Society, vol. 86, no. 5, pp. 681-9.

Johnson, D.P. & Wilson, J.S. 2009, 'The socio-spatial dynamics of extreme urban heat events: the case of heat-related deaths in Philadelphia', Applied Geography, vol. 29, no. 3, pp. 419-34.

Kalma, J.D., McVicar, T.R. and McCabe, M.F., 2008. Estimating land surface evaporation: A review of methods using remotely sensed surface temperature data. Surveys in Geophysics, 29(4-5), pp.421-469.

Kidder, S.Q. & Wu, H.-T. 1987, 'A multispectral study of the St. Louis area under snow-covered conditions using NOAA-7 AVHRR data', Remote Sensing of Environment, vol. 22, no. 2, pp. 159-72.

Kim, Y.-H. & Baik, J.-J. 2005, 'Spatial and temporal structure of the urban heat island in Seoul', Journal of Applied Meteorology, vol. 44, no. 5, pp. 591-605.

Kłysik, K. and Fortuniak, K., 1999. Temporal and spatial characteristics of the urban heat island of Łódź, Poland. Atmospheric environment, 33(24-25), pp.3885-3895.

Kolokotroni, M. and Giridharan, R., 2008. Urban heat island intensity in London: An investigation of the impact of physical characteristics on changes in outdoor air temperature during summer. Solar energy, 82(11), pp.986-998.

Kotak, Y., Gul, M.S., Muneer, T. and Ivanova, S.M., 2015, April. Investigating the Impact of Ground Albedo on the Performance of PV Systems. In Proceedings of CIBSE Technical Symposium, London, UK (pp. 16-17).

Kurihara, Y., Murakami, H. and Kachi, M., 2016. Sea surface temperature from the new Japanese geostationary meteorological Himawari-8 satellite. Geophysical Research Letters, 43(3), pp.1234-1240.

Lee, H.-Y. 1993, 'An application of NOAA AVHRR thermal data to the study of urban heat islands', Atmospheric Environment. Part B. Urban Atmosphere, vol. 27, no. 1, pp. 1-13.

Lehmann, S. and Sharifi, E., 2014. Local measures to mitigate the urban heat island effect in hot and humid climate: comparative case study of Sana'a, Bushehr and Dubai Marina. International Journal of Development and Sustainability, 3(1), pp.38-54.

Liu, W., Ji, C., Zhong, J., Jiang, X. & Zheng, Z. 2007, 'Temporal characteristics of the Beijing urban heat island', Theoretical and Applied Climatology, vol. 87, no. 1-4, pp. 213-21.

Lu, D., Hetrick, S. and Moran, E., 2010. Land cover classification in a complex urban-rural landscape with QuickBird imagery. Photogrammetric Engineering & Remote Sensing, 76(10), pp.1159-1168.

Lu, D. and Weng, Q., 2009. Extraction of urban impervious surfaces from an IKONOS image. International Journal of Remote Sensing, 30(5), pp.1297-1311.

Mills, G., 1997. An urban canopy-layer climate model. Theoretical and applied climatology, 57(3-4), pp.229-244.

Mirzaei, P.A. & Haghighat, F. 2010, 'Approaches to study urban heat island– abilities and limitations', Building and Environment, vol. 45, no. 10, pp. 2192-201.

Morris, C. & Simmonds, I. 2000, 'Associations between varying magnitudes of the urban heat island and the synoptic climatology in Melbourne, Australia', International Journal of Climatology, vol. 20, no. 15, pp. 1931-54.

Morris, C.J.G., Simmonds, I. and Plummer, N., 2001. Quantification of the influences of wind and cloud on the nocturnal urban heat island of a large city. Journal of Applied Meteorology, 40(2), pp.169-182.

Nunez, M. & Oke, T. 1976, 'Long-wave radiative flux divergence and nocturnal cooling of the urban atmosphere', Boundary-Layer Meteorology, vol. 10, no. 2, pp. 121-35.

Odindi, J.O., Bangamwabo, V. and Mutanga, O., 2015. Assessing the Value of Urban Green Spaces in Mitigating Multi-Seasonal Urban Heat using MODIS Land Surface Temperature (LST) and Landsat 8 data. International Journal of Environmental Research, 9(1), pp.9-18.

Oke, T.R., 1979. Advectively-assisted evapotranspiration from irrigated urban vegetation. Boundary-Layer Meteorology, 17(2), pp.167-173.

Oke, T.R., 1982. The energetic basis of the urban heat island. Quarterly Journal of the Royal Meteorological Society, 108(455), pp.1-24.

Parker, A. 2013, 'Melbourne urban heat island contamination of temperature trend maps in Victoria, Australia', Nonlinear Engineering, vol. 2, no. 1-2, pp. 39-62.

Platt, R.H., Rowntree, R.A. & Muick, P.C. 1994, The ecological city: preserving and restoring urban biodiversity, Univ of Massachusetts Press.

Ramamurthy, P., Li, D. and Bou-Zeid, E., 2017. High-resolution simulation of heatwave events in New York City. Theoretical and applied climatology, 128(1-2), pp.89-102.

Rainis, R., 2003. 16 Application of GIS and Landscape Metrics in Monitoring Urban Land Use Change. Urban ecosystem studies in Malaysia: A study of change, p.266.

Ramírez, A.Z. & Muñoz, C.B. 2012, Albedo effect and Energy efficiency of cities, INTECH Open Access Publisher.

Rashed, T. & Jürgens, C. 2010, Remote sensing of urban and suburban areas, vol. 10, Springer Science & Business Media.

Razzaghmanesh, M., Beecham, S. and Salemi, T., 2016. The role of green roofs in mitigating Urban Heat Island effects in the metropolitan area of Adelaide, South Australia. Urban Forestry & Urban Greening, 15, pp.89-102.

Richards, J.A. and Richards, J.A., 1999. Remote sensing digital image analysis (Vol. 3). Berlin et al.: Springer.

Ridd, M.K. 1995, 'Exploring a VIS (vegetation-impervious surface-soil) model for urban ecosystem analysis through remote sensing: comparative anatomy for cities†', International journal of remote sensing, vol. 16, no. 12, pp. 2165-85.

Roth, M., Oke, T. & Emery, W. 1989, 'Satellite-derived urban heat islands from three coastal cities and the utilization of such data in urban climatology', International Journal of Remote Sensing, vol. 10, no. 11, pp. 1699-720.

Rouse Jr, J., Haas, R.H., Schell, J.A. and Deering, D.W., 1974. Monitoring vegetation systems in the Great Plains with ERTS.

Ruslan, R., 2003. Application of GIS and landscape metrics in monitoring urban land use change. Urban Ecosystem Studies in Malaysia: A Study of Change; Hashim, NM, Rainis, R., Eds, pp.267-278.

Runnalls, K.E. and Oke, T.R., 2000. Dynamics and controls of the near-surface heat island of Vancouver, British Columbia. Physical Geography, 21(4), pp.283-304.

Schatz, J. and Kucharik, C.J., 2014. Seasonality of the urban heat island effect in Madison, Wisconsin. Journal of Applied Meteorology and Climatology, 53(10), pp.2371-2386.

Schwartz, M.D., Ahas, R. & Aasa, A. 2006, 'Onset of spring starting earlier across the Northern Hemisphere', Global Change Biology, vol. 12, no. 2, pp. 343-51.

Sharifi, E. & Lehmann, S. 2014, 'Comparative Analysis of Surface Urban Heat Island Effect in Central Sydney', Journal of Sustainable Development, vol. 7, no. 3, p. p23.

Sharifi, E., Philipp, C. & Lehmann, S. 2014, 'Multi-scale analysis of the surfacelayer urban heat island effect in five higher-density precincts of central Sydney', Low Carbon Cities: Transforming Urban Systems, p. 375.

Sidiqui, P., Huete, A. and Devadas, R., 2016, July. Spatio-temporal mapping and monitoring of Urban Heat Island patterns over Sydney, Australia using MODIS and Landsat-8. In Earth Observation and Remote Sensing Applications (EORSA), 2016 4th International Workshop on (pp. 217-221). IEEE.

Skoulika, F., Santamouris, M., Kolokotsa, D. & Boemi, N. 2014, 'On the thermal characteristics and the mitigation potential of a medium size urban park in Athens, Greece', Landscape and Urban Planning, vol. 123, pp. 73-86.

Stefanov, W.L. & Netzband, M. 2005, 'Assessment of ASTER land cover and MODIS NDVI data at multiple scales for ecological characterization of an arid urban center', Remote sensing of Environment, vol. 99, no. 1, pp. 31-43.

Streutker, D.R. 2003, 'Satellite-measured growth of the urban heat island of Houston, Texas', Remote Sensing of Environment, vol. 85, no. 3, pp. 282-9.

Studer, S., Stöckli, R., Appenzeller, C. & Vidale, P. 2007, 'A comparative study of satellite and ground-based phenology', International Journal of Biometeorology, vol. 51, no. 5, pp. 405-14.

Suppiah, R. & Whetton, P. 2007, 'Projected changes in temperature and heating degree-days for Melbourne and Victoria, 2008-2012', CSIRO Marine and Atmospheric Research: Aspendale, Victoria, Australia.

Taha, H., 1997. Urban climates and heat islands: albedo, evapotranspiration, and anthropogenic heat. Energy and buildings, 25(2), pp.99-103.

Torok, S.J., Morris, C.J., Skinner, C. & Plummer, N. 2001, 'Urban heat island features of southeast Australian towns', Australian Meteorological Magazine, vol. 50, no. 1, pp. 1-13.

Tapper, N. 2012, 'Adapting Urban Environments to Climate Change: A Case Study of Melbourne Australia', Schooling for Sustainable Development:, Springer, pp. 185-98.

Veroustraete, F., Patyn, J. & Myneni, R. 1994, 'Application of remote sensing in regional scale estimates of vegetation carbon budgets: The Belfix project'.

Voogt, J.A. & Oke, T.R. 2003, 'Thermal remote sensing of urban climates', Remote sensing of environment, vol. 86, no. 3, pp. 370-84.

Wang, Q., Shi, W., Li, Z. and Atkinson, P.M., 2016. Fusion of Sentinel-2 images. Remote sensing of environment, 187, pp.241-252.

Wang, Y., Du, H., Xu, Y., Lu, D., Wang, X. and Guo, Z., 2018. Temporal and spatial variation relationship and influence factors on surface urban heat island and ozone pollution in the Yangtze River Delta, China. Science of the Total Environment, 631, pp.921-933.

Weng, Q. 2001, 'A remote sensing GIS evaluation of urban expansion and its impact on surface temperature in the Zhujiang Delta, China', International journal of remote sensing, vol. 22, no. 10, pp. 1999-2014.

Weng, Q. 2002, 'Land use change analysis in the Zhujiang Delta of China using satellite remote sensing, GIS and stochastic modelling', Journal of environmental management, vol. 64, no. 3, pp. 273-84.

Weng, Q. 2003, 'Fractal analysis of satellite-detected urban heat island effect', Photogrammetric engineering & remote sensing, vol. 69, no. 5, pp. 555-66.

Weng, Q., 2011. Remote sensing of urban biophysical environments. In Advances in Environmental Remote Sensing (pp. 525-546). CRC Press.

Weng, Q., 2014. Global urban monitoring and assessment through earth observation. Crc Press.

Weng, Q., Lu, D. and Schubring, J., 2004. Estimation of land surface temperature–vegetation abundance relationship for urban heat island studies. Remote sensing of Environment, 89(4), pp.467-483.

Wilby, R.L., 2003. Past and projected trends in London's urban heat island. Weather, 58(7), pp.251-260.

Wu, J., Xu, J. & Yue, W. 2005, 'VIS model for cities that are experiencing rapid urbanization and development', IGARSS, pp. 1503-6.

Xie, Y., Sha, Z. & Yu, M. 2008, 'Remote sensing imagery in vegetation mapping: a review', Journal of plant ecology, vol. 1, no. 1, pp. 9-23.

Xu, H., 2006. Modification of normalised difference water index (NDWI) to enhance open water features in remotely sensed imagery. International journal of remote sensing, 27(14), pp.3025-3033.

Yang, Y., Titus, S.J. & Huang, S. 2003, 'Modeling individual tree mortality for white spruce in Alberta', Ecological Modelling, vol. 163, no. 3, pp. 209-22.

Yuan, F. & Bauer, M.E. 2007, 'Comparison of impervious surface area and normalized difference vegetation index as indicators of surface urban heat island effects in Landsat imagery', Remote Sensing of Environment, vol. 106, no. 3, pp. 375-86.

Yumimoto, K., Nagao, T.M., Kikuchi, M., Sekiyama, T.T., Murakami, H., Tanaka, T.Y., Ogi, A., Irie, H., Khatri, P., Okumura, H. and Arai, K., 2016. Aerosol data assimilation using data from Himawari-8, a next-generation geostationary meteorological satellite. Geophysical Research Letters, 43(11), pp.5886-5894.

Zha, Y., Gao, J. and Ni, S., 2003. Use of normalized difference built-up index in automatically mapping urban areas from TM imagery. International journal of remote sensing, 24(3), pp.583-594.

Zhao, L., Lee, X., Smith, R.B. & Oleson, K. 2014, 'Strong contributions of local background climate to urban heat islands', Nature, vol. 511, no. 7508, pp. 216-9.

Zhao, X., Shen, S., Yang, S., Xie, X. & Chen, T. 2010, 'Analyzing the Seasonal Variations of Urban Heat Island in Nanjing Using Remote Sensing Data', Multimedia Technology (ICMT), 2010 International Conference on, IEEE, pp. 1-4.

Zhu, G. and Blumberg, D.G., 2002. Classification using ASTER data and SVM algorithms;: The case study of Beer Sheva, Israel. Remote sensing of Environment, 80(2), pp.233-240.

Zhou, J., Chen, Y., Zhang, X. & Zhan, W. 2013, 'Modelling the diurnal variations of urban heat islands with multi-source satellite data', International journal of remote sensing, vol. 34, no. 21, pp. 7568-88.

Zhou, J., Chen, Y., Wang, J. & Zhan, W. 2011, 'Maximum nighttime urban heat island (UHI) intensity simulation by integrating remotely sensed data and meteorological observations', Selected Topics in Applied Earth Observations and Remote Sensing, IEEE Journal of, vol. 4, no. 1, pp. 138-46.

Zhou, L., Dickinson, R.E., Tian, Y., Fang, J., Li, Q., Kaufmann, R.K., Tucker, C.J. & Myneni, R.B. 2004, 'Evidence for a significant urbanization effect on climate in China', Proceedings of the National Academy of Sciences of the United States of America, vol. 101, no. 26, pp. 9540-4.

Zhou, Y. & Shepherd, J.M. 2010, 'Atlanta’s urban heat island under extreme heat conditions and potential mitigation strategies', Natural Hazards, vol. 52, no. 3, pp. 639-68.

Zhou, D., Zhao, S., Zhang, L., Sun, G. and Liu, Y., 2015. The footprint of urban heat island effect in China. Scientific reports, 5, p.11160.

Chapter 2: Spatial and Temporal Analysis of Land Surface Temperature in Urban – peri-urban Surroundings for Estimating and Quantifying the Urban Heat Island

Abstract

Cities tend to have higher surface/air temperature relative to nearby rural areas. This type of phenomena is called the Urban Heat Island (UHI) effect. The UHI effect is reported to occur mostly at nighttime. However, few field studies found that the maximum UHI can be reached at different times of the day, before and after sunset or midnight or even during the daytime. Moreover, the effect has specific seasonal characteristics, which need to be explored over time and space. In this study, we aim at investigating the land surface temperature (LST) and UHI spatial and temporal variations across two major Australian cities (Sydney and Melbourne), at diurnal, monthly, seasonal, and yearly scales to characterise the UHI in both selected cities. To implement the proposed study, 15 years of Terra/Aqua MODIS based LST data from 2003 to 2017 were analysed. Land use land cover (LULC) data from the Australian Bureau of Statistics (ABS) were used to delineate the urban, rural and water class for the selected cities. The UHI intensities were extracted from LST images by subtracting original from modelled rural LST surfaces for each date.

Significant differences in LST between urban and rural pixels were found throughout the day with daytime being the higher and nighttime smaller intensity. The results, indicated maximum intensities in daytime periods, particularly during the summer season. The daytime UHI intensity was as large as 7 - 8°C for Sydney and 2 - 3°C for Melbourne in summer days. UHI intensities were observed in night-time with intensity up to 2 - 3°C for both cities in summer and spring days. Satellite data of MODIS provided useful results for monitoring, mapping and characterising UHI patterns over time and space.

2.6 Introduction

Alteration of the landscape through urbanisation causes the changes in the radiative, thermal, moisture, and aerodynamic characteristics of the Earth's surface (Weng et al., 2011; Weng et al., 2014). This effect impacts the exchange of heat and moisture between the land surface and lower atmosphere creates the urban heat island (UHI) phenomenon and influences local, mesoscale, and even larger scale climate (Imhoff et al., 2010). UHI effect is the best-documented example of anthropogenic climate modification due to urbanisation.

The studies conducted on UHI showed that the effect was dominant mostly at nighttime in metropolitan areas (Sharifi and Lehmann, 2014; Streutker et al., 2003; Voogt and Oke, 2003; Morris et al., 2011). On the other hand, few more studies indicated that the effect was present at daytime as well with much higher intensity than at nighttime (Taha et al., 1997a; Kolokotroni and Giridharan, 2008; Bonafoni and Anniballe, 2015; Bounoua and Zhang, 2015; Azevedo and Chapman, 2016; Sidiqui and Huete, 2016) and it could be as much as 1 to 6°C in summer days (Taha et al.,1997b). Apart from the daytime and nighttime variations in UHI intensity, the literature also pointed out towards distinct seasonal patterns in the UHI spatially and temporally (Zhao and Shen, 2010; Zhou and Shepherd, 2010; Liu et al., 2007).

In Australia, few studies reported higher temperature measurements in urban to rural zones (Sharifi and Lehmann 2014; Razzaghmanesh and Beecham, 2016). In Melbourne, a transect across the city on the 25th August 1992 observed nighttime UHI intensity of 7.1 °C (Torok and Morris, 2001). The urban areas in Brisbane were reported to have a UHI of approximately 2°C (Deilami and Kamruzzaman, 2017). For Adelaide city in Australia, studies showed an intense nighttime heat island effect (Razzaghmanesh and Beecham, 2016b). However, it is clear from the literature that the studies were limited to certain spatial extents and times across the day.

Moreover, less attention was placed on the seasonal and diurnal variations in UHI both spatially and temporally. Not much emphasis was given on modelling the resulting UHI patterns in space and time. Thus, satellite-based measurements provide unique opportunities to conduct large-scale analysis to better understand and model the UHI patterns and assess its temporal evolution under the last few decades with the rise in population and infrastructure in urban zones.

Satellite data offers detailed spatial and temporal mapping of surface conditions. The sensors are enabled to record data in the wide electromagnetic range covering from microwave, optical, thermal to shortwave infrared bands. The data not only offers synoptic coverage but also provides archives of twenty or thirty years. MODIS sensor onboard Aqua/Terra satellites offer four passes each day in thermal, optical and near-infrared bands.

In this study, I analysed the spatial patterns and temporal dynamics of MODIS-derived LST across two major Australia cities, Sydney and Melbourne from 2003 to 2017. Specifically, I aimed to (1) investigate spatially explicit variations in the direction, intensity, and duration of LST variations across urban to rural zones; (2) quantify the difference in LST at diurnal and seasonal scale; and (3) model and quantify the evolution of UHI formation in selected cities. Results from this study will not only guide the design of Australian cities but will also generate essential knowledge for understanding the urban thermal dynamics.

2.7 Data and Methods

2.7.1 Land use land cover (LULC) & Digital elevation model (DEM) data

For elevation, SRTM based digital elevation model (DEM) was acquired and downloaded from USGS Earth Explorer website. The DEM was processed to eliminate the elevation difference in the study area. A threshold of 200 m above sea level was set to mask out pixels above this. This threshold of 200 m was selected for Sydney and 300 m for Melbourne to give maximum coverage to the urban boundary in the study zone. The maximum height of Greater Sydney region reaches as high as 1300 m and for Melbourne it was 1400 m. Fig.2.1 (a) and (b) shows the DEM for selected cities. Elevation may play a significant role in studies related with spatial distribution of LST such as UHI, climate change and evapotranspiration, hence, the effect of change in elevation needs to be considered for better analysis (Khandelwal et al., 2018a). In this subject study, to minimise the elevation effect, pixels with elevations greater than 200 m for Sydney and 300 m for Melbourne were eliminated based on the DEM data to avoid the influence of the elevation's cooling effect on the UHI quantification. The subject threshold was chosen for each city on the basis of the highest elevation point in urban and urban core zones. Hence, the adjacent non-urban LULC zones that were located outside the urban class and with elevations not greater than 200 m for Sydney and 300 m for Melbourne were flagged as rural pixels (Khandelwal et al., 2018b). This was done to avoid overshadowing effects of the urbanisation on temperature (Imhoff et al., 2010; Zhou et al., 2015; Zhou et al., 2016). The dominating land cover in the rural areas that obtained a similar elevation as the city were mostly pastures and parts of forest.

The Australian Statistical Geography Standard (ASGS) Volume 1 Mesh blocks information from Australian Bureau of Statistics (ABS) were utilised to derive the information on LULC data. The Mesh blocks are the smallest geographical area defined by the Australian Bureau of Statistics (ABS); they broadly identify land use such as ‘residential’, ‘commercial’, ‘primary production’, ‘parklands (forest, parks)’, ‘industrial’, ‘commercial’, ‘education’, ‘hospital’, ‘transport’, ‘water’ and ‘other’ covering the whole Australia without gaps or overlaps. For our analysis, we merged the built class as ‘urban’ that comprised of ‘residential’, ‘education’, ‘transport’, ‘commercial’; and non-built class as ‘rural’ that comprised of ‘other’, ‘pasture’ and ‘forest’. As per ABS, the ‘other’ class represents highly mixed land use, which could not be placed in other nine categories. The ‘pasture’ class in selected LULC data is general LULC class that represents ‘primary production’ or ‘agriculture’ land covers in rural zones. The data is updated every five years (2006, 2011 and 2016). Fig.2.1 (c) and (d) shows the Mesh block release by ABS in 2016; we have merged the built class as urban. This data were used to define urban and rural LULC zones.

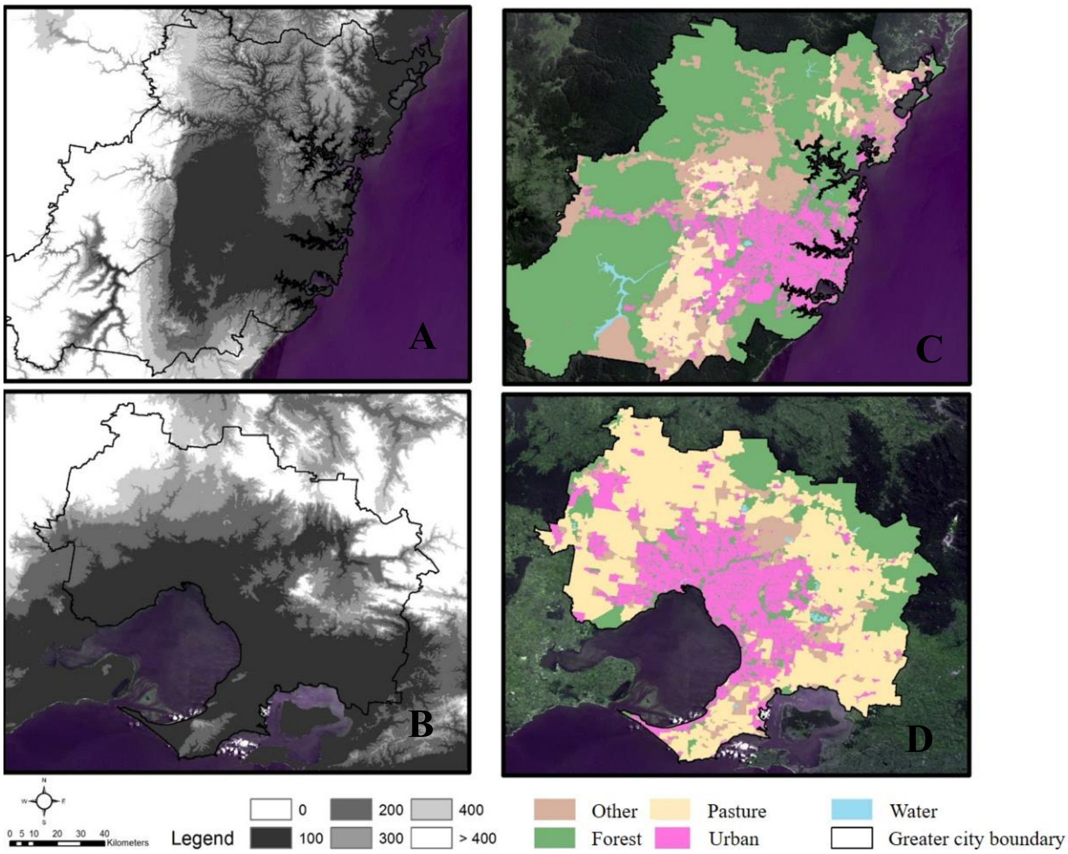

Figure 2.1. (a) SRTM DEM (30 m) overlayed by Greater city boundary for Sydney and (b) Melbourne, (c) Land Use Land Cover (LULC) map acquired from mesh boundaries data of Australian Bureau of Statistics (ABS) for Sydney (d) Land Use Land Cover (LULC) map acquired from mesh boundaries data of Australian Bureau of Statistics (ABS) for Melbourne.

2.7.2 Land Surface Temperature Data

For LST satellite data, Terra/Aqua MODIS LST 8-Day (1km) composite products volume 06 (MOD11A2 and MYD11A2) were acquired from NASA LP DAAC website (http://lpdaac.usgs.gov/modis/) for the period from 2003 to 2017. These datasets provided diurnal LST at 10 AM, 2 PM, 10 PM and 2 PM. These datasets were filtered based on the QA flags mentioned in the Quality Control (QC) layers provided with the respective products. The QA filtered datasets were reprojected from sinusoidal to geographic projection and converted to GeoTIFF format.

2.7.3 LST patterns across urban and rural zones (2003 to 2017)

To analyse inter-annual and seasonal patterns over time and space, the monthly LST data were converted into annual and climatic means over selected period using the weighted average technique. The year was further divided into summer, autumn, winter and spring. In the analysis, the months of January, April, July and October were chosen to represent summer, autumn, winter and spring seasons respectively in the region. The season of highest and lowest variability were selected to further plot histograms at diurnal scale for both urban and rural pixels. The programming interface R was used to plot histograms. Statistical tests such as F-test and t-tests were run on data to analyse the significance of distribution and the relative/absolute difference between urban and rural pixels' median.

2.7.4 Spatial and temporal patterns in UHI from 2003 to 2017

For understanding the spatial extent of UHI and its variation in space, we followed the following method to map UHI (Sidiqui, Huete & Devadas 2016; Streutker 2002). To map the spatial extent of UHI, we first masked out urban zones from LST image of the study area, leaving only rural pixels in the image. Secondly, the rural pixels were used to create a new surface using least square fit model (equation 1). Thirdly, the original LST images were subtracted from the modelled rural surface to calculate UHI (equation 2). LST in the rural regions were used to model a rural surface using least square fit method which was then used as reference to derive the resulting UHI footprint on the ground.The process was applied to all images of LST from 2003 to 2017. Finally, climatic average UHI were generated over selected fifteen years of the period.

$$\mathrm{LST}(x,y)_{\mathrm{rural}} = \mathrm{LST}_0 + a_1x + a_2y \qquad \text{Equation (1)}$$

$$\mathrm{UHI}(x,y) = \mathrm{LST}(x,y)_{\mathrm{original}} - \mathrm{LST}(x,y)_{\mathrm{rural}} \qquad \text{Equation (2)}$$

In equation (2) and equation (3), (x,y) represents the coordinate of single pixel, $\mathrm{LST}(x,y)_{\mathrm{original}}$, $\mathrm{LST}(x,y)_{\mathrm{rural}}$ and $\mathrm{UHI}(x,y)$ represent original LST measurement, planar fitted rural LST measurement and isolated UHI intensity at x, y pixel position, respectively. LST_0, a_1 and a_2 represent coefficients describing the spatial gradient of the rural temperature. The analysis gives us pixel based output, which was utilised to visualise the spatial variance in UHI over last fifteen years.

2.7.5 UHI Inside the city

To analyse the UHI means over various suburbs, Local Governing Area (LGA) boundary data from ABS (last updated on 2016) for both selected cities were utilised. We chose a few residential/commercial suburbs (LGAs) and parks within both cities and calculated the average UHI (diurnal and seasonal). A table was generated of UHI values to analyse the UHI means over parks inside the cities and complete residential/commercial parts of LGAs.

2.7.6 Workflow

Fig.2.2 shows the methodology followed for this chapter.

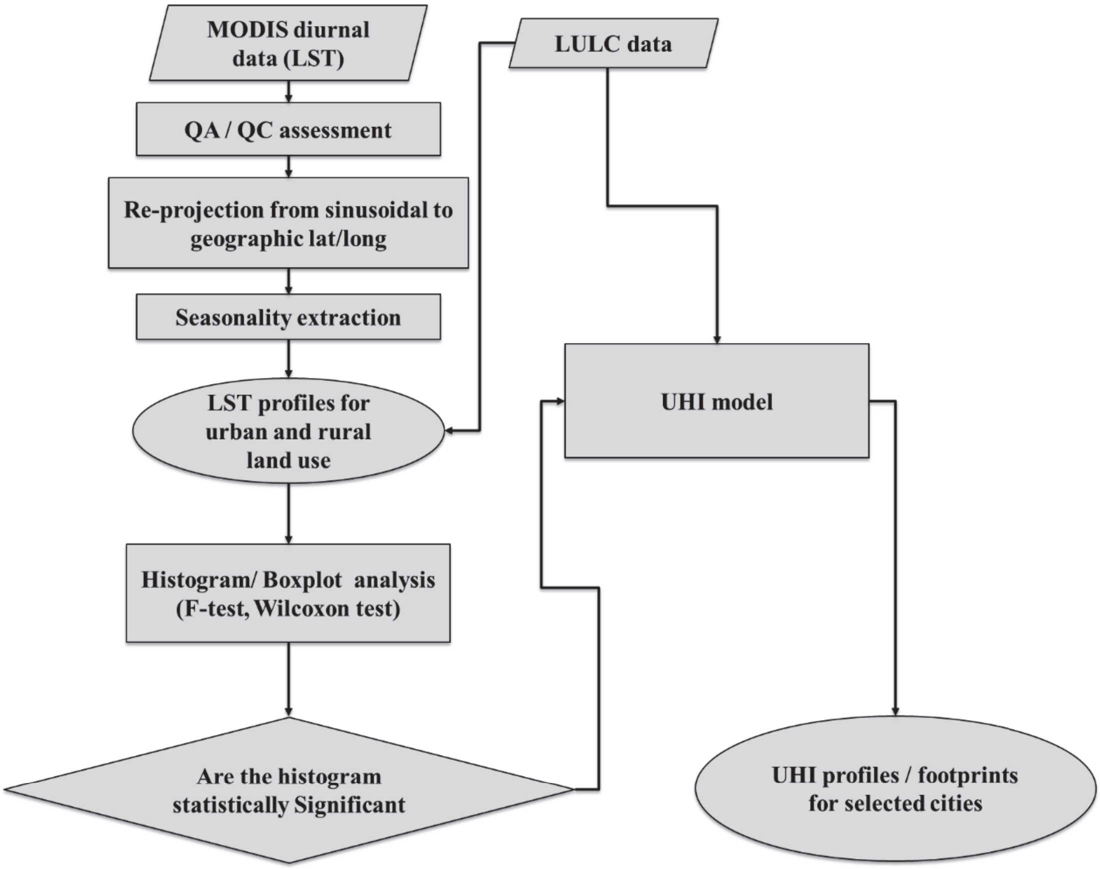

Figure.2.2. Workflow followed to implement the set objectives for chapter 2.

2.8 Results

2.8.1 LST spatial patterns over Sydney and Melbourne

Spatial variability of diurnal patterns in LST for both Sydney and Melbourne in last fifteen years (2003 - 2017) is shown in Fig.2.3 to Fig.2.4 respectively. Fig.2.3 illustrates that the city of Sydney shows urban to rural contrast in LST, which is more explicitly visible in months of summer season particularly at daytime with traces less observable during nighttime. The three months, December, January and February represent summer season in south-east Australia according to Bureau of Meteorology (BOM). In these figures, it can be comprehended that Sydney illustrates the most significant relative variations in LST for the month of summer.

In contrast, Melbourne indicates urban to rural variations in daytime LST specifically in the spring (Fig.2.4), where months of September, October and November represent spring season in the Australian region. This means the urban region indicates relatively higher temperatures than its surrounding rural regions throughout the year, however, the gradient of temperature becomes stronger during Spring season. On the other hand, the nighttime LST contrast in Melbourne is evident throughout the year with more explicitly visible traces in the summer months (Fig.2.3, Fig.2.4). Thus, both cities indicate nighttime variations across urban to the rural zone having peaks in summer and spring season for Sydney and Melbourne respectively. These observations suggest that the local thermal modifications are evident in the urban regions of both cities throughout the day with stronger contrast at daytime and weaker contrast at nighttime. The city of Melbourne, however, points towards more significant variations in nighttime LST in comparison to Sydney throughout the year. Furthermore, it is interesting to see that Melbourne does not observe specific daytime LST difference between urban and rural areas like Sydney where we see explicit daytime heat island. However, the 'spring' season in Melbourne indicates a difference in LST along southeast Melbourne, pointing towards a possible daytime UHI particularly in 'spring' season.

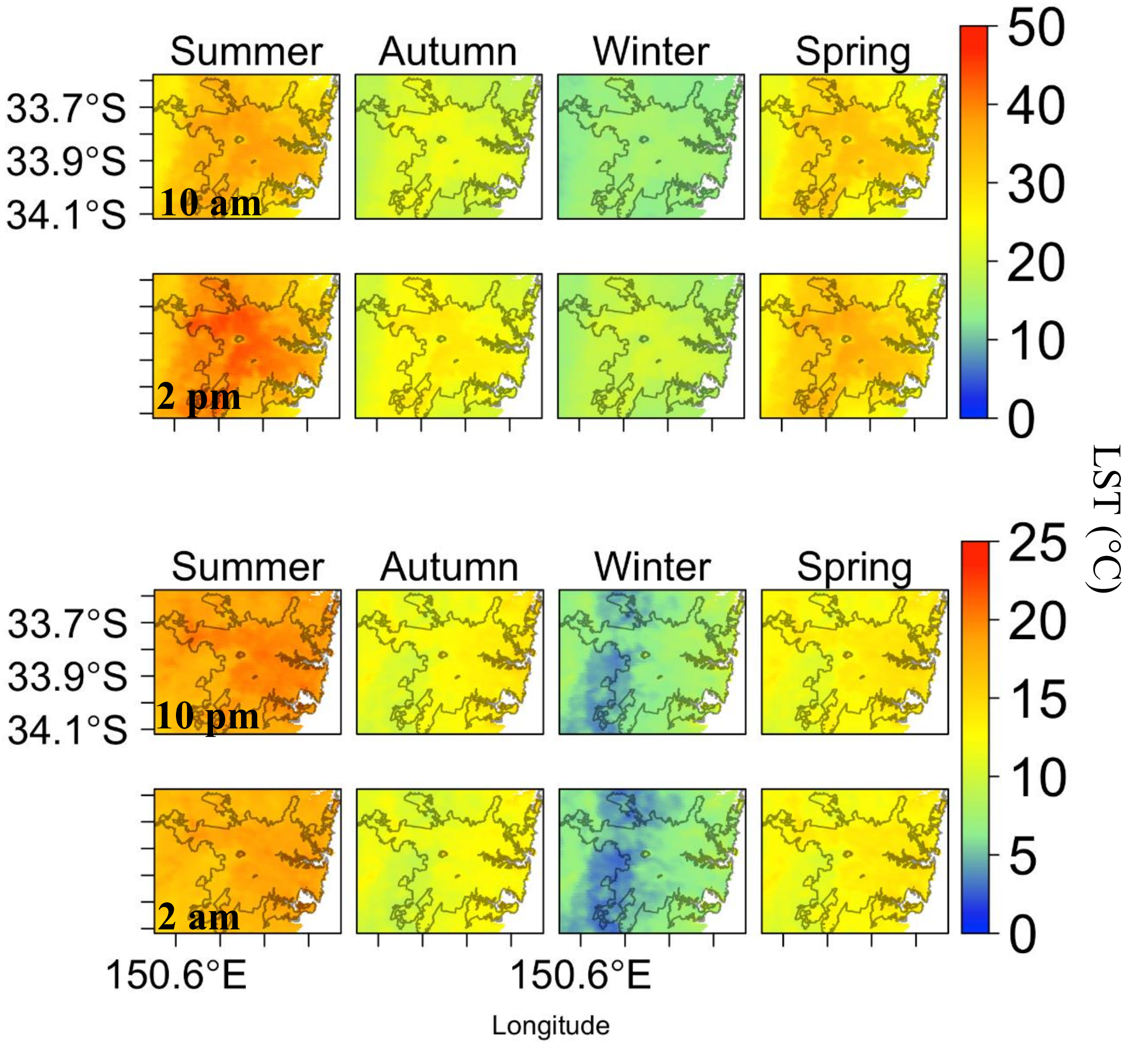

Figure 2.3. LST (daytime and nighttime) averaged over Sydney for fifteen years (2003 – 2017) through January, April, July and October representing summer, autumn, winter and spring seasons respectively. The black colour polygon represents the urban boundary as per ABS (2016) data.

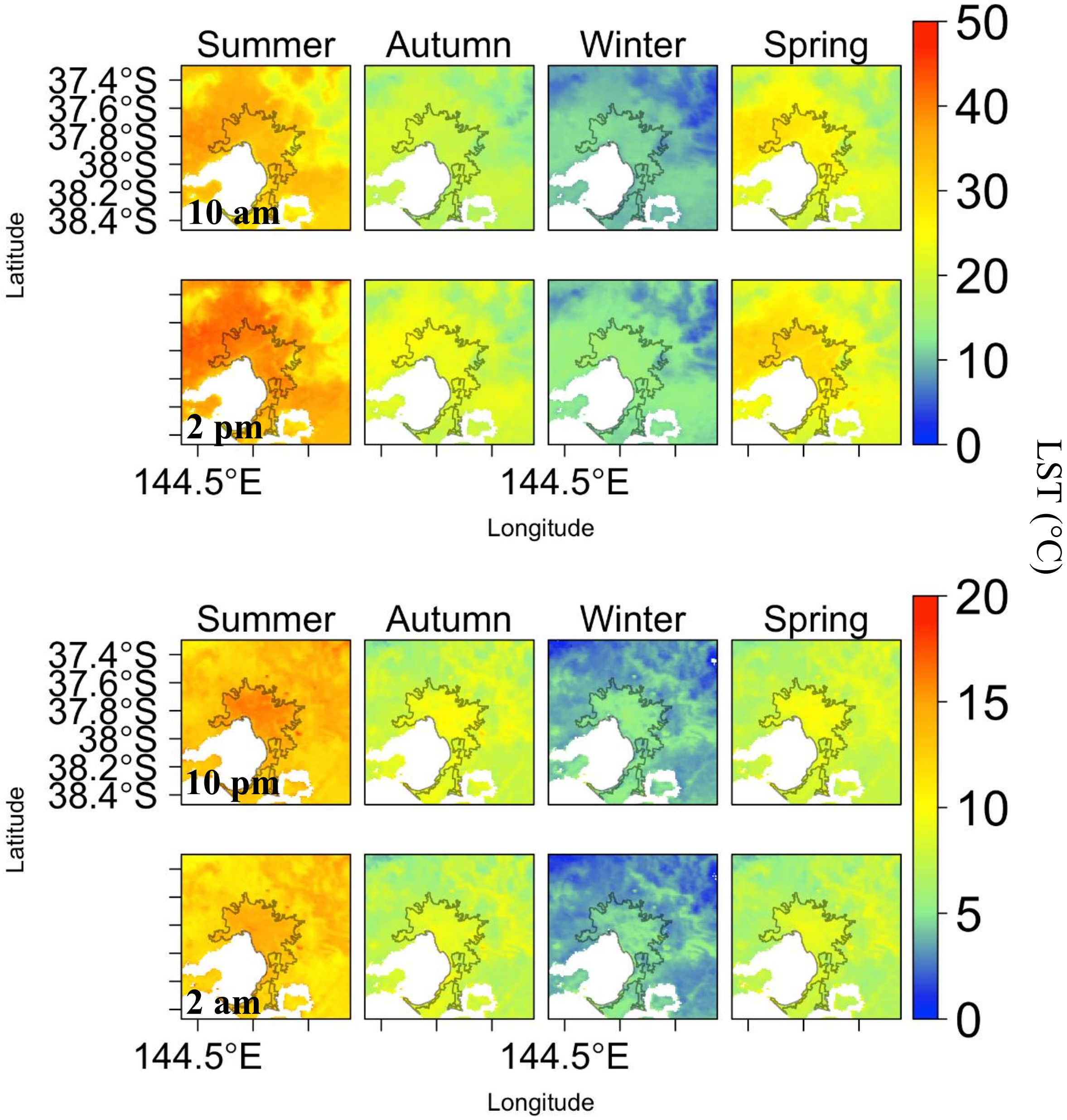

Figure 2.4. LST (daytime and nighttime) averaged over Melbourne for fifteen years (2003 – 2017) through January, April, July and October representing summer, autumn, winter and spring seasons respectively. The black colour polygon represents the urban boundary as per ABS (2016) data.

The spatial variations in LST over urban to rural are also noticeable in winter. However, the intensity is weaker as compared to one in summer, particularly at 2 pm. These observations indicate the local thermal modifications are evident in the urban regions of Sydney both at daytime and nighttime; however, the daytime variations in LST are significantly more significant than the nighttime particularly in summer and spring for Sydney. A further substantial indication of higher urban to rural LST contrast during the daytime, which is stronger in summer and weaker in 'winter'.

2.8.2 Urban and Rural LST Histogram

To better classify the urban to rural contrast we generated histograms and analysed their statistical significance, Fig.2.5 and Fig.2.6 shows histogram distribution of urban and rural pixels in summer and winter season at 10 am, 2 pm, 10 pm and 2 am for Sydney. Results indicate that the LST datasets at 10 am and 2 pm are right-skewed histograms in summer. The nighttime histograms at 10 pm and 2 am illustrates bell-shaped histograms for summer months. On the other hand, the winter season illustrates right-skewed and left-skewed histograms for urban and rural pixels with the minimal relative and absolute differences in medians.

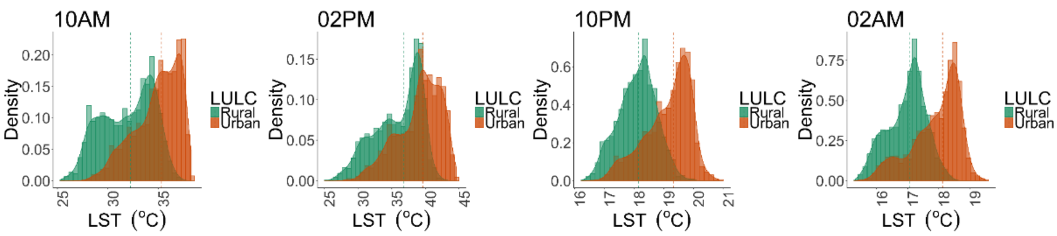

Figure 2.5. Shows LST pixels distribution in urban and rural regions over Sydney in summer season.

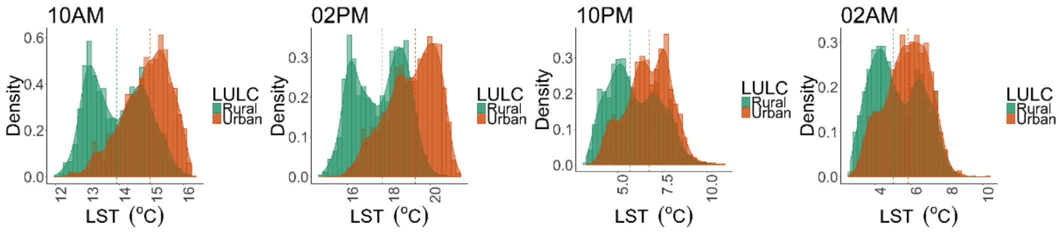

Figure 2.6. Shows LST pixels distribution in urban and rural regions over Sydney in winter season.

Fig.2.7 and Fig.2.8 shows histogram distribution for Melbourne in summer and winter season. We have already seen in Fig.2.4, that Melbourne did not indicate daytime variations as explicitly as were evident in Sydney, particularly in the summer season. However, the median values for Melbourne still pointed out a significant daytime UHI, which is smaller in when compared with Sydney's daytime UHI in the summer season. The nighttime 10 pm and 2 am LST shows right-skewed and left skewed histograms for rural and urban respectively in both seasons summer and winter.

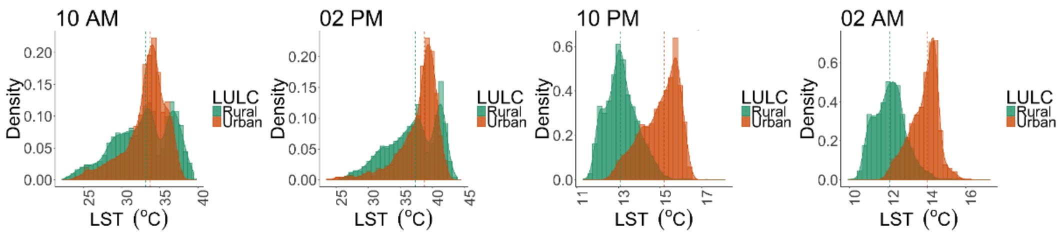

Figure 2.7. Shows LST pixels distribution in urban and rural regions over Melbourne in summer season.

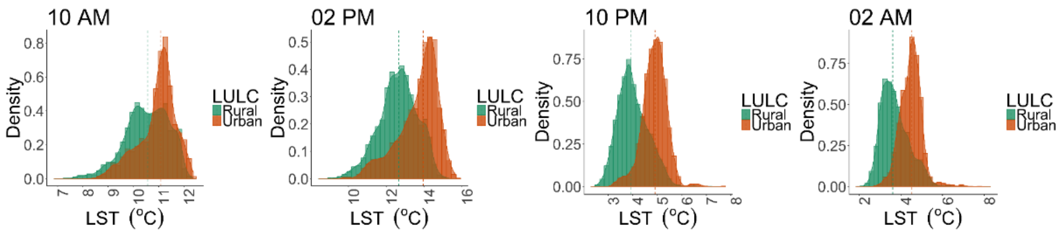

Figure 2.8. Shows LST pixels distribution in urban and rural regions over Melbourne in summer season.

Table.2.1 shows statistical tests that are calculated to verify the significance of histograms, such as F-test is seen to be significant indicating the data had similar variance. In addition to this, significant p-value for Wilcoxon test shows that the rural pixels median values are significantly different from that of urban pixels median values in the histogram. The table further illustrates the statistically absolute and relative differences of urban to rural pixel distribution. The table further indicates that the absolute difference of medians is highest particularly at daytime (2 pm) and in the summer season for both cities.

Furthermore, the relative difference indicates that both cities show 8% to 11% higher daytime LST values in urban zones relative to rural zone values. The winter season indicates smaller intensity for the absolute and relative difference over Sydney urban and rural pixels. However, Melbourne illustrates higher relative differences particularly at nighttime indicating stronger nighttime UHI for the city in the summer season. The analysis on histograms indicates that the nighttime difference in MODIS LST is most substantial in the summer season for both the cities. The daytime variations in MODIS LST are dependent on seasons; Sydney indicates strong LST gradient between rural and urban zones in summer whereas Melbourne shows the LST gradient to be most active in the spring season. These results only provide LST analysis and indicate strong evidence of daytime and nighttime UHI for both cities. We further analysed the data to quantify UHI parameters in the next section.

Table 2.1. Shows statistical significance of histograms

Sydney							
SUMMER							
	F-test	Welch Two Sample t-test	Wilcoxon test	Median of rural pixels ℃ (X1)	Median of urban pixels ℃ (X2)	Absolute difference (X2-X1) ℃	Relative difference (X2/X1)
10 am	P-value <0.05	P-value <0.05	P-value <0.05	31.9	34.9	3	1.09
2 pm	P-value <0.05	P-value <0.05	P-value <0.05	35.9	39.1	3.2	1.08
10 pm	P-value <0.05	P-value <0.05	P-value <0.05	18.1	19.1	0.9	1.06
2 am	P-value <0.05	P-value <0.05	P-value <0.05	16.9	17.9	1	1.06
WINTER							
10 am	P-value <0.05	P-value <0.05	P-value <0.05	13.9	14.9	1	1.07
2 pm	P-value <0.05	P-value <0.05	P-value <0.05	17.6	19.3	1.7	1.09
10 pm	P-value <0.05	P-value <0.05	P-value <0.05	5.7	6.7	1	1.17
2 am	P-value <0.05	P-value <0.05	P-value <0.05	5.0	5.8	0.8	1.16
Melbourne							
SUMMER							
	F-test	Welch Two Sample t-test	Wilcoxon test	Median of rural pixels ℃	Median of urban pixels ℃	Absolute difference (X2-X1) ℃	Relative difference (X2/X1)
10 am	P-value <0.05	P-value <0.05	P-value <0.05	23.4	25.6	2.2	1.09
2 pm	P-value <0.05	P-value <0.05	P-value <0.05	25.3	28.4	3.1	1.1
10 pm	P-value <0.05	P-value <0.05	P-value <0.05	7.6	9.2	1.6	1.2
2 am	P-value <0.05	P-value <0.05	P-value <0.05	6.9	8.4	1.5	1.2
WINTER							
10 am	P-value <0.05	P-value <0.05	P-value <0.05	10.6	11.0	0.4	1
2 pm	P-value <0.05	P-value <0.05	P-value <0.05	12.6	14.0	1.4	1.1
10 pm	P-value <0.05	P-value <0.05	P-value <0.05	3.9	4.9	1	1.2
2 am	P-value <0.05	P-value <0.05	P-value <0.05	3.6	4.5	0.9	1.5

2.8.3 Quantifying UHI

Fig.2.9 and Fig.2.10 shows spatial variations in UHI across Sydney and Melbourne respectively. Relatively stronger intensity in the summer season with less visible traces in the winter season are observed in both the cities in the nighttime UHI variations. Moreover, the summer nighttime UHI intensity reaches as high as 3°C in Melbourne and as high as 1°C in Sydney.

The daytime UHI variations are missing in Melbourne and do not indicate clear UHI pattern across the city whereas Sydney indicates a clear daytime UHI footprint for the city throughout the year with intensities reaching as high as 10°C particularly in the summer season. In contrast, the winter season marks the lowest daytime UHI for Sydney. However, The spring season marks high daytime UHI for Melbourne which is also true for Sydney which indicates strong daytime UHI with intensities as high as 8°C for few parts of the city. The winter season marks the lowest daytime UHI for Sydney. However, Melbourne shows daytime UHI in the spring season. The spring season marks high daytime UHI for Melbourne which is also true for Sydney which indicates strong daytime UHI with intensities as high as 6 - 7°C for few parts of the city.

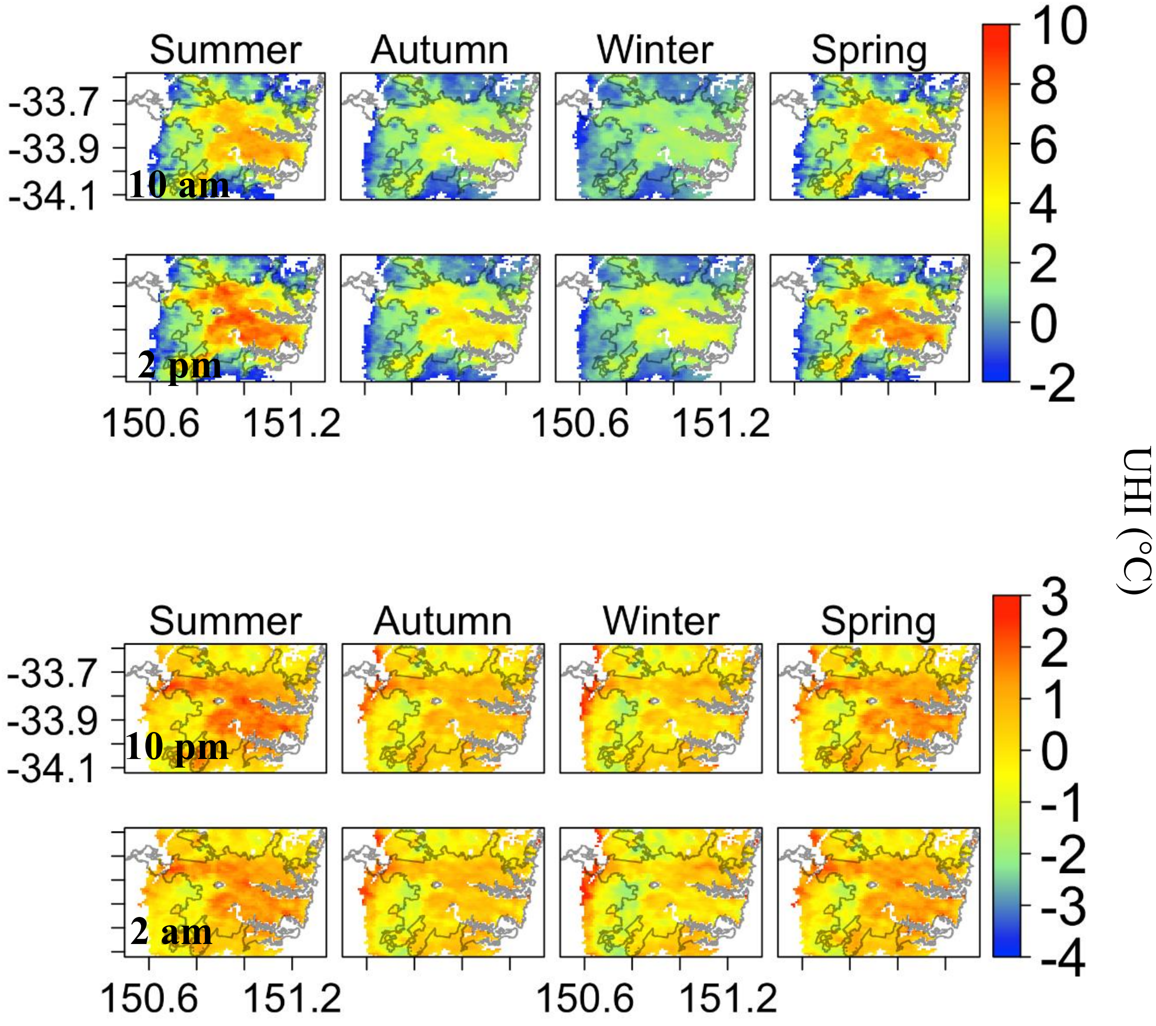

Figure 2.9. UHI (diurnal) averaged over fifteen years (2003 – 2017) through January, April, July and October representing summer, autumn, winter and spring seasons respectively over Sydney

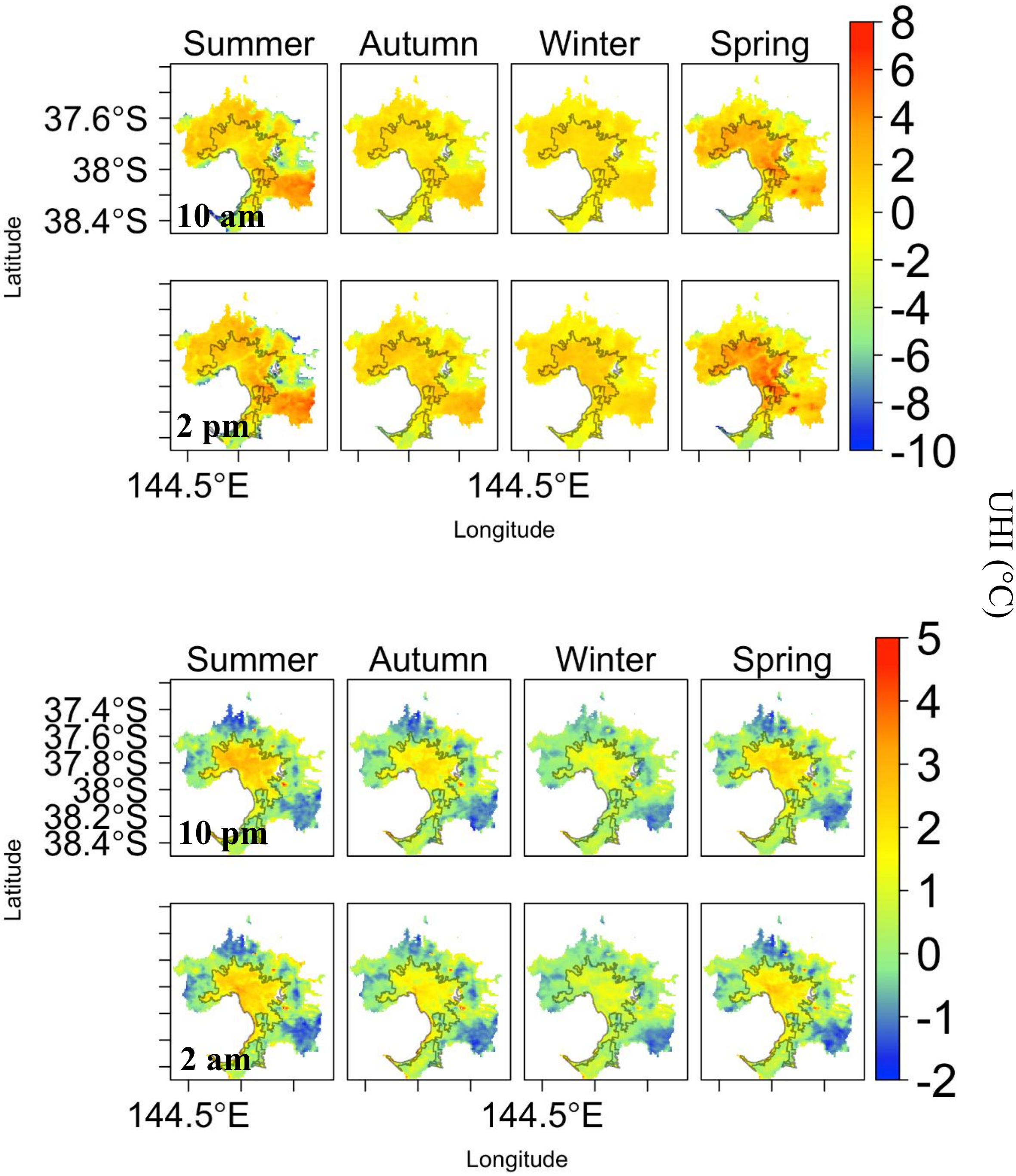

Figure 2.10. UHI (diurnal) averaged over fifteen years (2003 – 2017) through January, April, July and October representing summer, autumn, winter and spring seasons respectively over Melbourne.

2.8.4 *UHI inside city*

Table 2.2 shows the UHI values in few selected suburbs (local governing areas LGAs) inside the city with and without parks.

Table 2.2. UHI values inside city at different suburbs and parks

SYDNEY								
LGA	Summer		Autumn		Winter		Spring	
	2 pm ℃	10 pm ℃	2 pm ℃	10 pm ℃	2 pm ℃	10 pm ℃	2 pm ℃	10 pm ℃
Bankstown	7.6	1.6	4.6	0.6	3.4	0	7.1	0.8
Blacktown	6.7	1.3	3.9	0.6	2.9	0.2	6.1	0.9
Parramatta	6.8	2.6	4.1	0.8	3.4	0.6	6.3	1.2
Sydney Commercial	6.1	1.2	4.5	0.6	3.3	0.1	6.1	1.1
Parramatta Park	5.4	1.2	3.8	1.03	2.9	0.5	5.0	1.2
Centennial Park	5.0	0.7	3.4	0.7	2.5	0.2	4.3	0.8
Moore Park	4.8	1.7	3.0	1.1	2.4	0.9	5.0	1.7
Royal Botanical Garden	2.3	1.6	2.3	2.3	2.1	2.2	2.2	2.6
MELBOURNE								
LGA	Summer		Autumn		Winter		Spring	
	2 pm ℃	10 pm ℃	2 pm ℃	10 pm ℃	2 pm ℃	10 pm ℃	2 pm ℃	10 pm ℃
Greater Dandenong	3.3	2.2	1.9	1.5	1.6	1.1	5.2	1.8
Monash	2.2	2.2	1.1	1.8	1.4	1.2	4.2	2.0
Geln Eira	2.2	2.2	1.0	1.5	1.8	1.1	4.0	1.8
Melbourne CBD	-0.6	2.9	0.1	1.8	1.21	0.9	2.1	1.8
Port Phillip	-1.5	2.2	-0.4	1.5	0.8	0.5	1.6	1.6
Yarra	0	2.7	0.2	1.8	1.3	1.0	2.6	2.3
Stonnington	0.6	2.7	0.7	2.3	1.7	1.4	3.3	2.5
Alexendra Gardens	-0.6	2.6	0.1	1.9	1.2	0.9	2.3	2.4
Fawkner Park	-1.3	2.4	-0.3	2.2	1.0	0.8	1.7	2.4
Yarra Bend Park	-0.1	2.8	0.3	2.0	1.3	1.6	2.4	2.3

It can be seen that the parks are at lowest UHI values relative to residential/commercial suburbs, particularly at daytime. For example, the Sydney commercial LGA shows a mean UHI of 6.1℃ at daytime, and Parramatta LGA also indicates a mean UHI of 6.8℃ while the parks, such as Parramatta Park and Centinel Park indicates relatively 1℃ lower UHI values than in nearby residential/commercial suburbs (table.2.2). Similar is evident in Melbourne. However, the nighttime UHI seems to be independent of such effect.

2.8.5 UHI and its rural reference

The results based on the classic rural and urban pixel distributions, indcated that daytime UHI is present in both cities throughout the year with peak values occurring in summer and spring for Sydney and Melbourne respectively. Whereas, the winter season marks lowest daytime UHI values in both cities. To better understand the mechanism behind the variations in UHI intensity throughout year or a day, these seasonal and diurnal characteristics of UHI need to be further investigated. Since we know UHI is loosely speaking a differnce of temperature between urban and rural class. However, in our case, the rural class in both cities dominated by two different LULC classes such as forest and pasture. To better understand the underlying mechanism we processed the LST histograms for each dominant LULC class in rural zone in relation with urban class. These both classes (forest and pasture) have their particular characteristics that may drive the intensity of UHI in cities at diurnal and seasonal scale. Fig.2.11 and Fig.2.12 shows spatial variations in LST pixels across Sydney in urban and it's rural LULC classes which are pasture and forest.

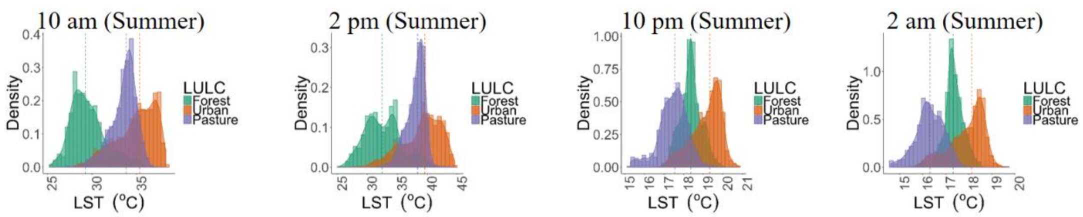

Figure 2.11. Shows LST pixel distribution in urban, forest and pasture regions over Sydney in summer season.

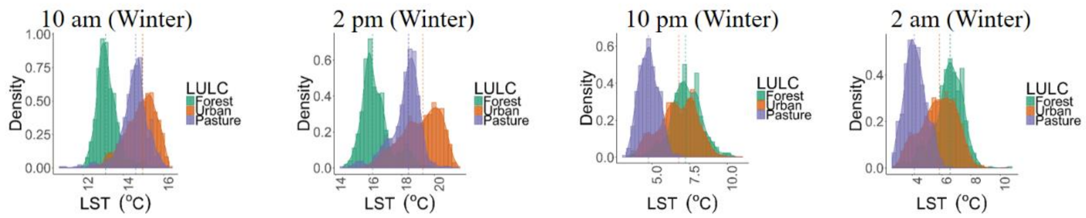

Figure 2.12. Shows LST pixels distribution in urban, forest and pasture regions over Sydney in winter season.

Fig.2.11 and Fig.2.12 indicates the LST distribution over rural zones adjacent to urban areas which are mainly dominated by forest and pastures. It can be seen here that these are the zones which are at elevation below 200 m for Sydney and below 300 m for Melbourne but outside the urban boundary. The figures further illustrate that forest pixels are coolest particularly at daytime and reverse is true at nighttime. This can be well explained by the fact that forest are cooler at daytime in relation to shallow rooted vegetation (grasses, pastures) due to evapotranspiration and warmer at nighttime in relation to open lands or grassland, however the nighttim warmth is lower in intensity relative to daytime cooling (Li, and Zhao, 2015). Hence, these results also show that urban temperatures are relatively highest in summer season pointing towards the summer UHI in city.

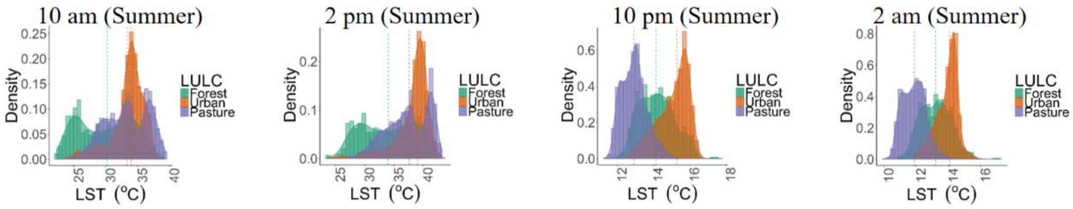

Figure 2.13. Shows LST pixels distribution in urban, forest and pasture regions over Melbourne in summer season.

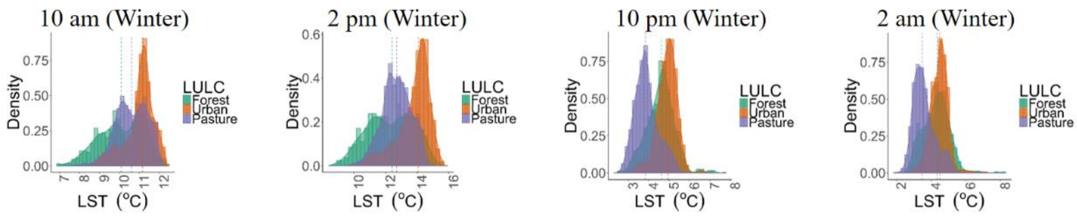

Figure 2.14. Shows LST pixels distribution in urban, forest and pasture regions over Melbourne in winter season.

Similar patterns are evident for Melbourne (Fig.2.13 and Fig.2.14). These figures indicates histogram distribution over urban and neighbouring forest and pasture class over Melbourne. Summer shows both pasture and urban pixels at higher temperature values particularly at daytime and nighttime. In summer the differnce between urban and pasture pixels increases due to the fact that open areas tend to be cooler at nighttime.

2.9 Discussion

This chapter presents a comprehensive study on characterising the UHI for the city of Sydney and Melbourne in Australia in space and time. In literature, not many studies have been done for Australian cities mainly using remote sensing datasets and products in the estimation of UHI. This study provides insight on the efficiency of remote sensing data sets that offer better spatial and temporal coverage when compared to data acquired from ground stations that is traditional way in which UHI measured, including station pairs or the use of transects. Most of the methods used meteorological observatory data to analyse air temperature gradients in urban and rural regions monitoring UHI (Bornstein and Lin, 2000; Gedzelman and Austin, 2003; Jin and Shepherd, 2005; Zhou and Chen, 2011). However, the data collected alone at meteorological stations in cities may not be suitable for representing urban weather conditions, as most stations are established for the purpose of synoptic forecasting at places where the parameters of the weather are not disturbed by urban structures or human activities (Lee et al., 1993). Whereas remote sensing provides better options and feasible ways of data acquisition and monitoring.

2.9.1 Diurnal characteristics of UHI

The analysis on day vs night revealed a clear UHI throughout the day for both cities, with daytime being highly seasonal and nighttime less dependent on seasonal variations. The daytime UHI reached as high as 10°C for Sydney and 6 - 7°C for Melbourne particularly at 2 p.m. In addition, it, should be kept in consideration that the reference surface for UHI calculation was all LULC classes as combined one rural zone which were used to generate a rural surface and then a UHI surface." The fact that the built or impervious surfaces have negligible latent heat flux as compared to surfaces covered by healthy vegetation (grass, shrubs, trees), which generates the difference in net radiation for impervious surfaces as compared to previous (vegetated) surfaces, causing the temperature to rise for urban zones, during the daytime. On the other hand, the nighttime UHI reached as high as 2°C - 3°C for both cities particularly at 10 pm in the evening. The nighttime UHI is supported by the fact that urban areas release more long wave radiation back to the atmosphere compared with rural areas.

2.9.2 *Seasonal characteristics of UHI*

The results indicated that the UHI, particularly at daytime, showed explicitly clear seasonality for both cities. It was observed that in Sydney, the daytime UHI reached its maximum in summer days while in Melbourne the daytime UHI was dominant in spring days. On the other hand, nighttime UHI was present in both cities throughout the year with summer being peak season for both cities. Melbourne also showed a positive UHI in spring days. However, the role of rural surfaces as references need to be further monitored to better understand the seasonality in UHI and its driving parameters.

2.9.3 *UHI and Choice of Rural Class as Reference*

The analysis on LST values for urban, forest and pasture LULC class, indicated that the forested regions were at most cooling temperatures relative to urban and pasture zones particularly at daytime and in summer months. Forests tend to be at lower temperatures in summer due to more evapotranspiration from trees than from grasses or pastures. Moreover, our analysis also shows forests warmer at nighttime, where, we know that during the night, most forests are warmer than open areas, with relatively lower intensity than that of the daytime cooling (Li and Zhao, 2015). These histograms point towards the underlying mechanism behind UHI calculated values at seasonal, annual and daily scale in cities. To better characterise we need to investigate further the trends and attribute these trends to its drivers. Hence, to further investigate UHI and their trends, we divided our rural class into sub-rural classes meaning sub-rural references and analysed the daytime UHI trends concerning each LULC separately in the rural zone, to better understand the UHI behaviour over last two decades in selected cities. The results are given in the next chapter.

2.9.4 Limitations

There remain some limitations that need to be further assessed. In the subject study, we utilised static LULC maps for urban and rural areas (ABS derived LULC data 2006, 2011 and 2016). For better analysis, more dynamic maps would have helped to understand the phenomena of UHI more effectively. Furthermore, the data resolution was 1 Km. Therefore, that also held us back from analysing at higher spatial resolution. However, the data were helpful in mapping and monitoring the UHI at diurnal scale. On the other hand, the method of deriving UHI surface may offer some limitations and uncertainties, since a least squares approach is being used to estimate the best fit surface for a set of data points by minimising the sum of the offsets or residuals of points from the plotted surface. Hence potential improvements can be noted for future research.

2.10 Conclusion

In this chapter, I tried to address the questions regarding the diurnal and seasonal nature of UHI in selected Australian cities. Moreover, the data were analysed over a long period of fifteen years to better map the day vs night characteristics and seasonal amplitudes of UHI. It was concluded from the above study that daytime UHI was highly seasonal and peaked in the summer months for Sydney city and in the spring months for Melbourne. The nighttime UHI was evident throughout the year for both cities with relatively smaller intensity. From the above analysis, it is further concluded that satellite data can provide better spatial and temporal coverages. Due to the efficiency of satellite data, we were able to monitor and map the diurnal characteristics along with seasonal patterns in UHI for both selected cities.

This study provided evidence of an absolute presence of UHI for both cities; the next step is to understand the long-term trends in UHI and what factors are driving this seasonal behaviour of UHIs in our cities.

2.11 References

Azevedo, J.A., Chapman, L. and Muller, C.L., 2016. Quantifying the daytime and night-time urban heat island in Birmingham, UK: A comparison of satellite derived land surface temperature and high resolution air temperature observations. Remote Sensing, 8(2), p.153.

Bonafoni, S., Anniballe, R. & Pichierri, M. 2015, 'Comparison between surface and canopy layer urban heat island using MODIS data', Urban Remote Sensing Event (JURSE), 2015 Joint, IEEE, pp. 1-4.

Bornstein, R. & Lin, Q. 2000, 'Urban heat islands and summertime convective thunderstorms in Atlanta: three case studies', Atmospheric Environment, vol. 34, no. 3, pp. 507-16.

Bounoua, L., Zhang, P., Mostovoy, G., Thome, K., Masek, J., Imhoff, M., Shepherd, M., Quattrochi, D., Santanello, J. & Silva, J. 2015, 'Impact of urbanization on US surface climate', Environmental Research Letters, vol. 10, no. 8, p. 084010.

Deilami, K. and Kamruzzaman, M., 2017. Modelling the urban heat island effect of smart growth policy scenarios in Brisbane. Land Use Policy, 64, pp.38-55.

Gedzelman, S., Austin, S., Cermak, R., Stefano, N., Partridge, S., Quesenberry, S. & Robinson, D. 2003, 'Mesoscale aspects of the urban heat island around New York City', Theoretical and Applied Climatology, vol. 75, no. 1-2, pp. 29-42.

Imhoff, M.L., Zhang, P., Wolfe, R.E. & Bounoua, L. 2010, 'Remote sensing of the urban heat island effect across biomes in the continental USA', Remote Sensing of Environment, vol. 114, no. 3, pp. 504-13.

Jin, M. & Shepherd, J.M. 2005, 'Inclusion of urban landscape in a climate model: How can satellite data help?', Bulletin of the American Meteorological Society, vol. 86, no. 5, pp. 681-9.

Kolokotroni, M. and Giridharan, R., 2008. Urban heat island intensity in London: An investigation of the impact of physical characteristics on changes in outdoor air temperature during summer. Solar energy, 82(11), pp.986-998.

Li, Y., Zhao, M., Motesharrei, S., Mu, Q., Kalnay, E. and Li, S., 2015. Local cooling and warming effects of forests based on satellite observations. Nature communications, 6, p.6603.

Liu, W., Ji, C., Zhong, J., Jiang, X. & Zheng, Z. 2007, 'Temporal characteristics of the Beijing urban heat island', Theoretical and Applied Climatology, vol. 87, no. 1-4, pp. 213-21.

Lee, H.Y., 1993. An application of NOAA AVHRR thermal data to the study of urban heat islands. Atmospheric Environment. Part B. Urban Atmosphere, 27(1), pp.1-13.

Morris, C. 2011, 'Urban heat islands and climate change—Melbourne, Australia'.

Razzaghmanesh, M., Beecham, S. and Salemi, T., 2016. The role of green roofs in mitigating Urban Heat Island effects in the metropolitan area of Adelaide, South Australia. Urban Forestry & Urban Greening, 15, pp.89-102.

Sharifi, E. & Lehmann, S. 2014, 'Comparative Analysis of Surface Urban Heat Island Effect in Central Sydney', Journal of Sustainable Development, vol. 7, no. 3, p. p23.

Sidiqui, P., Huete, A. and Devadas, R., 2016, July. Spatio-temporal mapping and monitoring of Urban Heat Island patterns over Sydney, Australia using MODIS and Landsat-8. In Earth Observation and Remote Sensing Applications (EORSA), 2016 4th International Workshop on (pp. 217-221). IEEE.

Streutker, D.R. 2003, 'Satellite-measured growth of the urban heat island of Houston, Texas', Remote Sensing of Environment, vol. 85, no. 3, pp. 282-9.

Taha, H., 1997. Urban climates and heat islands: albedo, evapotranspiration, and anthropogenic heat. Energy and buildings, 25(2), pp.99-103.

Torok, S.J., Morris, C.J., Skinner, C. & Plummer, N. 2001, 'Urban heat island features of southeast Australian towns', Australian Meteorological Magazine, vol. 50, no. 1, pp. 1-13.

Voogt, J.A. & Oke, T.R. 2003, 'Thermal remote sensing of urban climates', Remote sensing of environment, vol. 86, no. 3, pp. 370-84.

Weng, Q., 2011. Remote sensing of urban biophysical environments. In Advances in Environmental Remote Sensing (pp. 525-546). CRC Press.

Weng, Q., 2014. Global urban monitoring and assessment through earth observation. Crc Press.

Zhao, X., Shen, S., Yang, S., Xie, X. & Chen, T. 2010, 'Analyzing the Seasonal Variations of Urban Heat Island in Nanjing Using Remote Sensing Data', Multimedia Technology (ICMT), 2010 International Conference on, IEEE, pp. 1-4.

Zhou, J., Chen, Y., Wang, J. & Zhan, W. 2011, 'Maximum nighttime urban heat island (UHI) intensity simulation by integrating remotely sensed data and meteorological observations', Selected Topics in Applied Earth Observations and Remote Sensing, IEEE Journal of, vol. 4, no. 1, pp. 138-46.

Zhou, Y. & Shepherd, J.M. 2010, 'Atlanta's urban heat island under extreme heat conditions and potential mitigation strategies', Natural Hazards, vol. 52, no. 3, pp. 639-68.

Chapter 3: UHI Time Series Trends and their Drivers.

Abstract

Urban heat island (UHI) is loosely defined as urban temperature variance minus rural temperature. The behaviour of the UHI over the year does not remain constant nor does over the day; instead, it demonstrates certain seasonal and diurnal UHI variations. Past studies looked upon UHI drivers, such as wind direction, urban impervious surface percentage and population density. However, very few looked upon the fact that the heterogeneity and nature of the land use land cover (LULC) in the adjacent rural areas may also have specific implications on the measured UHI variance in space and time.

In this study, we are investigating the long-term trends in diurnal UHI variations and attributing these trends to their drivers in the selected Australian cities (Sydney and Melbourne). The aims of this study are to investigate (1) how the reference LULC 'rural' class influence seasonal and long term UHI patterns and (2) attribute the drivers of these influences. This chapter provides a long-term analysis (2003 - 2017) on UHI inter-annual trends and its dependencies on its drivers. To carry out the subject study Satellite-based land surface temperature (LST), enhanced vegetation index (EVI), and albedo data at daily, 08 days, 16 days, monthly and annual scale are acquired and processed accordingly.

The inter-annual trends in UHI revealed a significant increasing trend in daytime UHI (p-value < 0.01) for both selected cities with significant decreasing trend in daytime LST in neighbouring rural zones. The heterogeneity in rural LULC made a big difference on retrieved UHIs, with intensity varying between 6°C - 10°C. Retrieved UHI values were highest when the relatively 'cooler' forests were used as the rural reference. However, the UHI values were weaker when pasture / cropland class were used as the rural class. The results further indicated that the incline in daytime UHI trend was attributed to a significant rising trends in greenness in rural to urban zones. Albedo trends were shown

to decline in urban zones and increase in rural zones, with no strong relationship with UHI. A robust direct relationship was further observed between UHI and greenness.

This analysis presents a study on satellite-based UHI analysis. This chapter also points towards the nature of uncertainty in calculations of intensity and trends in UHI in literature, particularly when an unstable LULC class dominates the rural zone. In addition to this, the study provides an excellent example of integrating satellite data products to be used efficiently in urban studies, which still need to be explored and analysed when monitoring, mapping and characterising LST and UHI patterns over time and space.

3.1 Introduction

The UHI in cities responds in different ways during different times of day and season of the year; depending upon local climate (arid, semi-arid to humid), elevation, size of the city (Zhou and Rybski, 2017), slope and proximity to ocean (Ganbat and Han, 2013; Grimm and Faeth, 2008; Zhou and Chen, 2011; Zhou and Chen, 2013). Many studies in the literature have analysed various UHI drivers and relationships with UHI over time and space such as radiation balance, weather parameters, urban LULC, vegetation / greenness cover in cities, population density, etc. to understand the UHI behaviour. However, less attention is placed upon the fact that UHI can also be a function of heterogeneity in LULC in specific urban to rural transition zones. It means, not only urban areas are dominated by high heterogeneity in LULC, but even the surrounding rural areas may also have different ecosystems. Xu and Zhao (2018) pointed out in his research work that the rural class and the nature of LULC in rural zones could play a vital role in driving the UHI measurements and patterns in various ways. It was further reported that the the definitions of the urban and rural regions may cause the intercomparison study of UHI among various cities challenging (Li and Zhou, 2017; Li and Zhou 2018). Since rural class can be dominated by different biomes, for example vegeatation or pasture lands which may have certain seasonality, desert or forest. These settings will eventually affect the UHI amplitude in adjacent cities in a day and over a year.

In Australia, UHI studies were limited to certain spatial and temporal extents (Sharifi and Lehmann, 2014; Razzaghmanesh and Beecham, 2016) and not much attention were given to adjacent rural LULC biomes and their contribution in UHI variance in space and time. Thus, satellite-based measurements provide unique opportunities to conduct large-scale analysis to better understand and model the UHI patterns and assess their temporal evolution in time and space.

In this study, I analysed the spatial patterns and temporal dynamics of MODIS-derived UHI across two major Australia cities, Sydney and Melbourne from 2003 to 2017. Specifically, I aimed to (1) report the significant shifts in slope and trend over a period of fifteen years for UHI (2) attribute UHI trends to its drivers such as (green) EVI, precipitation and albedo and (3) explore the impact of LULC heterogeneity in rural zones as a reference on UHI dynamics and its indicators/drivers seasonally and inter-annually. This analysis was carried out using remotely sensed data from Aqua / Terra satellite and LULC data (mesh block data) acquired from the Australian Bureau of Statistics.

3.2 Data and Methods

The MODIS based LST datasets acquired and processed in the previous chapter (2003 – 2017) were further utilised in this chapter as well. The LULC data (ABS, 2016) and UHI datasets (Streutker et al., 2003; Bonafoni and Anniballe, 2015; Sidiqui and Huete, 2016) prepared in the previous chapter were also utilised here. In addition to, the following additional data sets were also acquired and processed to analyse the stated objectives.

3.2.1 Satellite based greenness (EVI)

The Enhanced Vegetation Index (EVI) is an 'optimized' vegetation index designed to enhance the vegetation signal with improved sensitivity in high biomass regions and improved vegetation monitoring through a de-coupling of the canopy background signal and a reduction in atmosphere influences (Huete et al. 1997). EVI is widely used as proxy of canopy "greenness", which is defined as an integrative composite property of green leaf area, green foliage cover, structure, and leaf chlorophyll content (Huete et al., 2002; Glenn et al., 2008). For the subject study, the enhanced vegetation index (EVI) products derived from MODIS L3 Global 250m (MCD13Q1) and 1Km (MYD11A3) at 16-day and monthly scale were acquired from NASA LP DAAC website (http://lpdaac.usgs.gov/modis/). The data were processed accordingly to further analyse the long-term inter-annual and seasonal trends spatially and temporally.

3.2.2 Urban Green Deficit (UGD)

The Urban Green Deficit (UGD) is defined as a measure of lack of green spaces in urban areas in relation to neighbouring rural zones in order to relate it with UHI, which is excess of temperature in urban areas in relation to rural land. To calculate the UGD we subtracted rural greenness from urban greenness (Equation 1). The UGD provided measure of urban greening relative to neighbouring rural areas.

$$\mathrm{UGD} = \mathrm{EVI}_{\mathrm{urban}} - \mathrm{EVI}_{\mathrm{rural}} \qquad \text{Equation (1)}$$

Where $\mathrm{EVI}_{\mathrm{urban}}$ and $\mathrm{EVI}_{\mathrm{rural}}$ represents EVI values averaged over urban and rural polygons. To generate footprints of UGD, each image was subtracted from its urban EVI mean.

3.2.3 Albedo

Surface albedo products derived from MODIS L3 Global 500m (MCD43A3) (shortwave broadband) processed on 16-day average were acquired from NASA LP DAAC website (http://lpdaac.usgs.gov /data_access/data_pool). The MCD43A3 is combined albedo product from MODIS sensor onboard Aqua, and Terra Satellites and produced data at DAAC website is from corrected radiances using a BRDF model (Houldcroft and Grey, 2009). For our analysis, we acquired data (shortwave broadband) and processed to monthly composites using a weighted average algorithm. The shortwave broadband is the combination of albedo in visible and near-infrared wavelengths. The data were then processed to analyse the long-term inter-annual and seasonal trends spatially and temporally.

3.2.4 Delta Albedo

Similarly, delta albedo was also calculated, to estimate the change in surface albedo over urban zones with respect to rural zones. Delta Albedo was calculated by subtracting albedo values over urban zone to rural zones. It is defined here as the difference of albedo in urban to its adjacent rural (non-built) zones. Equation 2 further simplifys our definition of delta albedo.

$$\text{Delta Albedo} = \text{Albedo}_{\text{urban}} - \text{Albedo}_{\text{rural}} \qquad \text{Equation (2)}$$

In Equation 2, $\text{Albedo}_{\text{urban}}$ is albedo mesurements averaged over urban area and $\text{Albedo}_{\text{rural}}$ is albedo measurments averaged over rural areas.

3.2.5 Urban Heat Island (UHI)

Since UHI is the difference of temperature between urban and rural zones, we calculated mean of LST values over urban class and subtracted it from the mean value of LST of rural class (equation 3). That however gave us point data which were utilised in graphs to analyse seasonality and inter-annual trends.

$$\mathrm{UHI} = \mathrm{LST}_{\mathrm{urban}} - \mathrm{LST}_{\mathrm{rural}} \qquad \text{Equation (3)}$$

For understanding the spatial extent of UHI and its variation in space, we followed following method to map UHI (Sidiqui, Huete & Devadas 2016; Streutker 2002). The method is explained in chapter 2.

3.2.6 UHI trends and attributing these trends to its drivers

To analyse inter annual and seasonal trends over time and space the LST, UHI and EVI data were converted into monthly, annual and climatic means over selected period using weighted average technique. To understand the seasonality and temporal trends in UHI, we plotted 'monthly' time series of UHI and LST (urban) at diurnal scale (2 PM and 10 PM) by generating raster plots and graphs. Trend analysis were carried out on the datasets to analyse the significant variations in UHI over 2003 - 2017. To analyse the role of indicators/drivers the variations in trend and seasonality were also plotted for LST, EVI and albedo data. In addition to it, to see the breakpoints in the time series I also applied Breaks for Additive Season and Trend (BFAST), which is an R package. BFAST is applied to integrate and decompose the time series into its components and estimate abrupt changes and its magnitude within a times series.

3.2.7 *Rural LULC and its impacts on UHI variance*

To analyse the uncertainties related with rural LULC classes, a zonal average analysis were carried out over all monthly LST images using three general LULC classes over Greater Sydney region; that were, 'urban', 'forest', and 'pasture'. Similarly, the UHIs for each rural sub-class were calculated by only subtracting the 'urban' LST means from 'forest', 'pasture' and 'rural' LST means. This analysis gave us three different UHIs, which means 'UHI_{forest}' , '$UHI_{pasture}$', and '$UHI_{overall}$'; where '$UHI_{pasture}$' can be defined as monthly mean LST over 'urban' minus monthly mean LST over 'pasture' class. The line plots were generated and the Pearson correlation coefficient, p-value and slope were calculated to further estimate the trends in LST and UHI measurement for each LULC class from 2003 - 2017. This complete analysis was carried out in R programming interface.

3.2.8 *Workflow*

Fig.3.1 shows the methodology followed for this chapter.

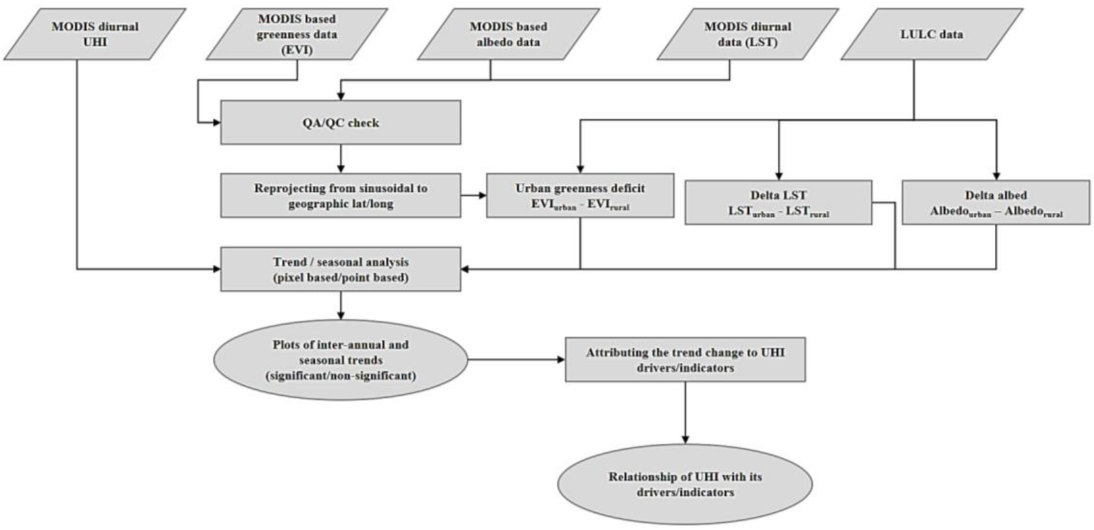

Figure 3.1. Workflow of the methodology followed in chapter 03

3.3 Results

3.3.1 Seasonal and inter-annual variations in UHI

Fig.3.2 and Fig.3.3 illustrate an increasing trend in daytime UHI from 2003 to 2017 for both cities with significant p-values (<0.05). The trends give slope value of 0.008, and 0.007 at daytime for Sydney and Melbourne respectively. In addition to it, Melbourne indicates a sudden lift in 2010, which causes the time series to illustrate a rise in UHI daytime values. On the other hand, nighttime UHI variations do not show any significant rise or drop in trends over the past fifteen years (2003 to 2017), and it is evident for both cities. Seasonal patterns are visible here in time series as well where the daytime and nighttime UHI both peak in summer for Sydney (Fig.3.2). Similarly, Melbourne also indicates summer as peak season for nighttime UHI. However, the daytime UHI in Melbourne reaches its peak values particularly in spring season (Fig.3.3). The seasonal trends are further explored in the next chapter.

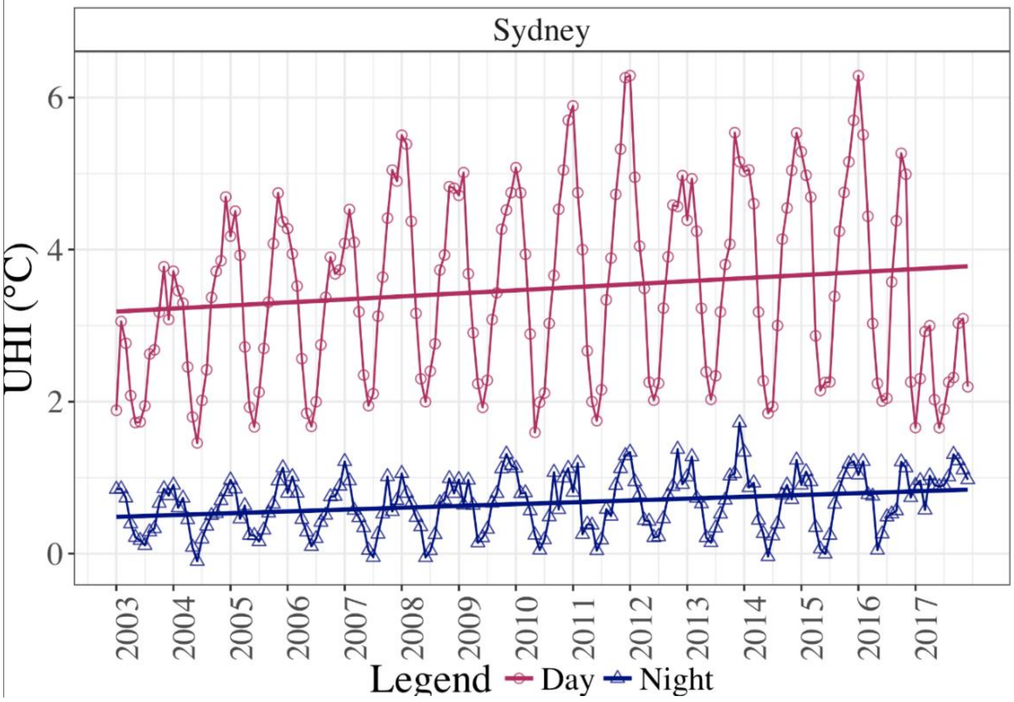

Figure 3.2. UHI trends over fifteen years from 2003 to 2017 Sydney

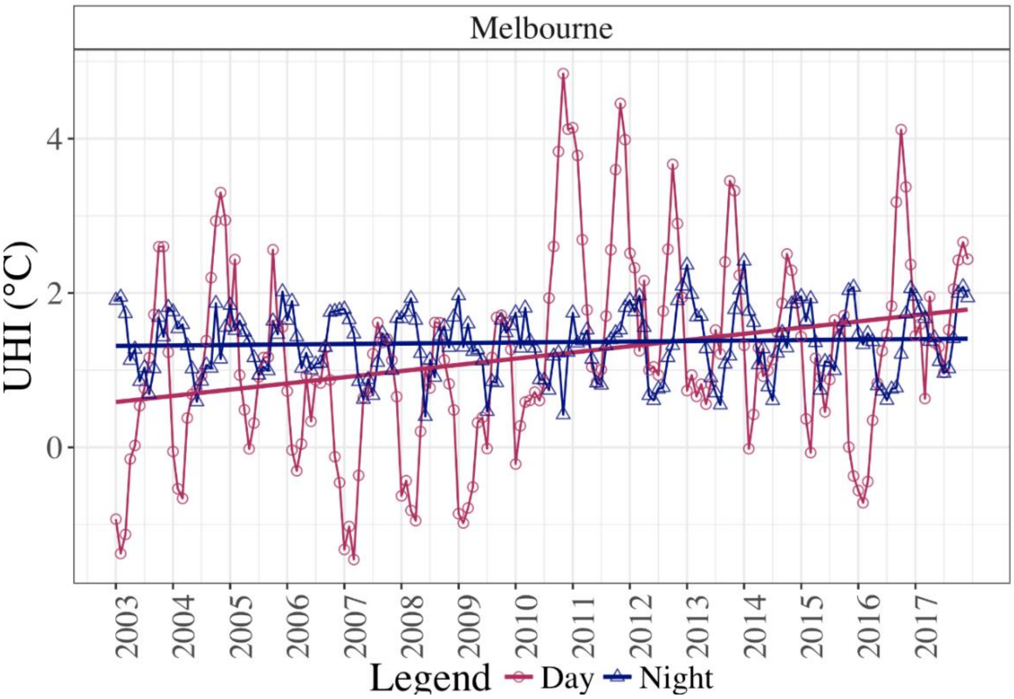

Figure 3.3. UHI trends over fifteen years from 2003 to 2017 over Melbourne

Now let's look at the pixel-based trends in both cities. Fig.3.4 and Fig.3.5 shows maps of pixel based slopes in which the p-value is less than 0.05, over past fifteen years over Sydney and Melbourne respectively. These results illustrate that the urban areas experienced a significant rise in daytime UHI over the past fifteen years (Fig.3.4(a) and Fig.3.5(a)). In contrast, nighttime UHI remains non-significant change for both cities (Fig.3.4(b) and Fig.3.5(b)).

The pixel-based slope maps further indicate that parts of the city experienced relatively faster growth in daytime UHI values. For example, we can see the areas with relatively steeper slope values inside the city highlighted by black colour circle in Fig.3.4(a) and Fig.3.5(a) for both cities. Hence, this may be attributed to increased urban activities in these parts which may have triggered a relatively steeper slope of daytime UHI in the past fifteen years. In contrast, the overall nighttime UHI was not seen to be significant in both cities. However, Sydney shows a few parts of the city particularly in its east with significantly rising nighttime UHI values (Fig.3.4(b)). A red colour circle is drawn on the Fig.3.4(b) to highlight the part of the city with relatively increased UHI in the last fifteen years, particularly at night. Overall the city of Sydney does not show a rise in nighttime UHI values.

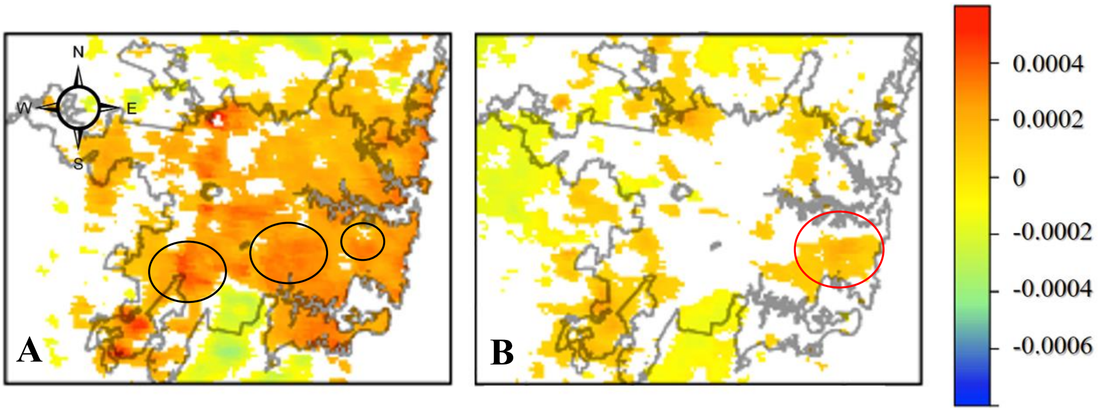

Figure 3.4. Pixel based slope with p-value <0.05 over Sydney (a) Day-time, where the black colour circle indicates areas with relatively steeper slopes; (b) Night-time, where red circle shows the pixels with relatively higher slope values.

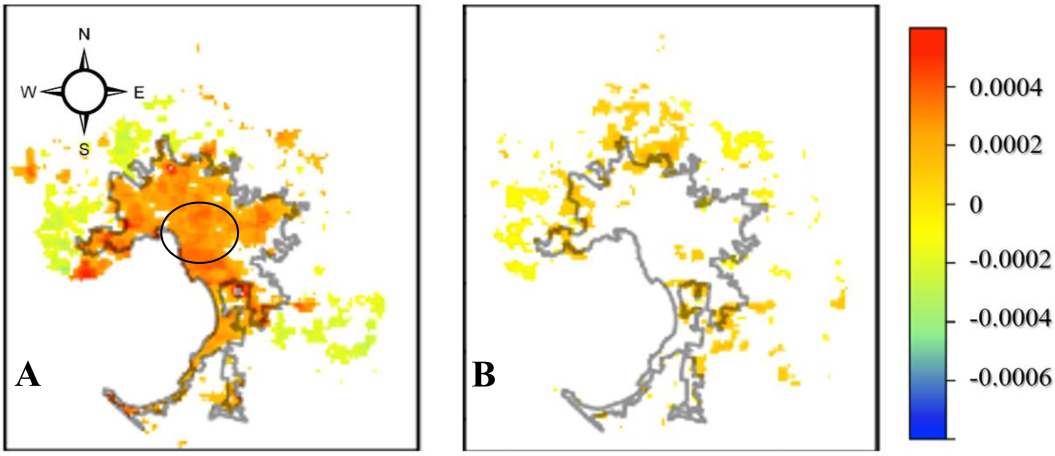

Figure 3.5. Pixel based slope with p-value <0.05 over Melbourne; (a) Day-time, where the black colour circle indicates areas with relatively steeper slopes; (b) Night-time.

These results are of very much interest, as these indicate a significant rise in daytime UHI values at both the pixel level and overall city level in both cities. These results immediately raised many questions like what factors caused the slope to be significant in daytime UHI values and did not alter nighttime UHIs. Since UHI is loosely defined as the difference of temperature in urban to rural zones, it was further required to consider the fact that the rural class is also the combination of various land use land covers (LULC). For example in Sydney, the rural class was dominated by 'forest', 'pasture' and similar was the case for Melbourne. In addition, in the previous chapter, we showed the results where each rural class indicated different seasonal patterns and ultimately affecting the measured UHIs. Hence, to further investigate UHI and the factors that are driving these trends, we divided our rural class into sub-rural classes, meaning sub-rural references, and analysed the daytime UHI trends concerning each LULC separately in the rural zone, to better understand the UHI behaviour over last two decades in selected cities. However, before proceeding to sub-rural classes, we also did a BFAST analysis to determine the breaks and seasonal attributes in time series (BFAST results are in section 3.3.6).

3.3.2 Influence of the non-urban, outside reference used to compute UHI

Fig.3.6 shows UHI variations with reference to sub-rural classes over the past fifteen years (2003 - 2015) for both cities. These results illustrate increasing trends in UHI with significant p-values for 'UHI_{forest}', '$UHI_{pasture}$'and '$UHI_{overall}$'. Furthermore, if we look at the results, the variations in daytime UHI with respect to 'pasture' class are highly unstable, as there are times when daytime UHI goes below zero, giving values in the negative (-2°C), which may depict a heat sink instead of a heat island in the city.

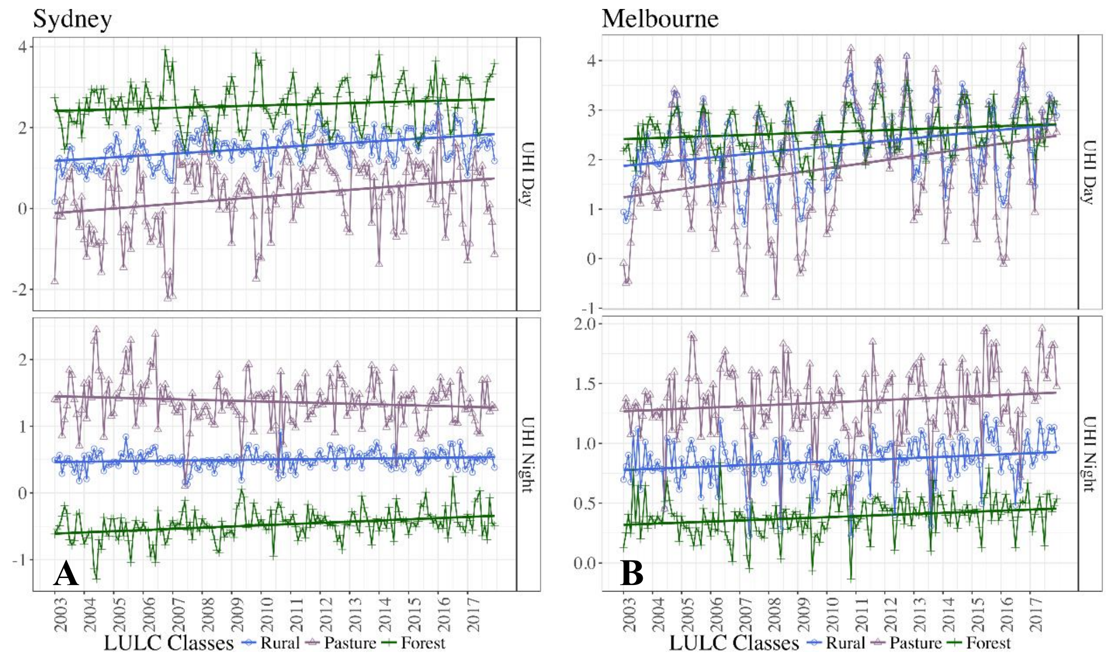

Figure 3.6. Shows time series of UHI spatial with respect to various rural LULC classes, used as the reference, for the past fifteen years (2003 - 2017) (a) over Sydney and (b) over Melbourne.

On the other hand, daytime UHI with reference to 'forest' depicts a consistent positive UHI in the city with relatively fewer variations over the selected period of fifteen years. Moreover, the daytime UHI also seem to be highly dependent on the choice of LULC class in rural zones, as UHI_{forest} and $UHI_{pasture}$ vary from 1°C to 4°C and -2°C to 2°C for Sydney respectively. Similarly, in Melbourne, UHI_{forest} and $UHI_{pasture}$ vary from 2°C to 3°C and -1°C to 4°C respectively. Hence, the choice of the rural class makes significant impacts on measured UHI values in a city, where in our case, 'forest' proves to be a more stable class to chose as a reference when calculating UHI. Whereas, 'pasture' remains unstable due to its seasonality features. The nighttime UHI measurements show relatively fewer variations and smaller intensity with reference to chosen rural LULC classes. In addition to it, these results also indicate that the increasing trends in the daytime and nighttime UHI dependent of LULC class chosen for reference. Thus, the slopes of

UHI may vary for each reference LULC class (Table.3.1). These results explicitly indicated that the rural LULC class is driving the UHI values at a broader scale. Furthermore, these results point towards a possible change in temperature between urban and its rural LULC classes. Does it mean, the urban zones are warming at a faster rate than rural LULC classes, or if other activities are happening in these zones which may have triggered such trends particularly at daytime? In order to understand the driving factors behind these trends, we processed LST trends in each LULC in the rural and urban zones for both cities. The results are further discussed in next section.

Table 3.1. Shows statistical significance and slope values of UHI variance over selected time for Sydney and Melbourne.

UHI	Sydney				Melbourne			
	Daytime		Nighttime		Daytime		Nighttime	
	P-value	Slope	P-value	Slope	P-value	Slope	P-value	Slope
UHI_{forest}	0.06	0.00005	<0.05	0.00005	<0.05	0.00005	<0.05	0.00002
$UHI_{pasture}$	<0.05	0.0002	0.06	-0.0003	<0.05	0.0002	<0.05	0.00002
UHI_{rural}	<0.05	0.0001	<0.05	0.00001	<0.05	0.0002	<0.05	0.00002

3.3.3 Causes for the increasing UHI trends. Is it LST trends in the city?

Fig.3.7 shows seasonal and inter-annual variations in LST monthly means over 'urban' and sub- rural classes for daytime and nighttime from 2003 to 2017 for Sydney and Melbourne. It is apparent from the results (Fig.3.7 (a)), that there is no increasing or decreasing trend seen in daytime urban temperature values over Sydney. However, the rural classes, show a drop in daytime LST measurements over the selected period with significant p-values. Hence, this indicates a clear reason of daytime UHI trending upwards significantly, where the urban daytime LST did not change instead a drop in daytime rural

LSTs triggered a rise in UHI measurements. On the other hand, nighttime LST in Sydney shows a significant rise in all classes, including urban and its neighbouring rural classes. Since all classes had an increase in temperature at nighttime, consequently the nighttimeUHIs remained the same over the time and did not face a significant rise in Sydney. Similar results were evident for Melbourne, where, the city area did not experience daytime warming temperatures, but the rural classes instead dropped with significant p-values (Fig.3.7(b)). Hence, the difference between the daytime temperature in urban and rural zones grew with time causing the UHI measurement to point towards a significant rise over the past fifteen years. The nighttime variations in Melbourne remain insignificant, hence no UHI nighttime rise or drop in past fifteen years.

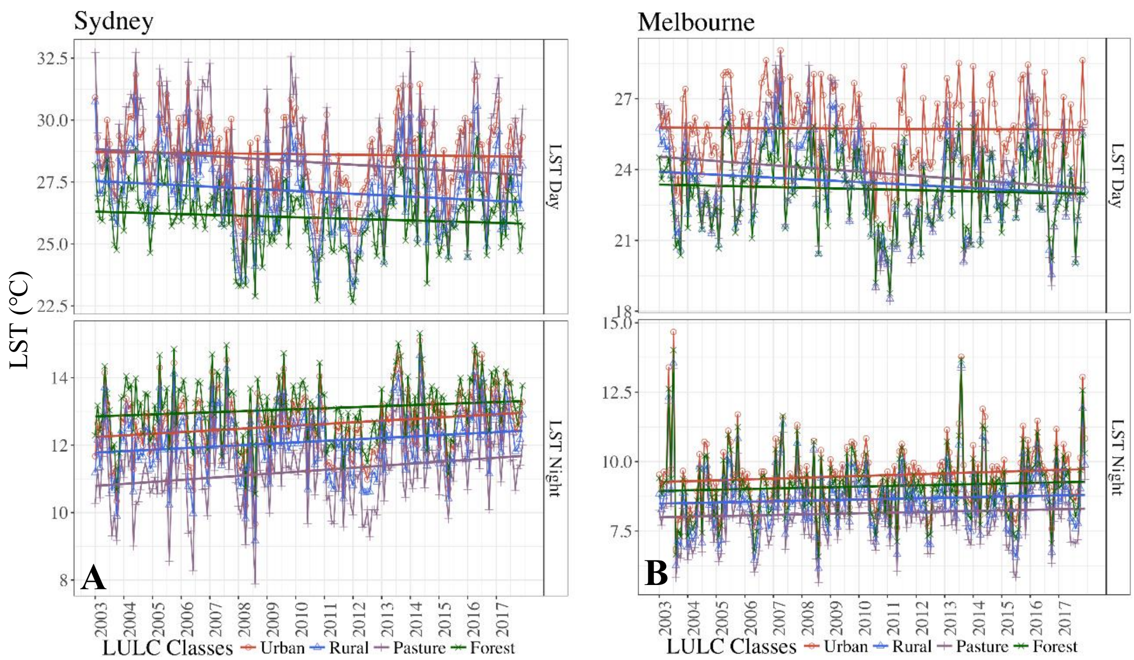

Figure 3.7. Shows time series of LST in urban and rural LULC classes for past fifteen years (2003 - 2017) (a) over Sydney and (b) over Melbourne.

Table.3.2 shows the p-values for LST over each rural LULC class and urban class in Sydney and Melbourne. These results indicated the drop in daytime LST measurements over the rural zones of our selected cities, particularly in pasture class, as was evident in

Table 3.2. Hence, this also points to possible increased activities of agriculture that may have dropped the temperature in pasture zones of rural class. In the next section, we tried to attribute the cause of the drop in daytime LSTs over rural zones and no change in daytime LSTs in urban zones. For this to analyse, we processed satellite-based greenness and albedo variations over the selected cities and in their adjacent rural zones. The results are given in the next section.

Table 3.2. Shows statistical significance and slope values of LST variance over selected time for Sydney and Melbourne urban and rural zones.

UHI	Sydney				Melbourne			
	Daytime		Nighttime		Daytime		Nighttime	
	P-value	Slope	P-value	Slope	P-value	Slope	P-value	Slope
LST_{urban}	0.5	-0.00005	<0.05	0.0001	0.78	-0.00002	0.15	0.00005
LST_{forest}	0.16	-0.00008	0.06	0.00008	0.34	-0.00005	0.33	0.00005
$LST_{pasture}$	<0.05	-0.00021	<0.05	0.0002	<0.05	-0.0002	0.38	0.00005
LST_{rural}	<0.05	-0.0002	<0.05	0.0001	0.05	-0.0002	0.36	0.00007

3.3.4 Attributing UHI to Greening

Fig.3.8 shows the trends in EVI over Melbourne. The results show a sharp, significant rise in satellite-based greenness measurements over a selected period, particularly in ‘pasture’ class. The figure further demonstrates that the EVI values over urban zone did not change over time. Instead, it remained constant with no rise or drop in values over the selected period (Fig.3.8(a)). The ‘forest’ and ‘pasture’ both classes are seen to increase in greenness over the past fifteen years. Fig.3.8 (b) indicates pixel based slopes for Melbourne with p-value < 0.05. These results also indicate rising EVI values in rural zones of Melbourne. Furthermore, it can be seen in pixel-based slope that particular areas show relatively higher slope values (Fig.3.8(b)). For example areas near south-west, highlighted by a black colour circle show relatively higher slope values (Fig.3.8(b)). The results also point towards areas near city boundary declining in greenness with negative slope values, these are highlighted by a red circle in the figure (Fig.3.8(b)).

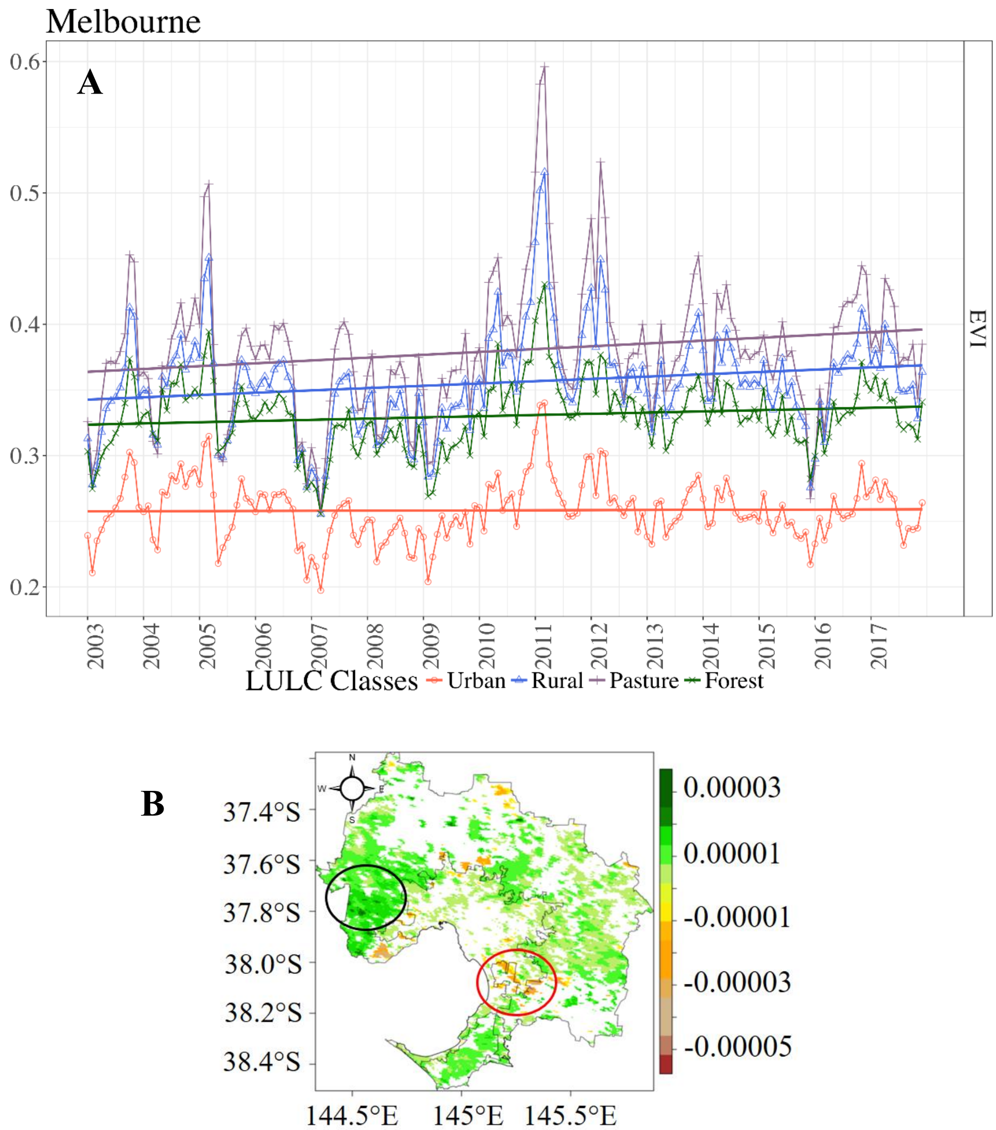

Figure 3.8. (a) Shows time series of EVI in urban and rural LULC classes for past fifteen years (2003 - 2017) over Melbourne region (b) Pixel based trend over Melbourne with p-value < 0.05; the black polygon shows relatively higher slope value pixels in the region and red polygon shows pixels with dropping EVI values over selected period.

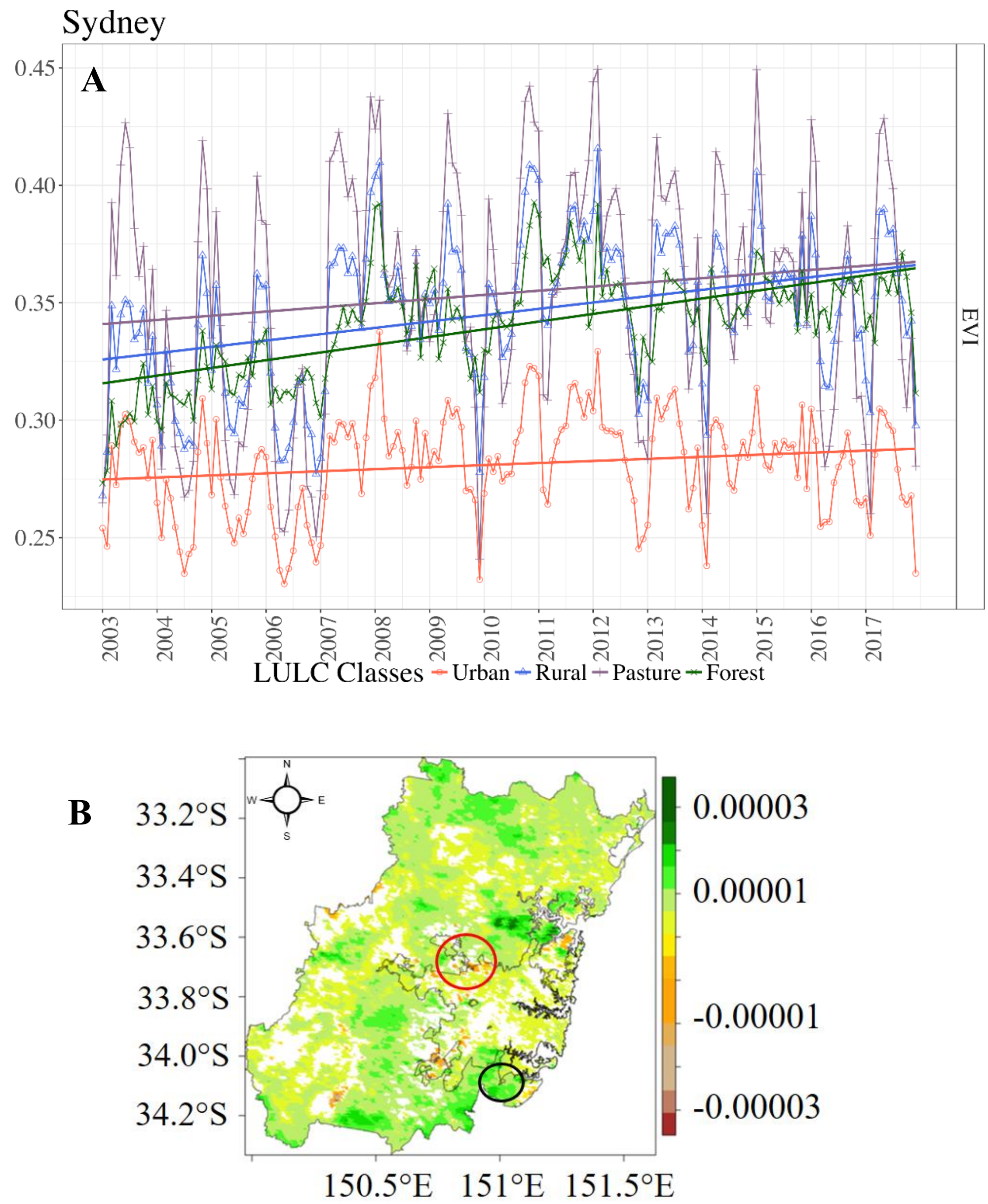

Figure 3.9. (a) Shows time series of EVI in urban and rural LULC classes for past fifteen years (2003 - 2017) over Sydney region (b) Pixel based trend over Sydney with p-value < 0.05; the black polygon shows relatively higher slope value pixels in the region and red polygon shows pixels with dropping EVI values over selected period.

Fig.3.9(a) shows EVI trends in Sydney and its rural sub-classes. In Sydney, the urban class illustrates no or minimal change in urban greenness with non-significant p-values. However, the 'pasture' class in rural zone shows the sharpest rise in EVI measurements with significant p-values (Fig.3.9(a)). 'Forest' class, also, shows the robust slope in all rural classes in the Sydney region. Pixel-based slopes also indicate similar results (Fig.3.9(b)) where the adjacent rural zones illustrate a significant rise in greenness over the past fifteen years. In Fig.3.9(b) the black and red colour circles indicate pixels with stronger greening and degreening trends respectively.

To better map the urban greenness in cities, we calculated UGD and plotted it over the selected period of fifteen years. Fig.3.10 shows the time series for UGD from 2003 to 2017 for Sydney and Melbourne. These results illustrate that the UGD is dropping significantly in both cities. It means rural areas are greener than urban areas and this difference is increasing with time. In Sydney, the urban greenness with respect to the forest was seen to be significantly dropping over the selected period (Fig.3.10(a)). Hence, this may also point towards a possible LULC change, where the forested zones being replaced by urban land use with increased growth of population in the city. Similarly, Melbourne also indicates the UGD trends to be significantly rising with the relatively higher slope for pasture class in the rural zone (Fig.3.10(b)), which also point towards activities related with replacing 'pasture' lands with urban land use.

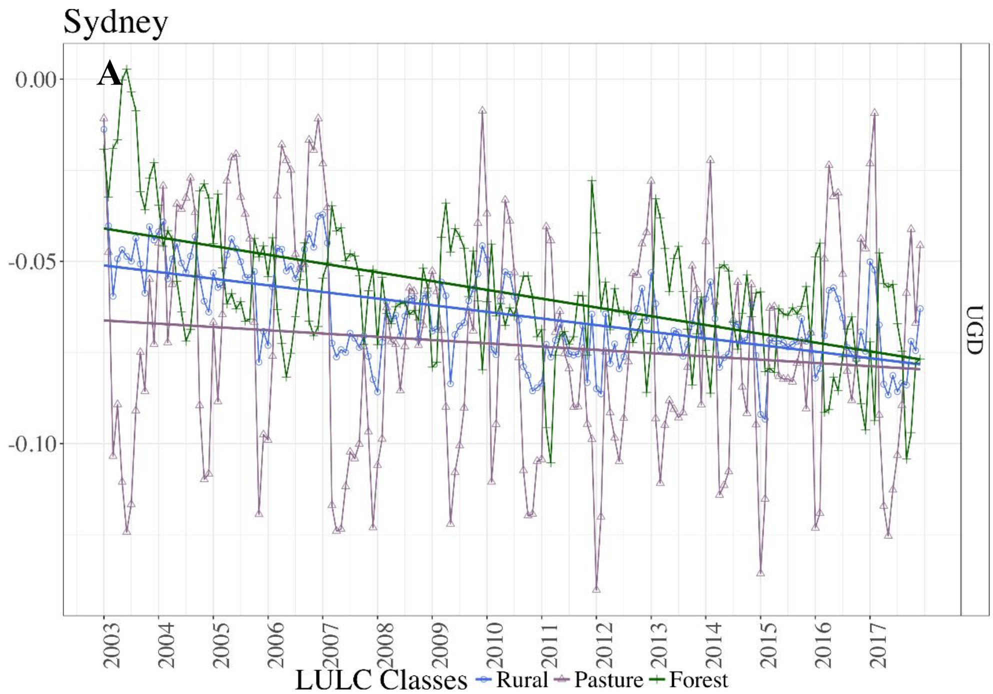

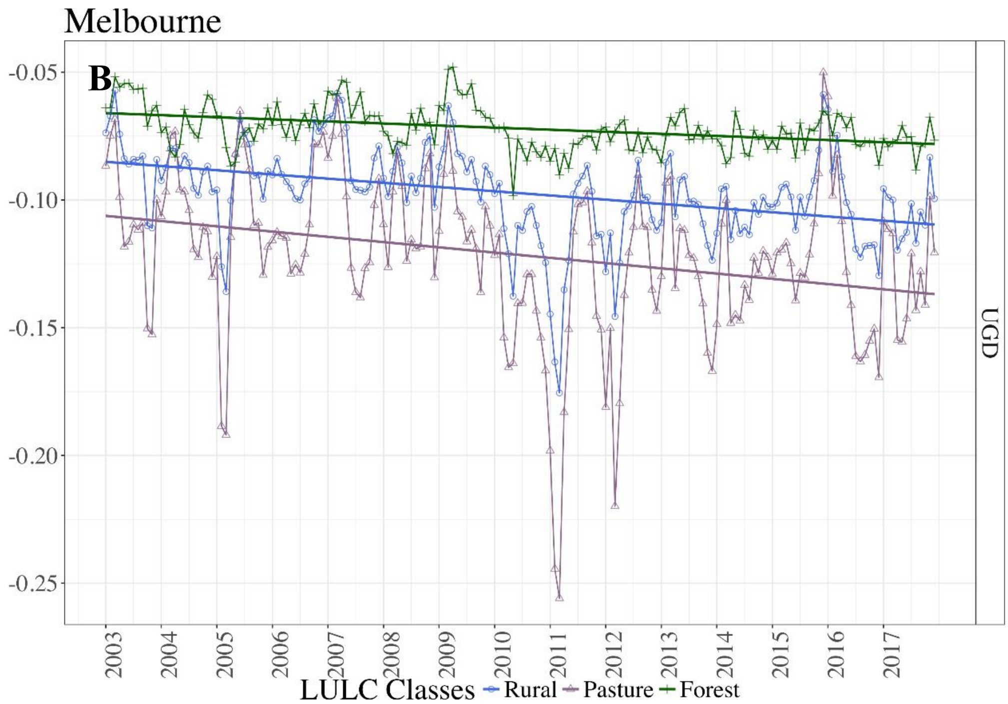

Figure 3.10. Shows time series of UGD in urban and rural LULC classes for past fifteen years (2003 - 2017) (a) over Sydney and (b) over Melbourne.

Fig.3.11 shows cross plots of UGD vs UHI (daytime). These results indicate an inverse (negative) relationship of UHI daytime with UGD. These results further confirm the role of rural LULC in UHI variance over time. The EVI curve further establishes the pattern of UHI where it shows a significant rise (p-value < 0.05) in greenness in rural classes as compared to urban. Therefore, the increase in UHI can be attributed to greening in rural class in comparison to urban class. The data indicated a significant drop in rural LST with no change in urban LST. It was also seen that EVI, which is the measure of greenness, showed a rise in rural class with significant p-values.

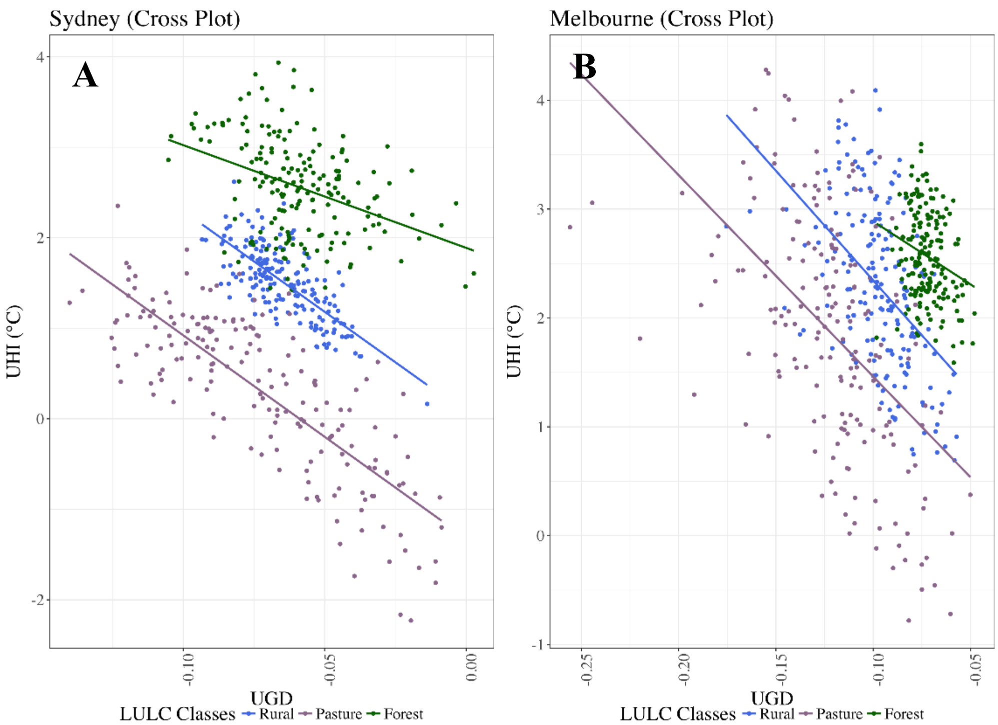

Figure 3.11. Shows cross plots of UHI day vs UGD for rural sub-classes over past fifteen years (2003 - 2017) (a) Sydney and (b) Melbourne.

3.3.5 Attributing to Albedo

Fig.3.12 shows the seasonal and inter-annual patterns in albedo (black sky) over fifteen years. Fig.3.12 (a) and Fig.3.12(b) shows that the albedo drops significantly in urban areas of Sydney and Melbourne respectively. The results also indicate that the rural zones show a rise in albedo measurements over the selected period for both cities. ‘Forest’ class shows a significant surge in albedo and a drop in ‘urban’ class in Sydney. Similarly in Melbourne ‘urban’ albedo depicts a decline in values over past fifteen years. The ‘pasture’ class does not show any rise or drop in albedo values for both cities. Fig.3.12(b) depicts the change in slope at pixel level for Sydney where, city is seen to drop in albedo values and rural areas are seen to rise in albedo values. These pixel based slopes show only signifcant trends (p-value <0.05). Similar results are evident for Melbourne (Fig.3.13).

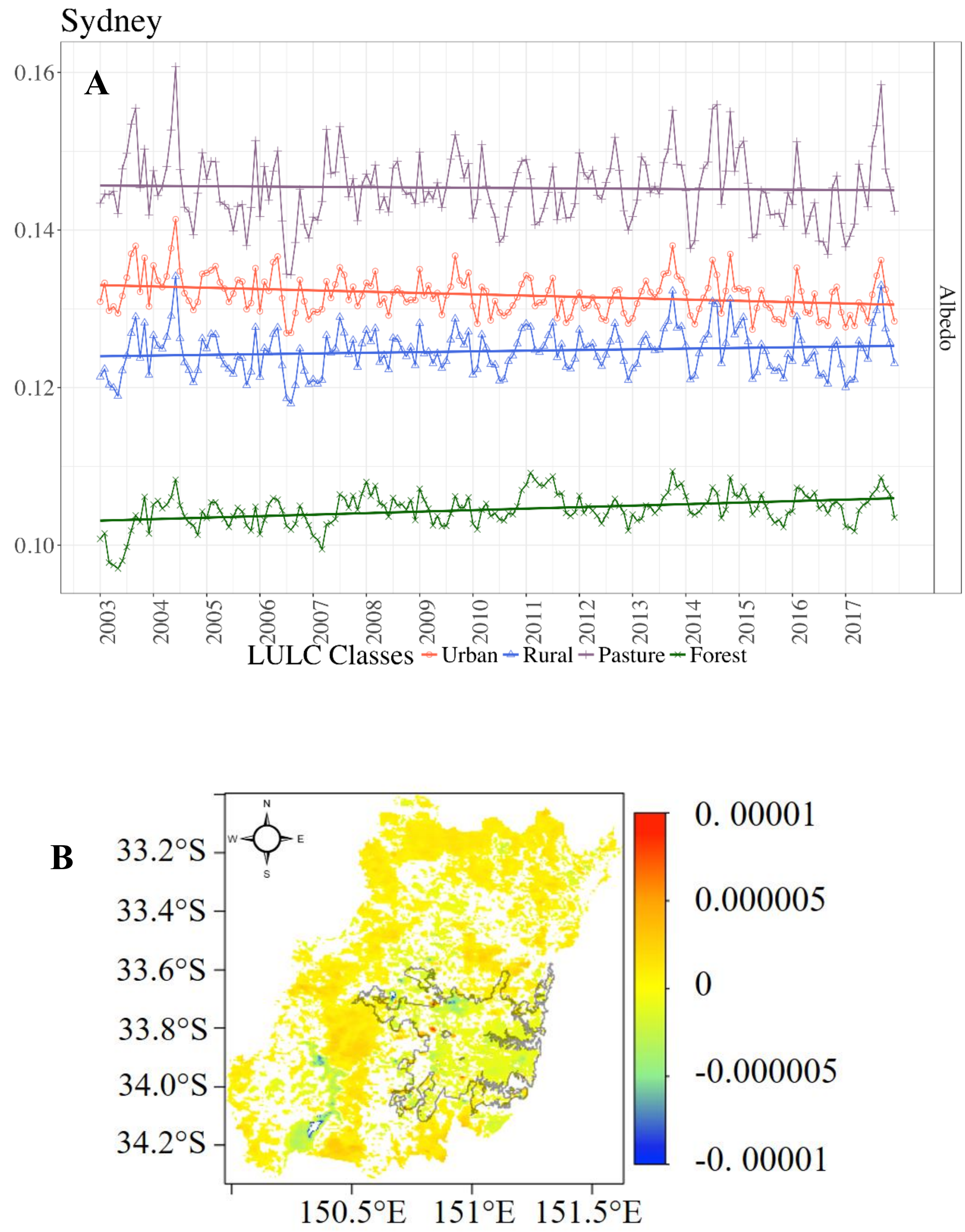

Figure 3.12. (a) Shows time series of albedo in urban and rural LULC classes for past fifteen years (2003 - 2017) over Sydney region (b) Pixel based trend over Sydney with p-value < 0.05.

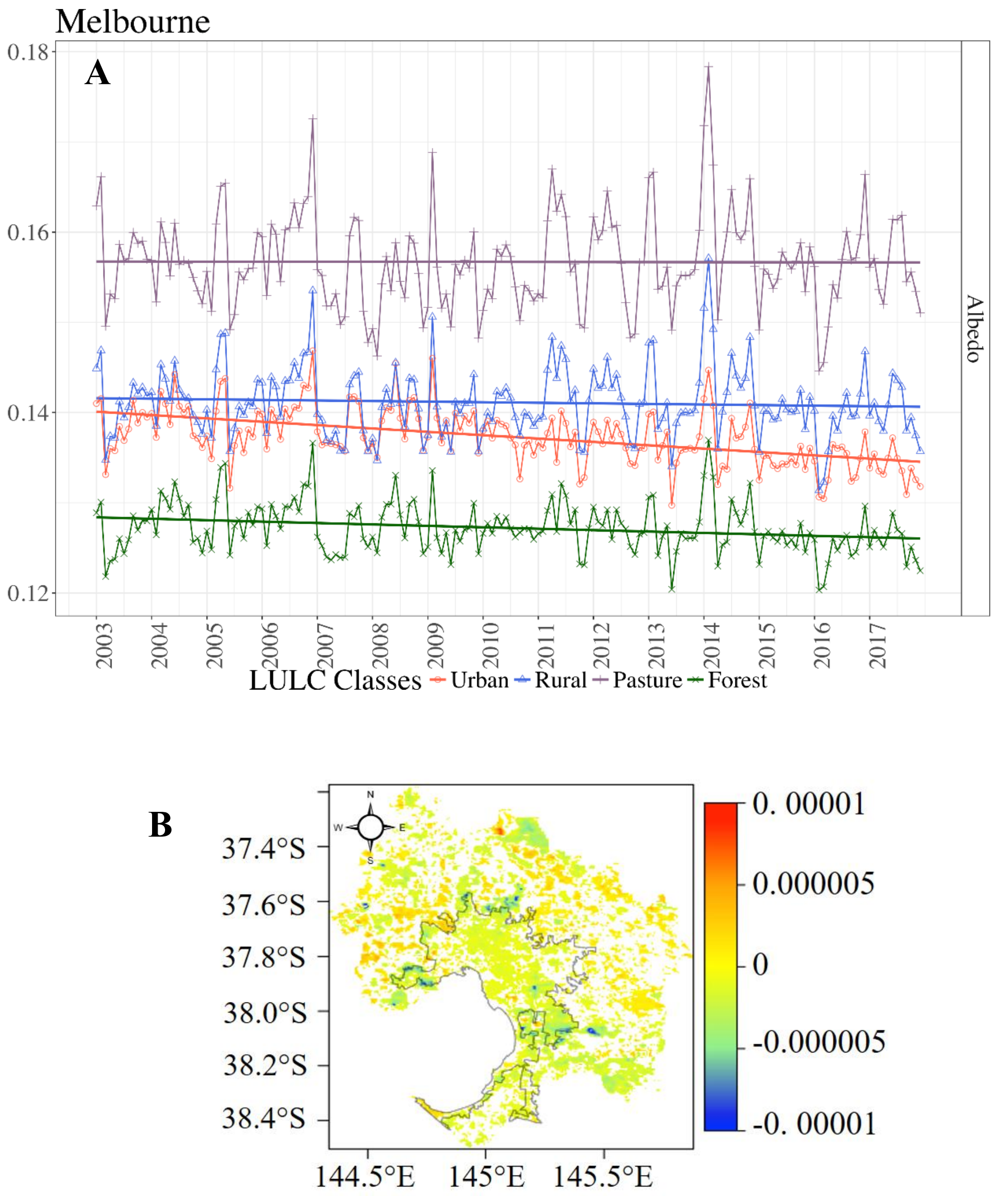

Figure 3.13. (a) Shows time series of albedo in urban and rural LULC classes for past fifteen years (2003 - 2017) over Melbourne region (b) Pixel based trend over Melbourne with p-value < 0.05.

Fig.3.14 shows delta albedo for Sydney and Melbourne. It is evident from the plots that the delta albedo dropped over the past fifteen years with significant p-values. Which indicates that sharp decline in urban albedo with respect to its adjacent rural areas, during the selected period.

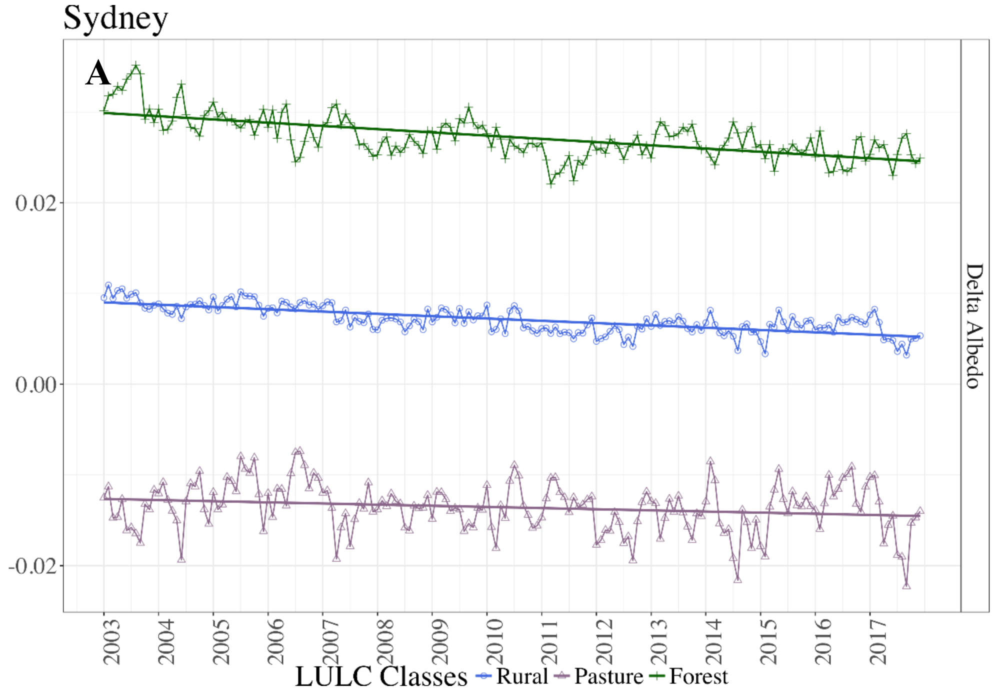

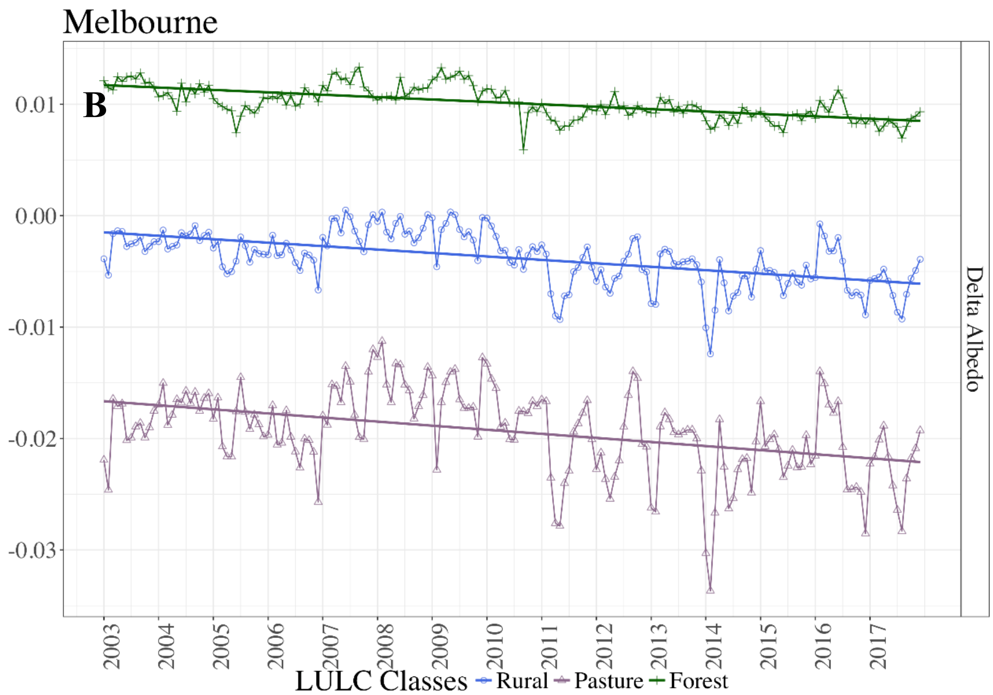

Figure 3.14. Shows time series of delta albedo in urban and rural LULC classes for past fifteen years (2003 - 2017) (a) over Sydney and (b) over Melbourne.

For further analysis, I also plotted cross plots for UHI and delta albedo. Fig.3.17 shows the cross plots for Sydney and Melbourne, where there is no significant relationship evident for albedo with daytime UHI over both cities.

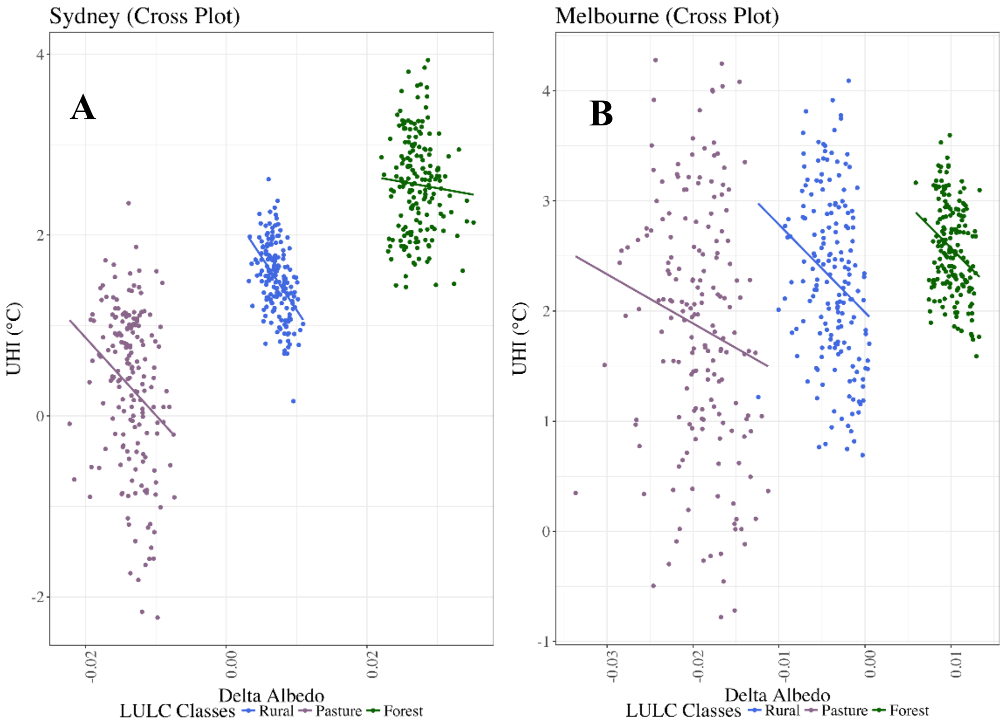

Figure 3.15. Shows cross plots of UHI day vs delta albedo for rural sub-classes over past fifteen years (2003 - 2017) (a) Sydney and (b) Melbourne.

3.3.6 BFAST results

Fig.3.16 and Fig.3.17 shows BFAST results for Sydney and Melbourne with one breakpoint. Fig.3.16 shows that Sydney has an increasing trend at both daytime and nighttime. The daytime shows one breakpoint in 2016 whereas nighttime does not indicate any such breakpoints. Fig.3.17 shows the BFAST results for Melbourne, where the algorithm shows decreasing trends in daytime UHI with one breakpoint at 2010. It further indicates that Melbourne has decreasing trends in UHI daytime with a significant UHI spike in 2010. On the other hand, the nighttime UHI for Melbourne shows rising trends. I applied BFAST to monitor any breakpoints in the time series.

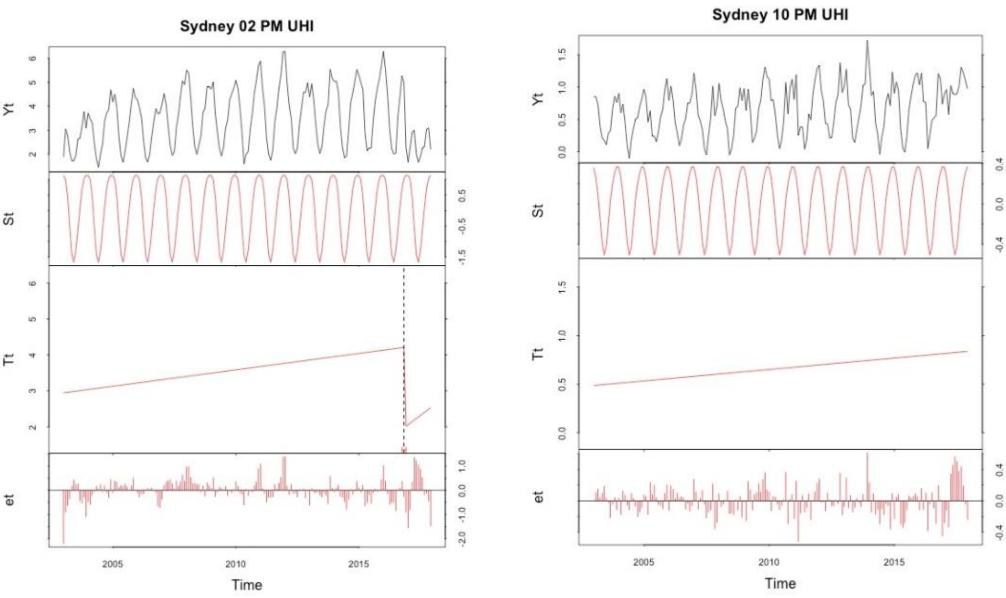

Figure 3.16. BFAST results for Sydney UHI time series at daytime and night-time.

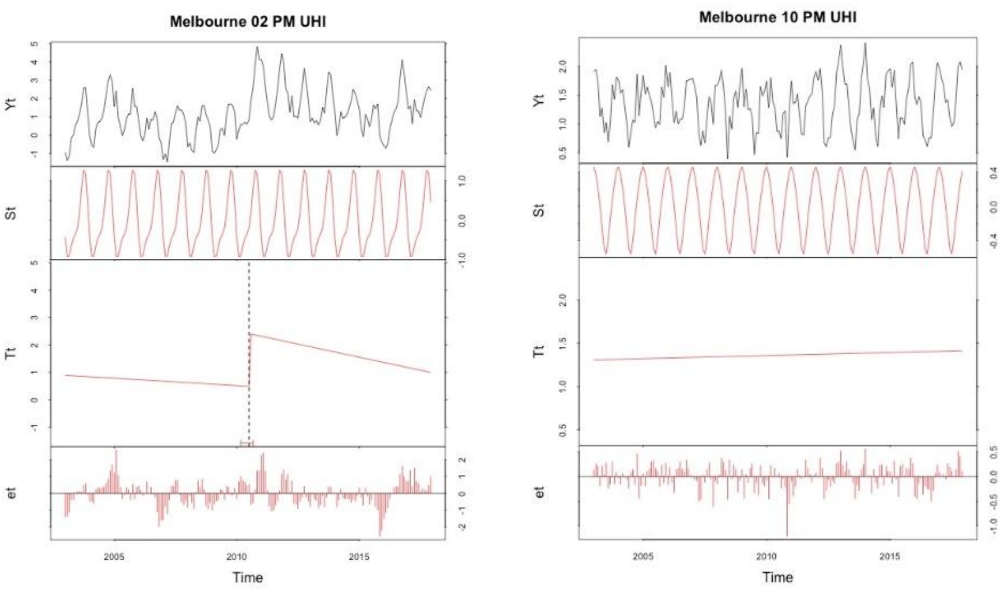

Figure 3.17. BFAST results for Melbourne UHI time series at daytime and night-time

3.4 Discussion

In this study, we investigated the urban and rural interactions on UHI patterns and dynamics of two Australian cities, Sydney and Melbourne. Using land surface temperature (LST), albedo, and vegetation index products from the MODIS sensor, we monitored greenness, UGD, albedo, delta albedo and temperatures, at diurnal, weekly, and monthly time scales across the urban to rural transition areas. The results were of very much importance as these highlighted variations and trends in the long term for UHI and its drivers such as EVI, UGD, albedo and delta albedo with reference to each LULC class in adjacent rural zones.

We found a year-round heat island in Sydney with no LST trends over the urban areas in past 15 years. This contrasted with a significant UHI increase in Sydney particularly at daytime, a consequence of rural areas becoming cooler over the same period, a result of increasing amounts of vegetation, confirmed by satellite greenness values. Similar results were found for Melbourne, but with surrounding pasture areas generating a negative heat island at certain times of the year.

3.4.1 The inter-annual trends in UHI and their drivers

The sharp daytime rise in UHI trends with a significant drop in rural LST measurements (daytime) pointed towards increased greenness in rural zones in relation to urban zones of both cities. Hence, the analysis indicated that in the past fifteen years there was an apparent increase in greenness in all rural classes with the significant p-values whereas urban class showed no increase or decrease in greenness (EVI) over the selected time. In addition to it, the results further indicated that the region was greening whereas the city due to infrastructure activities did not face any rise in greenness and eventually gave rise to daytime UHI, which had increased over time. Therefore, this could also be due to increasing cropping/agriculture activities in rural areas due to rising demand for food production with the growing population in urban zones.

The results did not illustrate any significant change in nighttime UHI trends over the past fifteen years for both cities. Hence, this was well explained by the fact that Melbourne experienced the rise in nighttime LSTs (p-value<0.05) all over the region, it means both urban and rural zones warmed at the same rate, eventually causing no change in UHI at nighttime. On the other hand, Sydney region did not experience any significant changes in nighttime LST, ultimately creating no significant difference in nighttime UHI. Furthermore, the nighttime LST showed a rise in temperature irrespective of greening in its rural surroundings pointing towards it independent nature from surrounding LULC classes in rural zones. The nighttime UHI usually exhibit due to the high thermal inertia of urban materials with a lower albedo that tends to store heat longer and release back to the atmosphere relatively slow.

The daytime UHI drop in 2017 indicate an unusual rise in temperatures in rural zones, which caused the difference of urban from rural LSTs to become minimal. If we further look at figure 3.6 in the same chapter, it can be seen that $UHI_{pasture}$ indicates a drop in 2017 summers whereas UHI_{forest} does not point to any such anomalous behaviour. It further illustrated that the decline comes from pasture zones in the overall UHI curve in figure 3.2. Furthermore, if we look at vegetation curves in figure 3.9 for Sydney, it can be seen, Sydney pasture zones that usually face two peaks in a year, experience only one peak in 2017. Hence, this anomalous effect of daytime UHI in 2017 summer can be linked with the unstable behaviour of pasture zones in rural class. It also points towards the need for further research into pasture zones and their dynamics in peri-urban regions and their role in driving UHI values for cities.

3.4.2 Greenness in rural zones

Greenness in rural zones was seen to drive the UHI trends over the selected period particularly at daytime. The UGD provided an excellent measure of the amount of greenness lacking in urban zones with reference to its rural zones. The trends in UGD further indicated that the over the selected period, the UGD trends increased with significant p-values, which pointed towards the fact that rural zones were greening and urban zones did not experience any increase in greenness over the selected period. It eventually gave birth to an increased daytime UHI in both cities. Therefore, it can be further argued that UGD may provide a measure of the amount of greenness required in cities to mitigate daytime UHI.

The cross-correlation also showed that EVI and UGD had a strong negative relationship with UHI (daytime). Hence, this means, the higher the greenness in rural zones with respect to urban zones; the higher will be daytime UHI values. It further showed us the role of vegetation in dropping the temperatures, as the rural zones, which were abundant in vegetation had lower LST at daytime and it created a difference of temperature between urban and rural zones, consequently causing a daytime UHI. It is also explained by the fact that during the daytime vegetation is cooler due to evapotranspiration, where urban surfaces due to no vegetation and impervious surfaces have higher relative surface temperatures.

3.4.3 Albedo change and its influence on UHI trends

Surface albedo variations did not show any significant relationship with daytime UHI variations. However, the form of relationship highly depends upon the wavelength and nature of surface (Houldcroft and Grey, 2009). In trend analysis, the mean albedo values indicated a substantial drop in urban zones and no change in rural zones over the selected period for both cities. The pixel-based slopes also reported a decrease in albedo values over all the urban area, with some rural spots showing increasing trends. In this study, we utilised shortwave broadband albedo measurements (BRDF corrected) which are approximated by averaging the visible and NIR broadband albedos (Jin and Dickinson, 2005). Hence, the sharp drop in albedo values in the city indicates a substantial increase in urban activities inside the city. In addition to it, the pixel-based slopes showed rural spots with increased albedo measurements which point towards increased activities related to agriculture cropping since NIR albedo will rise with increase vegetation.

3.4.4 The role of rural class as reference

The rural class and its each LULC showed their particular trends and their impacts on UHI analysis over the long term. When we further subdivided our rural class into its respective LULC classes, we saw that the LST means over each LULC class showed a decrease over the selected period with significant p-values. By dividing the rural into its respective LULC classes, we tried to point towards the uncertainties in calculations of UHI when the rural cover is dominated by multiple reference classes that may change the calculations. The 'UHI_{forest}', '$UHI_{pasture}$', and 'UHI_{rural}' showed significantly rising trends. However, the intensity and seasonality of each UHI were different and highly dependent on the choice of rural class chosen as reference. That means when the rural was considered to be 'forest', the intensity for 'UHIforest' reached as higher value, whereas when the rural was considered to be 'pasture' the 'UHIpasture' reached as lower value, and both not in the same time. Furthermore, 'UHIpasture' was seen highly variable with no clear seasonality however the rest of UHIs were more stable and showed clear inter-annual seasonality.

3.4.5 Past studies

This analysis has raised a big question mark on past studies where rural is being considered as one homogeneous surface irrespective of the fact that it may be dominated by non-stable LULC class such as in our case it was ‘pasture. It was further seen that, in spite of the fact that LULC in the rural zone was stable at ’forest’ side and non-stable at ’pasture’ side, it did not affect the increasing trend in UHI which remained to be significant with p-values <0.05.

3.4.6 Limitation

This chapter provided a comprehensive study carried out on a long term data from 2003 to 2017. However, there remains some limitation that held us back from reaching any fixed conclusion. For example, the study was carried out using LULC data of ABS, which is updated every five years (2016, 2011, and 2006). A more dynamic LULC data could have helped more to understand and track down the causes behind UHI variation across the selected time. In addition to this, the study was more of a regional study and conducted at broader scale using 1Km data, a better resolution along with temporal coverage could have helped more. Furthermore, we did not utilize Landsat data, because the city of Sydney was being covered in four tiles with two different path and rows. Hence, this caused the change in dates for each tile.

Since in our analysis we saw that UHI (daytime) had seasonality in both cities, with summer we saw UHI was dominant in Sydney and with spring the Melbourne reached its maximum daytime UHI. Furthermore, we also saw from the above analysis that the dynamics in rural zones are driving the UHI (daytime) characteristics. To better map the seasonal patterns of UHI we processed some phenological curves of vegetation in the rural zone and tried to link with seasonality in UHI. The results are further explored in the next chapter.

3.5 Conclusion

This chapter presented a complete study on UHI for the city of Sydney and Melbourne in Australia. We were able to conclude from this study that UHI calculations are very much dependent on the choice of rural class in its neighbouring non- urban areas. It is further found here that the change of reference in UHI calculations from a stable to an unstable LULC can make a difference in UHI intensity estimations and the seasonal and inter-annual fluctuations of UHI. Moreover, the study showed a strong, increasing daytime UHI in both selected cities which were driven by increased greenness cover in rural areas and relatively less green up inside the city. However, this analysis was entirely based on satellite data from MODIS; we further recommend investigating the air temperature trends along with other meteorological data sets.

3.6 References

Bonafoni, S., Anniballe, R. & Pichierri, M. 2015, 'Comparison between surface and canopy layer urban heat island using MODIS data', Urban Remote Sensing Event (JURSE), 2015 Joint, IEEE, pp. 1-4.

Ganbat, G., Han, J.-Y., Ryu, Y.-H. & Baik, J.-J. 2013, 'Characteristics of the urban heat island in a high-altitude metropolitan city, Ulaanbaatar, Mongolia', Asia-Pacific Journal of Atmospheric Sciences, vol. 49, no. 4, pp. 535-41.

Glenn, E., Huete, A., Nagler, P. and Nelson, S., 2008. Relationship between remotely-sensed vegetation indices, canopy attributes and plant physiological processes: What vegetation indices can and cannot tell us about the landscape. Sensors, 8(4), pp.2136-2160.

Grimm, N.B., Faeth, S.H., Golubiewski, N.E., Redman, C.L., Wu, J., Bai, X. & Briggs, J.M. 2008, 'Global change and the ecology of cities', science, vol. 319, no. 5864, pp. 756-60.

Houldcroft, C.J., Grey, W.M., Barnsley, M., Taylor, C.M., Los, S.O. and North, P.R., 2009. New vegetation albedo parameters and global fields of soil background albedo derived from MODIS for use in a climate model. Journal of Hydrometeorology, 10(1), pp.183-198.

Huete, A., Didan, K., Miura, T., Rodriguez, E.P., Gao, X. and Ferreira, L.G., 2002. Overview of the radiometric and biophysical performance of the MODIS vegetation indices. Remote sensing of environment, 83(1-2), pp.195-213.

Huete, A., Liu, H., Batchily, K.v. & Van Leeuwen, W. 1997, 'A comparison of vegetation indices over a global set of TM images for EOS-MODIS', Remote sensing of environment, vol. 59, no. 3, pp. 440-51.

Jin, M., Dickinson, R.E. & Zhang, D. 2005, 'The footprint of urban areas on global climate as characterized by MODIS', Journal of Climate, vol. 18, no. 10, pp. 1551-65.

Li, H., Zhou, Y., Li, X., Meng, L., Wang, X., Wu, S. & Sodoudi, S. 2018, 'A new method to quantify surface urban heat island intensity', Science of The Total Environment, vol. 624, pp. 262-72.

Li, X., Zhou, Y., Asrar, G.R., Imhoff, M. & Li, X. 2017, 'The surface urban heat island response to urban expansion: A panel analysis for the conterminous United States', Science of the Total Environment, vol. 605, pp. 426-35.

Razzaghmanesh, M., Beecham, S. and Salemi, T., 2016. The role of green roofs in mitigating Urban Heat Island effects in the metropolitan area of Adelaide, South Australia. Urban Forestry & Urban Greening, 15, pp.89-102.

Sharifi, E. & Lehmann, S. 2014, 'Comparative Analysis of Surface Urban Heat Island Effect in Central Sydney', Journal of Sustainable Development, vol. 7, no. 3, p. p23.

Streutker, D.R. 2003, 'Satellite-measured growth of the urban heat island of Houston, Texas', Remote Sensing of Environment, vol. 85, no. 3, pp. 282-9.

Xu, J., Zhao, Y., Zhong, K., Zhang, F., Liu, X. & Sun, C. 2018, 'Measuring spatio-temporal dynamics of impervious surface in Guangzhou, China, from 1988 to 2015, using time-series Landsat imagery', Science of The Total Environment, vol. 627, pp. 264-81.

Zhou, J., Chen, Y., Zhang, X. & Zhan, W. 2013, 'Modelling the diurnal variations of urban heat islands with multi-source satellite data', International journal of remote sensing, vol. 34, no. 21, pp. 7568-88.

Zhou, J., Chen, Y., Wang, J. & Zhan, W. 2011, 'Maximum nighttime urban heat island (UHI) intensity simulation by integrating remotely sensed data and meteorological observations', Selected Topics in Applied Earth Observations and Remote Sensing, IEEE Journal of, vol. 4, no. 1, pp. 138-46.

Zhou, B., Rybski, D. and Kropp, J.P., 2017. The role of city size and urban form in the surface urban heat island. Scientific Reports, 7(1), p.4791.

Chapter 4: Interactions of vegetation phenology with UHI

Abstract

From previous chapters, we know that an urban heat island (UHI) occurs when higher temperatures are encountered in built environments of cities compared with surrounding rural areas. This UHI effect does not remain stable over the year and instead exhibits particular intra-annual seasonal variations. UHI responses may depend on the thermal properties of its adjacent neighbouring land use and land cover (LULC), mainly when the rural zones are dominated by vegetation with specific seasonal patterns.

Many studies in the literature have investigated UHI seasonality. However, very few have looked at the causes behind resulting seasonal patterns. In previous chapters, we showed that both Melbourne and Sydney indicated increasing trends for UHI particularly at daytime which were driven by changes in rural land and variations in its thermal properties due to increased greenness over the selected period. In this chapter, we investigate the inter-annual seasonal variations in UHI, particularly at daytime and its dependency on vegetation phenology and resulting thermal patterns of rural lands.

The aims of this chapter were to investigate the urban and rural interactions of vegetation phenology on UHI patterns and inter-annual and seasonal dynamics of selected Australian cities, Sydney and Melbourne. Using land surface temperature (LST) and vegetation index data derived from the MODIS sensor, we monitored greenness, urban greenness deficit (UGD) and temperatures across the urban to rural transition areas. Results indicated that seasonal vegetation greenness peaks in rural areas drove peaks in UHI for daytime hours. The results further showed that Melbourne, where most of the rural land is ‘pasture’, peaked in spring due to the heavy influence of rural pasture lands and their respective thermal response. Sydney summer as the peak UHI season, where ‘forest’ and ‘pasture’ zones equally shared the rural land as reference class.

We conclude that continued urbanisation induces complex interactions and feedbacks among temperature, greenness, and phenology that impact UHI measures. Furthermore, phenological differences among land cover classes, and in particular between urban and rural reference areas will generate asynchronous effects on the derived UHI that may amplify or mitigate surface temperatures and associated UHI. Further research is needed to interpret the meanings of UHI in such dynamic environments.

4.1 Introduction

The interactions of urban surfaces with the atmosphere are governed by surface heat fluxes, the distribution of which is drastically modified by urbanisation (Landsberg et al., 1981; Dousset and Gourmelon, 2003; Nunez and Oke, 1976; Liu and Chen, 2004). Urban heat island (UHI) is one of the products of urbanisation that generates a temperature gradient between urban and rural zones (Oke et al., 1982; Kim and Baik, 2005; Gallo and Tarpley, 1995). UHI formation is one characteristic of urban land cover change that is of concern across science disciplines because the UHI signal reflects a broad suite of significant land surface changes impacting human health, ecosystem function, local weather and possibly climate (Imhoff and Zhang, 2010; Pickett and Cadenasso, 2011).

UHI measurements are not distributed evenly throughout the year. In the literature, a few studies found that UHI was intense during summer seasons and a few other studies observed it was dominant in autumn or winter (Zhang and Hou, 2005; Jin et al., 2012). Zhao and Shen (2010) found that UHI was strong in summer over Nanjing, China. Zhou & Shepherd (2010) observed strong daytime UHI intensity over Atlanta, USA in summer season. Liu and Ji (2007); Ganbat and Han (2013) reported strong UHI intensity in winter season. It can be summarised that many studies analysed the inter and intra-annual seasonal variations in UHI, however, less attention was given on its driving attributes. In addition to it, in spite of the fact, that the rural thermal properties have the ability to generate seasonal variations in the UHI (Oke et al., 1982; Oke et al., 1979), very few studies looked at the role and influence of rural LULC dynamics and its vegetation phenology on UHI seasonal and inter-annual variations. Phenology is defined as the study and analysis of the life cycles of flora and fauna and their interactions with climate and other seasonal environmental drivers (White & Thornton, 1997). In the last decade, some different methods have been developed to determine the timing of vegetation green-up and senescence (i.e., the start and end of growing season) using time series of vegetation indices derived from satellite data. Satellite based vegetation indices offer better ways of plotting phenology cuves for different biomes.

From previous chapters, we know that daytime UHI showed a strong relationship (negative cross-correlation) with the greenness in cities relative to its adjacent non-built/rural zones. Hence, this played an important role in driving the trends in UHI particularly at daytime in both selected cities. However, we still do not know if the vegetation in rural zones also influences the seasonality of UHI in the city. Since it is also known that UHI behaviour is not the same throughout the year, instead it depicts different seasons at peak times for both selected cities. In this study, I processed phenology profiles of greenness and urban greenness deficit to better understand the vegetation phenology and its influence on UHI. The objectives of this study were to (1) determine the variations in timing and duration of UHI with reference to rural vegetation cover seasonality, and (2) investigate the inter-annual responses and variations of rural and urban vegetation phenology on UHI variability.

4.2 Data and Methods

The land surface temperature (LST), land use land cover (LULC) data prepared in chapter 2 and enhanced vegetation index (EVI), urban greenness deficit (UGD) and UHI monthly data (2003-2017) generated in chapter 2 and chapter 3 were utilised in this study to investigate the set objectives for this chapter. To map the inter-annual seasonal patterns, the dataset were split into three time groups, one from 2003 to 2009, second for 2011 to 2013 and third for 2014 to 2017. The period was divided considering the fact that Australian region was hit by decadal millennium drought in 2001 to 2009, followed by a short wet pulse in 2010 and 2011 (Xie et al., 2016), which may have implications on vegetation profiles in selected regions.

4.2.1 Plotting UHI and LST climatic averages

The LST and UHI climatic means generated in the previous chapter were plotted inter-annually to map the seasonality of UHI in the selected regions. We divided our study period into three parts, one was chosen to be from 2003 to 2009 and second was from 2010 to 2013 and the third was from 2014 to 2017. These plots provided information about averaged seasonal behaviour of UHI over the 3 selected time periods. The UHIs were further classified with reference to each rural LULC class, which are ‘urban’, ‘pasture’ and ‘forest’, considering the fact that each rural LULC class had its distinct thermal properties.

4.2.2 Generating inter-annual and seasonal patterns

The monthly mean data of EVI and UGD from 2003 to 2017, prepared in the previous chapter, were utilised to generate the inter-annual and seasonal patterns of greenness in the selected regions. First data were averaged over 2003 to 2009, 2010 to 2013, and 2014 to 2017. Then, zonal statistics were run on each set of monthly averages and LULC data, to extract the EVI and UGD values over ‘urban’, ‘pasture’ and ‘forest’. Then plots were generated which are further discussed in the results section.

4.3 Results

4.3.1 Seasonal Patterns UHI

Fig.4.1 indicates the inter-annual response of daytime UHI over the selected period. It can be seen that the UHI computed using adjacent forests as the reference,

UHI_{forest}, shows a consistant seasonal pattern over the year in both cities. The plot further indicates that the peak season for UHI_{forest} is summer (December, January and February). However, when UHI is computed using adjacent pastures as reference, or $UHI_{pasture}$, remarkably different results occur in the seasonality patterns in both cities. Sydney shows much lower, year-round UHI values with slightly higher intensity in the summer (December, January and February), while Melbourne reaches its highest values in the spring (September, October and November) (Fig.4.1).

Similarly, the minimum UHI values are also very much dependent on the rural thermal properties which are highly variable for 'pasture' lands and more stable or consistent for the 'forest'. For example, it can be seen that $UHI_{pasture}$ records its lowest values in the end of summer and start of autumn for Melbourne, causing the city to be a heat sink instead of heat island. On the other hand, Sydney remains highly unstable concerning 'pasture' class, with $UHI_{pasture}$ fluctuating between -1°C to 1°C throughout the year. It can be seen from the results that 'forest' class acts as a more stable reference class keeping the UHI pattern consistent over the years with maximums in summer and minimums in winter for both cities. These seasonal curves of UHI further explain the role of rural lands and their dynamics in driving the daytime UHI sesaonal patterns.

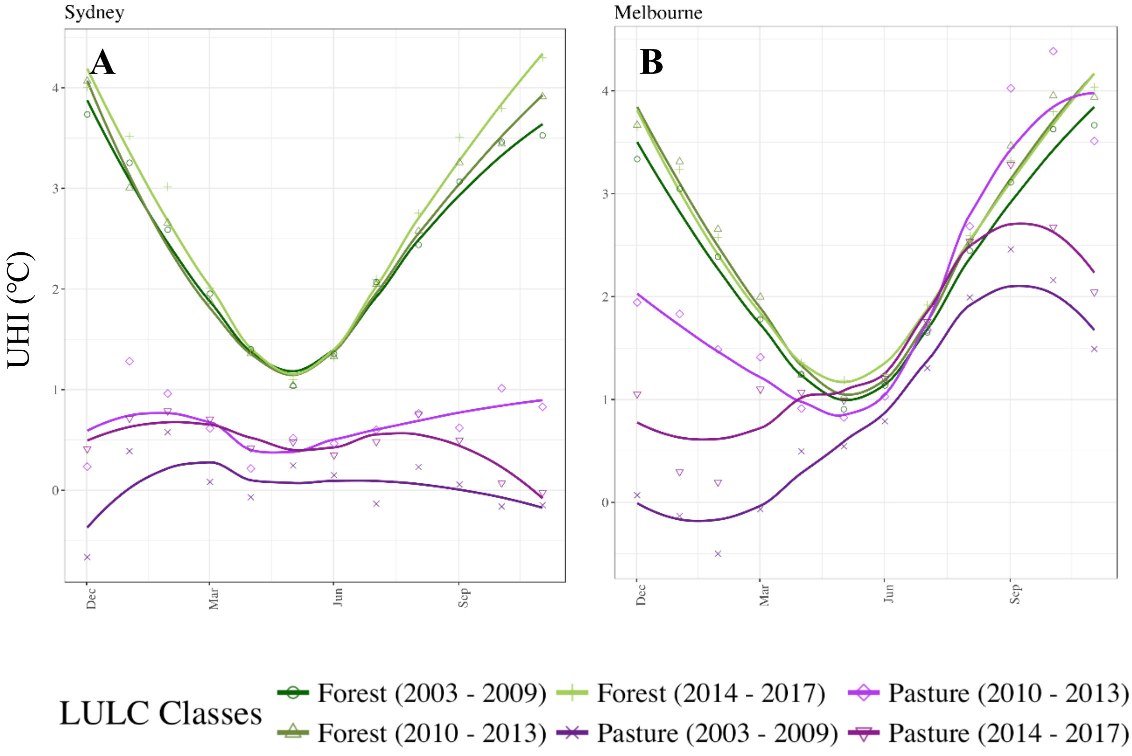

Figure 4.1. Shows inter-annual variations in UHI with reference to selected adjacent rural LULC classes, which are 'pasture' and 'forest' over (a) Sydney and (b) Melbourne.

4.3.2 Inter-annual Patterns - LST

Fig.4.2 illustrates the inter-annual response of daytime LST over Sydney and Melbourne from 2003 to 2017. Fig.4.2(a) indicates 'urban' and 'pasture' at relatively warmer temperatures than the 'forest' covered zones throughout the year over Sydney. On the other hand, Melbourne indicates metropolitan areas at relatively higher temperature than in pastures, particularly in the spring season. Forested zones remain relatively cooler than other LULC classes in the region, through out the year. On the other hand, 'pasture' class shows variable thermal response relative to other LULC classes in the region.

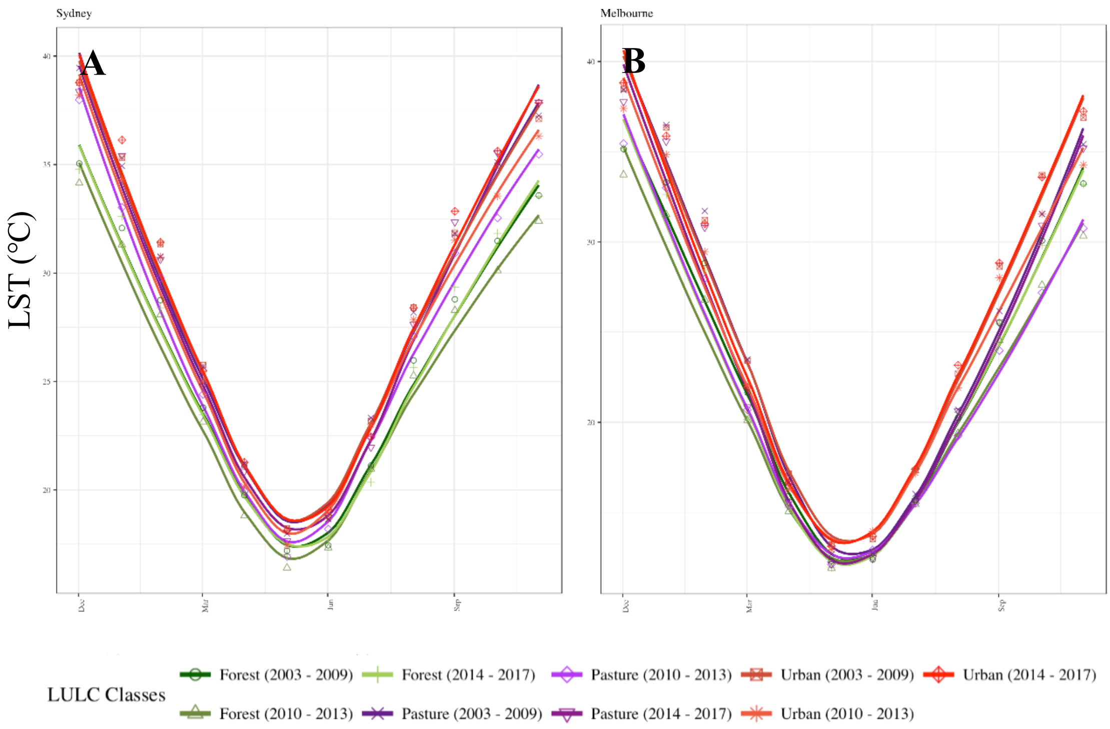

Figure 4.2. Shows inter-annual variations in LST over 'urban' and it's adjacent rural LULC classes, which are 'pasture' and 'forest' over (a) Sydney and (b) Melbourne.

4.3.3 Phenology curves for vegetation

Fig.4.3 illustrates the inter-annual seasonal patterns of greenness in selected LULC classes in both regions. These figures represent the patterns of vegetation phenology in selected LULC classes. Fig.4.3(a) indicates that in Sydney the 'pasture' class has the highest relative variability over a year, with maximum greenness reaching in summer season (particularly in February). It means grasses or crops in Sydney's 'pasture' dominated zones are at their peak season in February, eventually causing the temperatures of that zones to drop down in temperature values in summer months. Similar green patterns are evident inside the city, where vegetation peaks in summer, particularly in February. The second peak in vegetation is also apparent for Sydney which is seen in late winter (August). Fig.4.3(b) shows similar patterns for Melbourne, however, the greenness in pasture zones peak only in August, September and October (late winter and spring season). Hence, this further confirms the cooling of adjacent rural zones in spring, which is not visible in 'urban' zones due to relatively less vegetation greenness inside the city than outside.

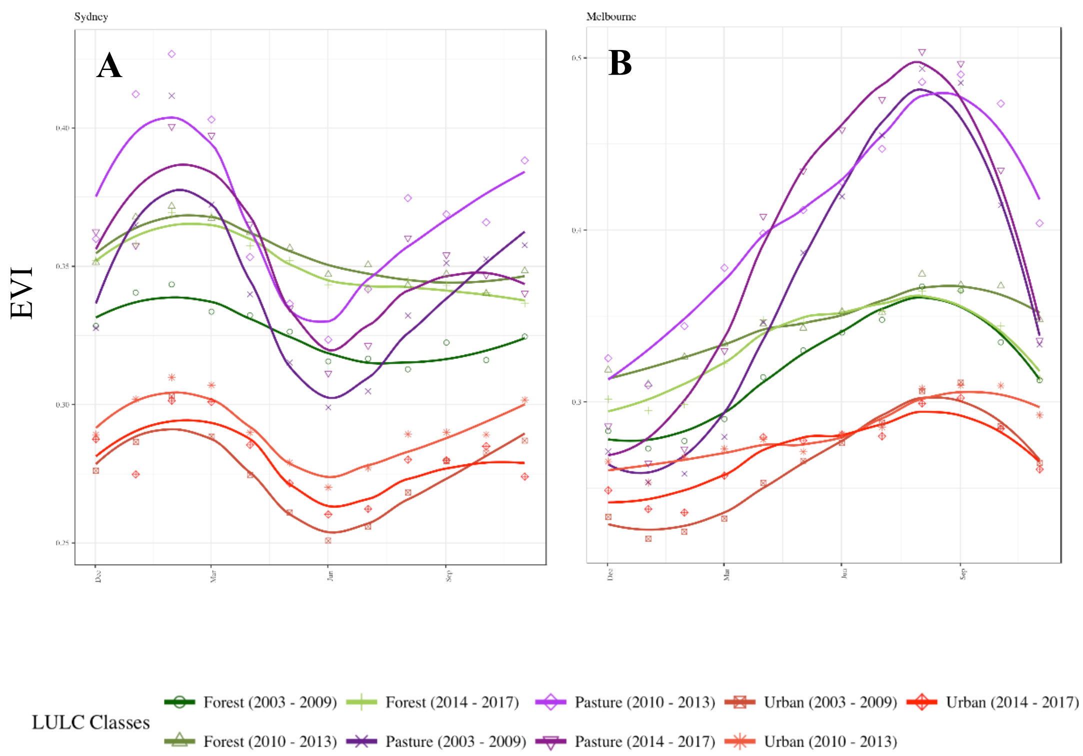

Figure 4.3. Shows inter-annual variations in EVI (satellite based greenness) over 'urban' and it's adjacent rural LULC classes, which are 'pasture' and 'forest' over (a) Sydney and (b) Melbourne.

Fig.4.4 indicates UGD patterns, which illustrate the lack of greenness inside the city than outside. Fig.4.4(a) shows the peak season for UGD_{forest} in Sydney is 'summer' particularly months of December and January. On the other hand, $UGD_{pasture}$ reaches its peak values in late summer, particularly in February. It means the difference of greenness in the city to its rural LULC reaches its peak values in summer months for Sydney, ultimately causing the variation of temperature between urban and adjacent rural lands due to different thermal responses of each zone.

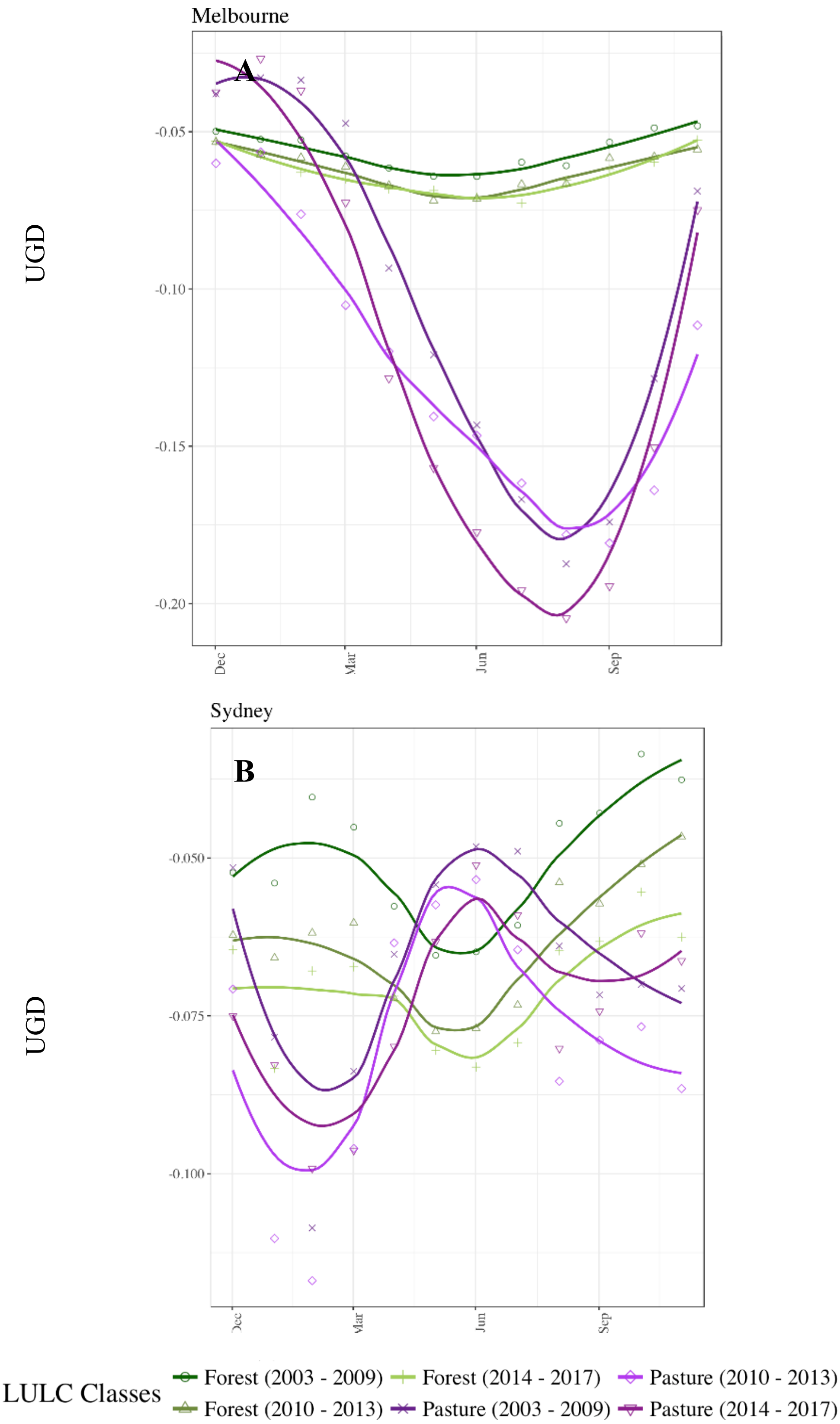

Figure 4.4. Shows inter-annual variations in UGD with reference to adjacent rural LULC classes, which are 'pasture' and 'forest' over (a) Sydney and (b) Melbourne.

4.4 Discussion

This chapter highlights a comprehensive study on UHI seasonal variability and its attributing drivers. The study is carried out for city of Sydney and Melbourne in Australia using recent remote sensing tools and techniques. This study provides insight on the efficiency of space-borne data and GIS tools for better spatial and temporal analysis.

4.4.1 UHI and LST seasonality

The thermal responses of rural lands play an important role in driving the daytime UHI values. In Sydney, the rural or adjacent zones to urban areas are dominated by two major LULC classes, which are 'forest' and 'pasture' (please refer to Fig.2.1 in chapter 2). Sydney is neighbouring with 'forest' in its east and 'pasture' in its west. Therefore both LULC classes contribute to generating the resulting UHI in the city for Sydney region. The 'pasture' class remains unstable even causing the cool urban island at certain times of the year instead of generating urban heat island. Hence, in Sydney, 'pasture' class does not play a vital role in driving the UHI values, since forested zones also have significant contribution in resulting UHI seasonal patterns.

On the other hand, Melbourne's rural land is mostly dominated by 'pasture' LULC class (please refer to Fig 2.1 in chapter 2). These 'pasture' zones were seen to reach their coolest temperatures in the spring season and ultimately triggering a $UHI_{pasture}$ which reaches its maximum values in that particular season. On the other hand UHI_{forest} peaks in summer much like Sydney.

To map the inter-annual seasonal patterns, the data were split into three-time groups, one from 2003 to 2009, the second for 2010 to 2013 and the third for 2014 to 2017. The period was divided considering the fact that Australia was hit by a decadal millennium drought from 2001 to 2009, followed by a short-wet pulse in 2010 and 2011. The results indicated that the $UHI_{pasture}$ values were affected by variations in dry years (2003 – 2009) and wet years (2010 – 2013), since results indicated the summer $UHI_{pasture}$ dropping during dry years (2003 – 2009) and rising in wet years (2010 – 2013) which was evident for both cities. UHI_{forest} was least affected by variations in dry years and wet years.

4.4.2 Vegetation Phenology

The vegetation phenology plays the most critical role in decreasing the temperatures in rural LULC classes and driving the specific thermal response of respective zones. Hence, when vegetation is at its peak and most green, it cools down the rural surfaces, on the other hand, urban due to no vegetation cover or relatively less vegetation cover remains at warmer temperatures, eventually giving rise to higher amplitudes of UHI for subject cities. In addition to it, in rural LULC classes, the 'pasture' class indicates particular seasonality and phenology patterns across the year, which eventually drives the UHI seasonality, particularly at daytime. For example, in Melbourne, the city experiences UHI in spring due to relatively lower temperatures in rural zones than in urban zones. The cooler temperatures are due to increased greenness in the region in that particular season. Since vegetation has the ability to cool the surfaces due to evapotranspiration, it is the main reason rural areas are cooler when vegetation is at its peak season. Ultimately it gives rise to particular seasonality in UHI causing Melbourne to peak in spring. Therefore, Melbourne exhibits a strong daytime UHI in spring.

However, the 'forest' remains independent of such patterns due to being green all year with no particular seasonal patterns across the year. The tree layer is predominantly evergreen and functionally active year round (Eamus and Hutley, 2001) and therefore does not show any specific seasonal pattern as is evident for pastures. Therefore, forests remain cooler in summer and throughout the year with respect to other LULC classes in the region. The summer is peak season for UHI_{forest} due to warmer temperatures in the area and 'forest' having the ability to cool down the temperatures.

The results were of very much importance as these highlighted seasonal, inter-annual variations in UHI and its drivers such as EVI, and UGD with reference to each LULC class in adjacent rural zones.

4.5 Conclusion

This chapter presented a comprehensive study on UHI for the city of Sydney and Melbourne in Australia. We conclude from this study that the rural LULC dynamics play a significant role in driving the seasonal and inter-annual response of UHI, particularly at daytime. Sydney had a peak UHI in summer which was influenced by 'forest' class, and Melbourne had a peak UHI in spring, and it was controlled by 'pasture' class in rural zones. We further conclude that vegetation phenology in peri-urban or rural zones has a controlling effect on UHI amplitudes in the cities. Furthermore, it can also be concluded that the 'pasture' class behaves as unstable with certain variations throughout the year and particularly during dry and wet years. Whereas 'forest' behaves more stable with less fluctuations due to climate or other factors."

The analysis was entirely carried out using space-borne data; we further suggest integrating ground-based observations for better analysis and understanding.

4.6 References

Bonafoni, S., Anniballe, R. & Pichierri, M. 2015, 'Comparison between surface and canopy layer urban heat island using MODIS data', Urban Remote Sensing Event (JURSE), 2015 Joint, IEEE, pp. 1-4.

Dousset, B. and Gourmelon, F., 2003. Satellite multi-sensor data analysis of urban surface temperatures and landcover. ISPRS journal of photogrammetry and remote sensing, 58(1-2), pp.43-54.

Eamus, D., Hutley, L.B. and O'Grady, A.P., 2001. Daily and seasonal patterns of carbon and water fluxes above a north Australian savanna. Tree Physiology, 21(12-13), pp.977-988.

Ganbat, G., Han, J.-Y., Ryu, Y.-H. & Baik, J.-J. 2013, 'Characteristics of the urban heat island in a high-altitude metropolitan city, Ulaanbaatar, Mongolia', Asia-Pacific Journal of Atmospheric Sciences, vol. 49, no. 4, pp. 535-41.

Huete, A., Didan, K., Miura, T., Rodriguez, E.P., Gao, X. and Ferreira, L.G., 2002. Overview of the radiometric and biophysical performance of the MODIS vegetation indices. Remote sensing of environment, 83(1-2), pp.195-213.

Huete, A., Liu, H., Batchily, K.v. & Van Leeuwen, W. 1997, 'A comparison of vegetation indices over a global set of TM images for EOS-MODIS', Remote sensing of environment, vol. 59, no. 3, pp. 440-51.

Imhoff, M.L., Zhang, P., Wolfe, R.E. & Bounoua, L. 2010, 'Remote sensing of the urban heat island effect across biomes in the continental USA', Remote Sensing of Environment, vol. 114, no. 3, pp. 504-13.

Kim, Y.-H. & Baik, J.-J. 2005, 'Spatial and temporal structure of the urban heat island in Seoul', Journal of Applied Meteorology, vol. 44, no. 5, pp. 591-605.

Landsberg, H.E., 1981. The urban climate (Vol. 28). Academic press.

Liu, W., Ji, C., Zhong, J., Jiang, X. & Zheng, Z. 2007, 'Temporal characteristics of the Beijing urban heat island', Theoretical and Applied Climatology, vol. 87, no. 1-4, pp. 213-21.

Nunez, M. & Oke, T. 1976, 'Long-wave radiative flux divergence and nocturnal cooling of the urban atmosphere', Boundary-Layer Meteorology, vol. 10, no. 2, pp. 121-35.

Oke, T.R., 1979. Advectively-assisted evapotranspiration from irrigated urban vegetation. Boundary-Layer Meteorology, 17(2), pp.167-173.

Oke, T.R., 1982. The energetic basis of the urban heat island. Quarterly Journal of the Royal Meteorological Society, 108(455), pp.1-24.

Pickett, S.T., Cadenasso, M.L., Grove, J.M., Boone, C.G., Groffman, P.M., Irwin, E., Kaushal, S.S., Marshall, V., McGrath, B.P., Nilon, C.H. and Pouyat, R.V., 2011.

Urban ecological systems: Scientific foundations and a decade of progress. Journal of Environmental Management, 92(3), pp.331-362.

Streutker, D.R. 2003, 'Satellite-measured growth of the urban heat island of Houston, Texas', Remote Sensing of Environment, vol. 85, no. 3, pp. 282-9.

White, M.A., Thornton, P.E. and Running, S.W., 1997. A continental phenology model for monitoring vegetation responses to interannual climatic variability. Global biogeochemical cycles, 11(2), pp.217-234.

Zhao, X., Shen, S., Yang, S., Xie, X. & Chen, T. 2010, 'Analyzing the Seasonal Variations of Urban Heat Island in Nanjing Using Remote Sensing Data', Multimedia Technology (ICMT), 2010 International Conference on, IEEE, pp. 1-4.

Zhou, Y. & Shepherd, J.M. 2010, 'Atlanta’s urban heat island under extreme heat conditions and potential mitigation strategies', Natural Hazards, vol. 52, no. 3, pp. 639-68.

Zhang, J., Hou, Y., Li, G., Yan, H. and Yao, F., 2005. The diurnal and seasonal characteristics of urban heat island variation in Beijing city and surrounding areas and impact factors based on remote sensing satellite data. Science in China Series D-Earth Sciences, 48(suppl Ⅱ), pp.220-220.

Chapter 5: Extreme Heat Waves and their influence on UHI

Abstract

Urban heat island (UHI) is a phenomenon where urban areas exhibit warmer temperatures than the surrounding rural landscapes. In the context of climate change, UHI patterns may modify the impact of heat waves in summer over metropolitan areas, critically testing the adaptive capacity of urban populations to respond to extreme events. However, the interactions and spatial patterns of extreme heat events with UHI of urban areas remain unknown and mostly untested.

In 2017, Sydney had its hottest summers on record. The city was hit by a number of heat waves in summer 2017, with most extreme occurring on 9 to 12 February 2017. In this chapter, the heat wave of summer 2017 and its interactions with UHI in Sydney city are studied. The objectives of this chapter are to analyse the diurnal variations in UHI and quantify its intensity around the metropolitan area during an extreme heat wave event. To do this high temporal resolution data of Himawari-8 was used. MODIS based observations were further used to detect the effect of the heat wave on UHI and compare the results with Himawari-8 data. LST and UHI diurnal patterns, anomalies and statistical significance were assessed in both urban and rural surroundings of the Sydney region. During the extreme heat waves the urban class showed 5°C – 6°C and forests 2°C – 3°C warmer temperatures respectively, relative to regular days, with their absolute difference remaining significant all day. Moreover, western Sydney showed relatively warmer temperatures than eastern and northern parts, suggesting a potential for mitigation options. This study presents innovative research on UHI, and extreme heat wave interactions using recently available satellite data.

5.1 Introduction

Heatwaves are the number one mortal risk among so-called natural hazards in today's world (Poumadere and Mays 2005). In general, there is no universal definition of a heatwave although it can be broadly defined as a extended period of extreme heat (Xiang and Bi, 2014). Beureau of Meteoroglogy (BOM) defines a heat wave as three or more days of anomoulous high temperatures (BOM, 2019). The heatwaves are silent killers,and the memories of the heat wave vanish once cooler weather arrives (Seneviratne and Nicholls 2012). Many people succumb to extreme heat events every year. Heat stress affects human health and manifests in various symptoms, such as lack of concentration, exhaustion, dehydration, circulatory disorder, and finally can result in death, as revealed in several studies (Abrahamson and Wolf, 2008; Kovats and Hajat, 2008; Gartland, 2010; Gabriel and Endlicher, 2011; Scherer and Diffenbaugh, 2014). During heatwave as temperatures rise and normal physiological processes can no longer regulate body temperature, as evidenced by increased hospitalisations and emergency calls during heatwaves (Kalkstein and Smoyer, 1993; Astrom and Bertil, 2011; Zhang and Nitschke, 2013). Heat mortality follows a J-shaped function with a steeper slope at higher temperatures (McMichael, and Haines 1996; Patz and Campbell 2005). It is further claimed that the deaths and illness caused by deadly heatwaves are preventable to some extent (Nakai and Itoh, 1999; Kovats and Kristie, 2006). Heatwaves are mainly linked with particularly hot sustained temperatures that may cause essential impacts on human mortality, regional economies and ecosystems (Meehl and Tebaldi, 2009).

Global average temperatures are projected to rise between 1.4℃ and 5.8℃ by the end of this century (Xu and Zhou, 2017; Kraaijenbrink and Bierkens, 2017). With climate change, hot days and heatwave events are projected to become more frequent and severe (Meehl and Tebaldi, 2007; Hayhoe and Sheridan 2010). In the context of projected climate change which is associated with the increase of heatwaves of higher intensities and longer durations (IPCC, 2018) along with rapid rise in urbanisation, the urban inhabitants can be at higher risk than ever before. Cities are where climate change will have the most significant impact on population health (Bambrick and Capon 2011).

Moreover, urban areas experience urban heat island (UHI) effect which causes the urban areas to be at a relatively warmer temperature than its adjacent rural zones (Oke et al., 1982; Taha et al., 1997). As urban areas and urban population grow, vulnerability to heat-related mortality seems likely to increase in the future (Patz and Campbell 2005). These UHIs during a heatwave may exacerbate extreme climatic events causing potentially negative impacts on human comfort levels (Dousset and Gourmelon, 2011; Tan and Zheng, 2010).

In Australia, temperatures have risen by about 1°C (on average) since 1950, and parts of eastern Australia have warmed by 2°C (Hanna and Kjellstrom 2011). As a wealthy, a highly urbanised country subject to extreme weather, Australia can provide a useful analogue for the potential consequences and opportunities elsewhere in the region (Bambrick and Capon 2011). Our knowledge of climate change vulnerability and, therefore, adaptation options, is not well developed. Understanding vulnerabilities and adaptation strategies involve interdisciplinary approaches linking physical, ecological, and social science. The effects of urbanisation on weather and climate at different temporal and spatial scales need further attention because of rapid urbanisation processes occurring over the last few decades. It is particularly important in cities to better understand the influence of urbanisation on temperatures and related processes to improve the adaptive capacity in cities.

To monitor the temperature changes particularly in cities and their impact on urban inhabitants during heatwaves, many studies have been conducted. However, most of the studies utilised ground based data since it offers high temporal coverage with data each hour, whereas satellite data was restricted to four passes a day (MODIS). The modern advnacements in technology have now allowed to monitor the surface with better temporal resolutions, such as geo-stationary satellites offer high temporal coverage with 10 min interval. For Australian region, geo-stationary satellite Himawari-8 to 9 provides real time data every 10 min. The satellite was launched by Japanese Aerospace Exploration Agency (JAXA) to monitor the earth. In this study we explored high temporal resolution data from Himawari-8 to map the diurnal characteristics of extreme heat wave influence on UHIs in Sydney, Australia.

In this chapter, I tried to mainly answer the research question about the unknown dynamics and impacts of extreme heat events on UHIs in cities. The first aim of this chapter is to demonstrate that the Himawari-8 high temporal resolution data can be used to monitor the diurnal foot prints of UHI intensity during a heatwave. This claim is demonstrated by analysing a case study of the UHI in Sydney which was hit by a series of heatwaves from January to February 2017. To the best of our knowledge, this study is the first to use such high temporal resolution data for monitoring heatwave impacts on UHI. The second aim of this chapter is to investigate UHI patterns during the heatwave. The third aim is to evaluate the within city variations in UHI during the heatwave. The results of this chapter reveal how UHI acts on extreme heat in urban areas. The objectives of this chapter will be as follows: (1) To analyse diurnal variations in UHI and quantify its intensity around the metropolitan area during a heat wave event using high temporal resolution data of Himawari-8. (2) Analyse MODIS based observations to further detect the effect of extreme heat wave on diurnal UHIs in cities.

5.2 Data and Methods

5.2.1 Study Area

The city of Sydney was selected to monitor the impacts of extreme climate on UHI footprints at diurnal scale.

5.2.2 Synoptic Background

According to reports published, the summer of 2016-17 in Australia broke more than 205 climate records and included several extreme heatwaves in January and February (BOM, 2017). In January and February, south-east Australia was hit by series of distinct heatwaves, with the deadliest one recorded over 9 to 12 February in 2017 (BOM, 2017). Sydney and Brisbane were the cities in Australia that experienced their hottest summers on record in 2017 (BOM, 2017). Fig.5.1(a) shows the heat wave condition as seen by BOM on 10^{th} of February in 2017 across south-east Australia Fig.5.1(b) shows Sydney reached its highest number of severing heat in 2017 summer. It was further reported that Sydney experienced temperatures in the 97th percentile in summer of 2017, which means the temperatures were in the range of the top 3% of all January/February days since 1911 (BOM, 2017).

A

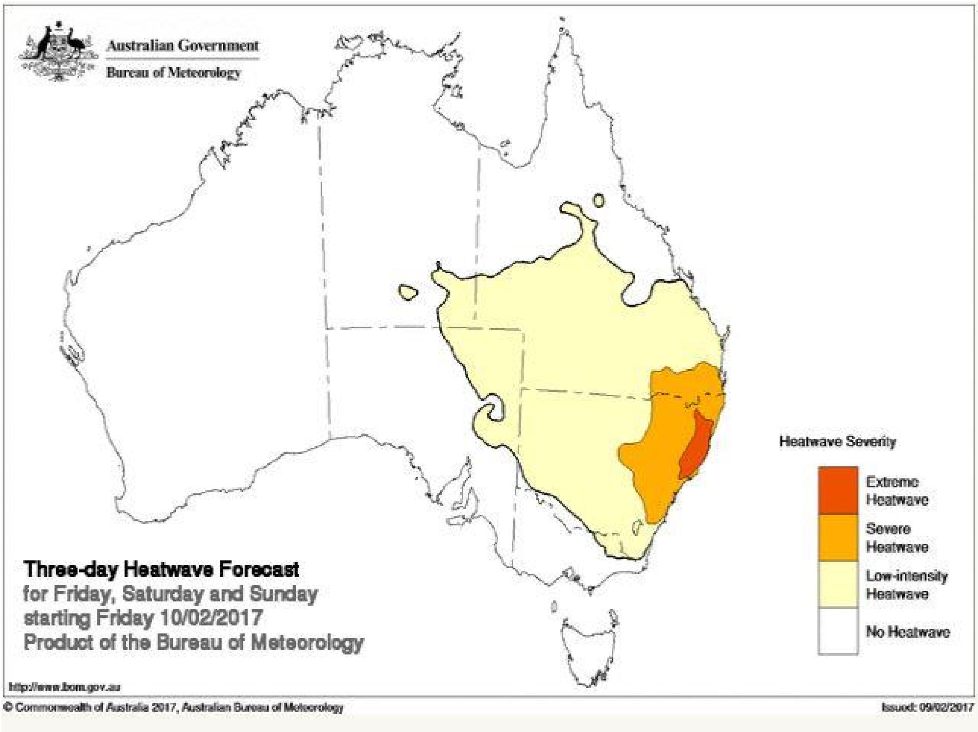

B

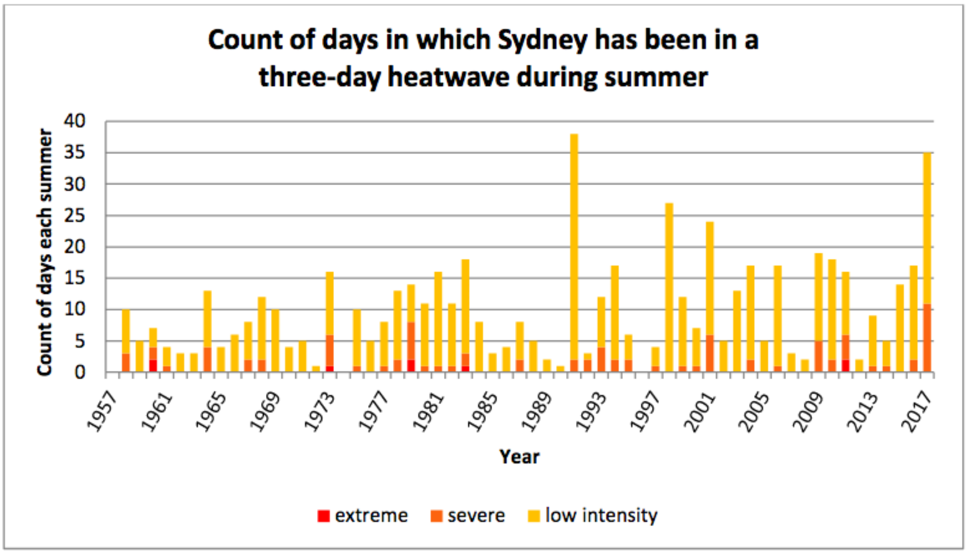

Figure 5.1. (a) Shows the heat wave plot for Friday, Saturday and Sunday (10-12 February 2017), the figure is modified from http://www.bom.gov.au/ dated 05 Oct 2017; (b) Count of days in which Sydney has been in a three-day heatwave during summer, where it can be seen 2017 summer has recorded one of the most of number of days as three-day heatwave after 1991, the figure is modified from http://www.bom.gov.au/ dated 12 Nov 2018.

5.2.3 MODIS based LSTs and UHI

MODIS-8 day products, which were utilised in previous chapters were acquired for the heat wave event dates. The daily data from MODIS may have contamination from clouds, including its thermal data, therefore 8 day composites were preferred in comparison to daily data. The analyses were carried out to show the initial results from MODIS. Since MODIS provided a comppsite of 8 days to look at the heat wave, a better temporal resolution data could be more useful. Hence, we acquired and processed Himawari-8 data to look at 10 min interval data for Sydney during the devasting heat wave of 2017 summer. We also acquired MODIS daily data for validation of Himawari-8 based LST products.

5.2.4 Himawari-8

Himawari-8 launched by Japan Meteorological Agency (JPA) carries an Advanced Himawari Imager (AHI) sensor similar to Advanced Baseline Imager (ABI) onboard the Geostationary Operational Environment Satellite sensor (GOES-16) of NASA. The Himawari-8 offers real-time data with a 10 min interval over Australian region. The data are available in level-1 and level-2 products at JPA website for download (http://www.jpa.com.jp). The products range from surface reflectance to brightness temperature with spatial resolution ranging from 500 m to 2 Km.

5.2.5 Himawari-8 derived LST Data

For the subject study, we acquired the brightness temperature data (BT) for the Sydney region in Australia from January to February 2017 with 10 minutes interval from JPA website (http://www.jpa.com.jp). To convert the BT data into LST, we utilised the formula derived from Split-Window LST (SW LST) algorithm of Ulivieri and Cannizzaro (1985) (Equation 1).

$$LST = C + A_1T_{14} + A_2(T_{14} - T_{15}) + A_3\frac{\varepsilon_{11.2} - \varepsilon_{12.3}}{2} + \mathrm{D}(T_{14} - T_{15})(\sec\theta - 1)$$

Equation (1)

Where, In Equation (1), T_{14}, and T_{15} represents brightness temperature in band-14 (wavelength = 11.2 µm), and band-15 (wavelength = 12.3 µm) in Himawari-8 respectively. ε and θ represents surface emissivityand satellite zenith angle respectively in respective bands. The constants used in equation (5.1) are given in table 5.1, which were adopted from the technical document, GEOS-R Advanced Baseline Imager (ABI) Algorithm Theoretical Basis Document for Land Surface Temperature by Yunyue et al. (2010).

Table 5.1. Shows the constants given in equation (1) and their values as adopted from technical document, GEOS-R Advanced Baseline Imager (ABI) Algorithm Theoretical Basis Document for Land Surface Temperature by Yunyue et al. (2010).

Condition	**C**	**A1**	**A2**	**A3**	**D**
Dry	45.257935	0.985361	1.332220	-41.750015	0.035390
Moist	52.651920	0.930713	2.408630	-35.962742	-0.219514

The coefficient presented in Table 5.1 are for Day (solar zenith angle < 85°) and two atmospheric conditions (Dry Atmosphere: water vapor < 2.0 g/cm2 and Moist Atmosphere: water vapor >2.0 g/cm2). The surface emissivity and water vapour needed in the implementation of LST algorithm were acquired from level-3 MODIS-Terra global products, MOD11A2 and MOD08_E3 available from NASA LAADS web (http://ladsweb.nascom.nasa.gov/). The MOD11A2 product contains 8-days composite (average value) of global LST (at day and nighttime) and emissivity data (at ~11 µm and 12 µm) for a clear-sky at 1 km spatial resolutions. The MOD08_E3 contains global 8-day composite (average value) of atmospheric data (atmospheric water vapour) at the spatial resolution of 1° X 1°. The derived LST were further validated using MODIS daily data.

5.2.6 Ancillary Data

Data on urban local governing areas (LGAs) were acquired from Australian Bureau of Statistics to analyse the LST/UHI variations inside the city. This was done by selecting a few suburbs in the west, east and north parts of the city area. Selecting a few LGAs in the city also gave an overall idea of UHI variations inside the city during a heat wave event. In this regard it was not found necessary to select all 44 LGAs in Sydney area. The means were calculated over each selected LGA to map particular suburban LSTs and UHIs over time. Then the means were calculated over each selected LGA to map particular suburban LSTs and UHIs over time. The LULC data were also acquired from ABS (2016) and were utilised to derive UHI maps and LST patterns in respective LULC classes during heatwave event.

5.2.7 UHI Quantification and Contour Plots

To analyse the UHI the methods used in chapter 3 were adopted. The LULC data were also acquired from ABS 2016 database.

5.2.8 Comparison of heat wave LST/UHI with average LST/UHI in summer

Plots were generated for BT, LST and normalised LST from 9 to 12 February, 2017. The data were normalised to analyse the timings of temperature drop and rise in each LULC class during heat wave event. By normalising I mean scaling the values between 0 and 1. To further understand the influence of heat wave on existing UHI, we compared the LST/UHI on heat wave event (9-12 February 201) with an average February LST/UHI data (2016). Both datasets were extracted from Himawari-8 derived LSTs and UHIs by compositing the data for selected dates. For example, for the heatwave, I did a composite over 9 to 12 February in 2017, and for monthly average, a composite was created over 01 February to 28 February in 2016. The composites were generated using the weighted average algorithm.

5.2.9 Workflow

Fig.5.2 shows the methodology followed for this chapter.

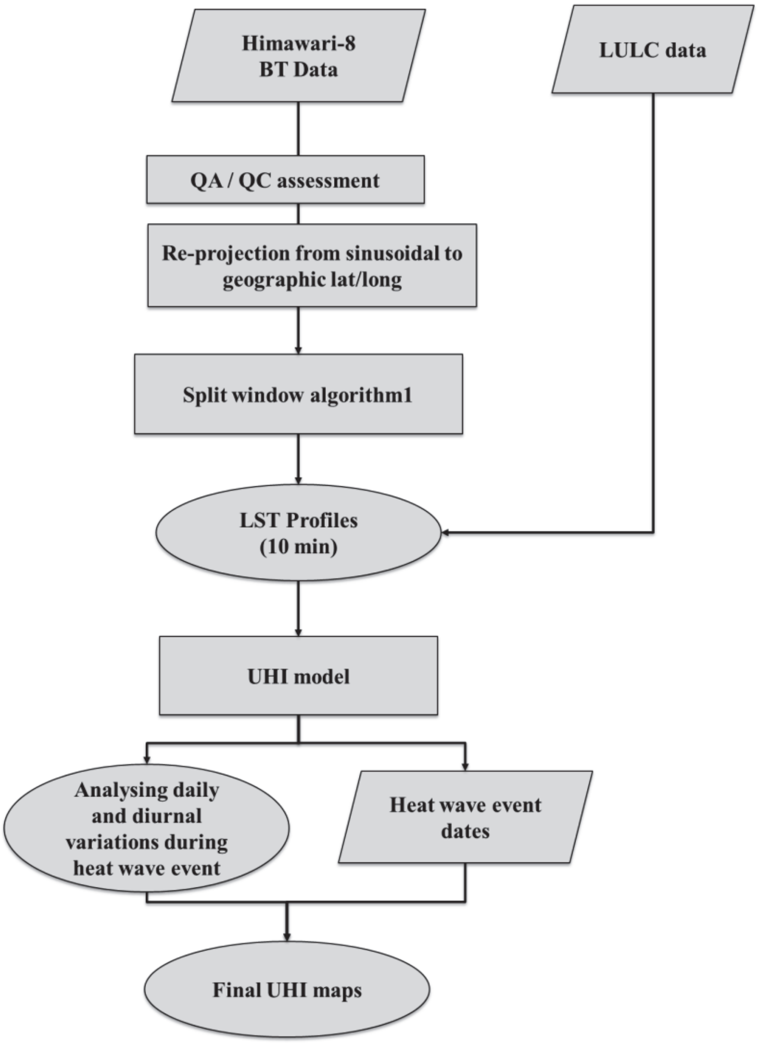

Figure 5.2. Workflow followed for Himawari-8 data analysis.

5.3 Results

5.3.1 Heat Wave as seen in MODIS

Fig.5.3 shows diurnal patterns in LST and UHI as extracted from MODIS 08-day composites over Sydney dated 08 February 2017. The images show warmer temperatures and eventually extreme UHI intensities in daytime particularly at 2 pm during the heat wave event in the region. These figures further illustrate that the Sydney experiences relatively warmer temperatures in its west, up to 50°C. The UHI was also as high as 10°C particularly at daytime (2 pm) in its west. However, the processed data in Fig.5.3 are derived from 08-day composites from MODIS sensor, to better understand the influence of heat wave on UHI footprints and intensity, we need to look at high temporal resolution data. Therefore, we processed high temporal resolution data of Himawari-8, the results are presented in the next section.

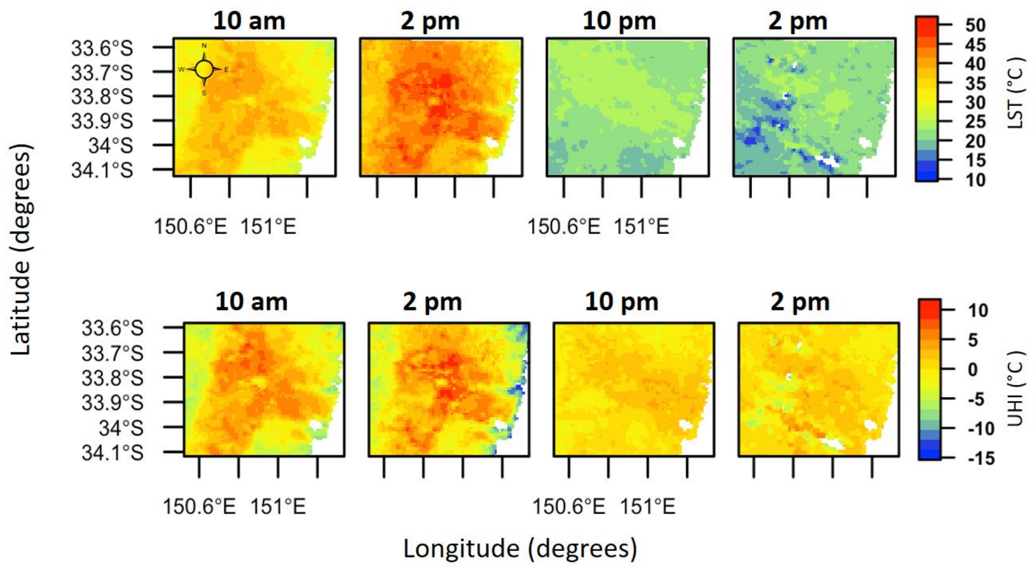

Figure 5.3. LST and UHI maps at diurnal scale over Sydney from derived from MODIS 08 day composites (10-02-2017).

5.3.2 Himawari-8 Brightness Temperature (BT) Results

Fig.5.3(a) illustrates the BT recorded at Himawari-8 sensor from 01 to 14 February in 2017 over urban Sydney. Since from above study we know that the heat wave started on 9 February and ended on 12 February, Fig.5.4 further illustrates us that city of Sydney recorded warmer temperatures and peaked particularly on 10th of February in 2017. BOM also reported 10th of February as the highest February temperature recorded at Sydney Airport in last few decades.

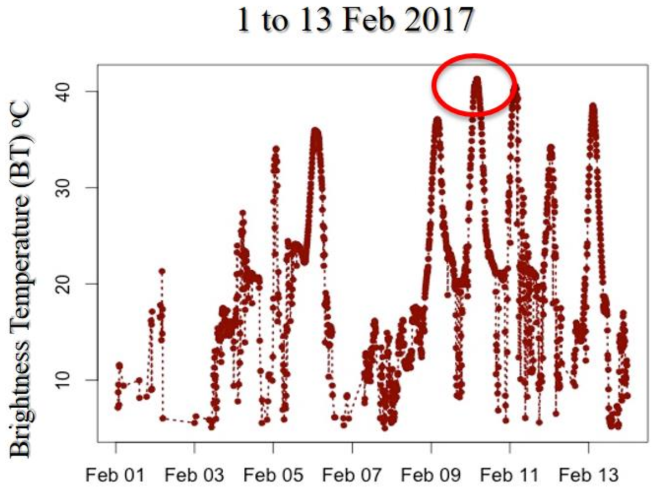

Figure 5.4. Brightness Temperature (BT) results as seen in Himawari-8 data from 1 February to 14 February in 2017 over Sydney region during the heat wave event

These results provided the evidence that Himawari-8 recorded the higher temperatures, to better analyse, we converted these BT values into LST values and processed, the results are given in the next section.

5.3.3 Himawari-8 derived LST

Fig.5.5(a) shows the scatter plot and the correlation coefficient between Himawari-8 derived LST with MODIS based daily LST product of NASA. Results indicated a good correlation coefficient for the derived LST values from Himawari-8 (R =0.8305). Fig.5.5 (b) shows the images for LST derived from Himawari-8 and MODIS based daily LST product of NASA for 10 February in 2017.

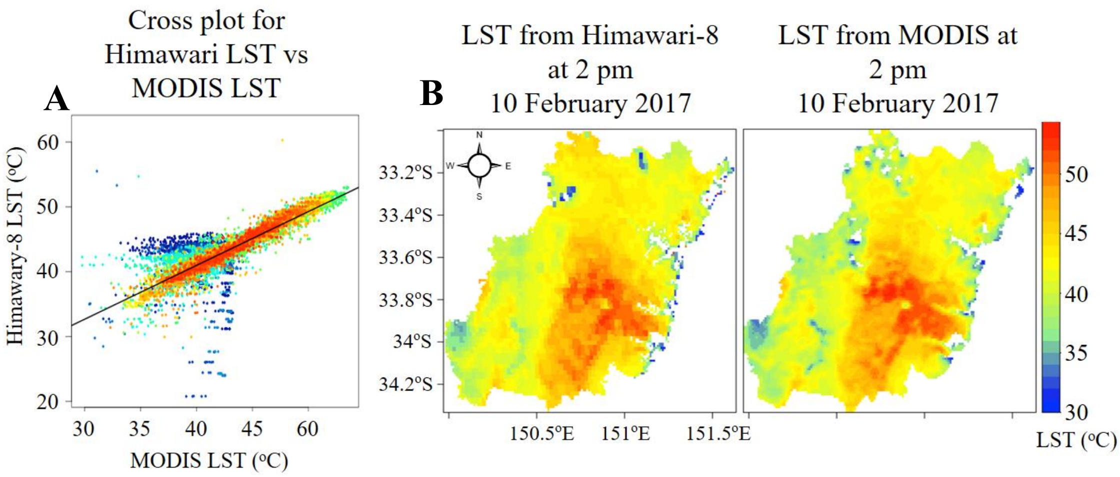

Multiple R-squared: 0.7461
Adjusted R-squared: 0.7461
R = 0.8305

Figure 5.5. (a) Cross plots, the solid line represents the correlation of 0.8305 between Himawari-8 derived LST and MODIS daily LST at 2 pm (b) images of MODIS derived LST and Himawari-8 LST MODIS LST dated 10 February 2017.

5.3.4 Himawari-8 LST results (9 to 12 February 2017)

Fig.5.6 shows the plot of LST derived from Himawari-08, over Sydney urban and its adjacent non-urban zones, from 9 February to 12 February in 2017. It can be seen that the urban zones during the heat stress are at relatively warmer temperatures at daytime, LST reaching as high as 44°C, 48°C, 47°C and 42°C on 9th, 10th, 11th and 12th February, particularly at daytime (1 pm to 4 pm) as on average. The rural zones, in our study area, are at relatively lower temperatures, particularly forested zones are cooler at daytime. From the previous chapter, we already know that forest acts as a stable class, while pasture remains highly dynamic due to its seasonality features. In our results, in Fig.5.6, pasture remains unstable throughout the heat wave event, with temperatures as high as the urban regions. Fig.5.7 shows the normalised LSTs, where it can be seen that the decreases in

LST occurred with the same timing for all LULC in all classes. These spikes seen in the evening of Feb 11 – 13 are due to noise in the data, since the data are 10-minute interval.

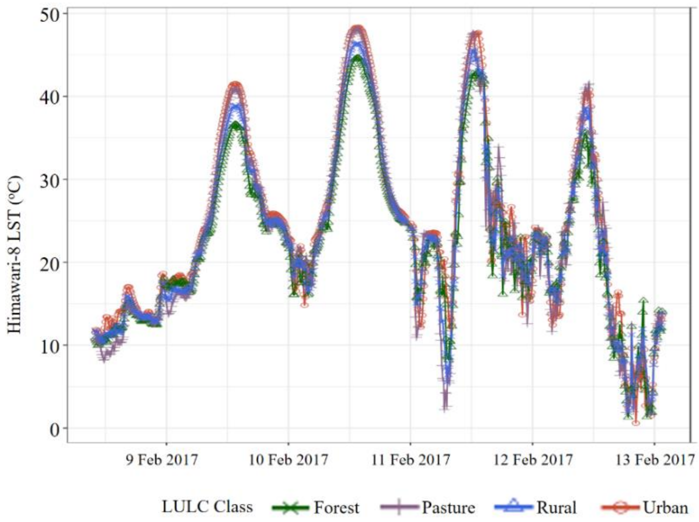

Figure 5.6. Himawari-08 derived LST means plotted from 9 February to 12 February, 2017 over urban, rural, pasture and forest LULC classes in Sydney region.

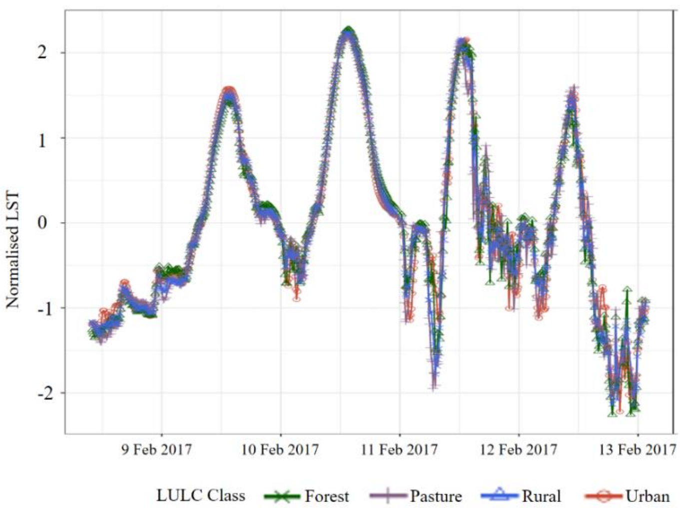

Figure 5.7. Normalised LST means from Himawari-8, plotted from 9 February to 12, 2017 over urban, rural, pasture and forest LULC classes in Sydney region.

Fig.5.8(a) shows the LST plot on 9th February 2017, where it can be seen that the urban areas reach their peak temperature on that day from 12 pm till 3 pm (LST> 40°C).

Forested zones remain relatively at cooler temperature (LST < 40°C). It can also be observed from these results that as temperature rises, the difference between urban and its surrounding areas also increases, including the difference between urban and forest peaks at 2 pm. Fig.5.8 (b) illustrates the LST maps at hourly intervals, where it can be seen that the urban areas are at relatively warmer temperatures. In addition, western Sydney is seen to remain at relatively warmer temperatures than eastern and northern Syndey. Fig.5.8(c) depicts the histograms for each class at hourly intervals. It can be seen from the results that the absolute difference between urban and forest medians remain significant all day and with varying intensity. Fig.5.9 and Fig.5.10 show the diurnal plots and maps on the 10th and 11th of February in 2017. These results show us that the urban zones are above 45°C on February 10 and 11, particularly in daytime. On the other hand, forested zones show much more resilience with the lowest temperatures during the heat wave event, which remained at below 45°C at daytime on February 10 and 11 (Fig.5.9 and Fig.5.10). The pixel-based slopes indicate that the city reaches its warmest temperatures at daytime particularly between 1 pm to 3 pm.

Moreover, the results further indicate that during the subject heat wave, the city was relatively warmer in its west than in its east or north (Fig.5.9(b) and Fig.5.10(b)). Fig.5.9(c) and Fig.5.10(c) shows histograms which indicate the distribution to be statistically significant (p-value <0.05). The next section shows results in western suburbs in the city and some eastern and northern suburbs and their LST pattern on selected dates.

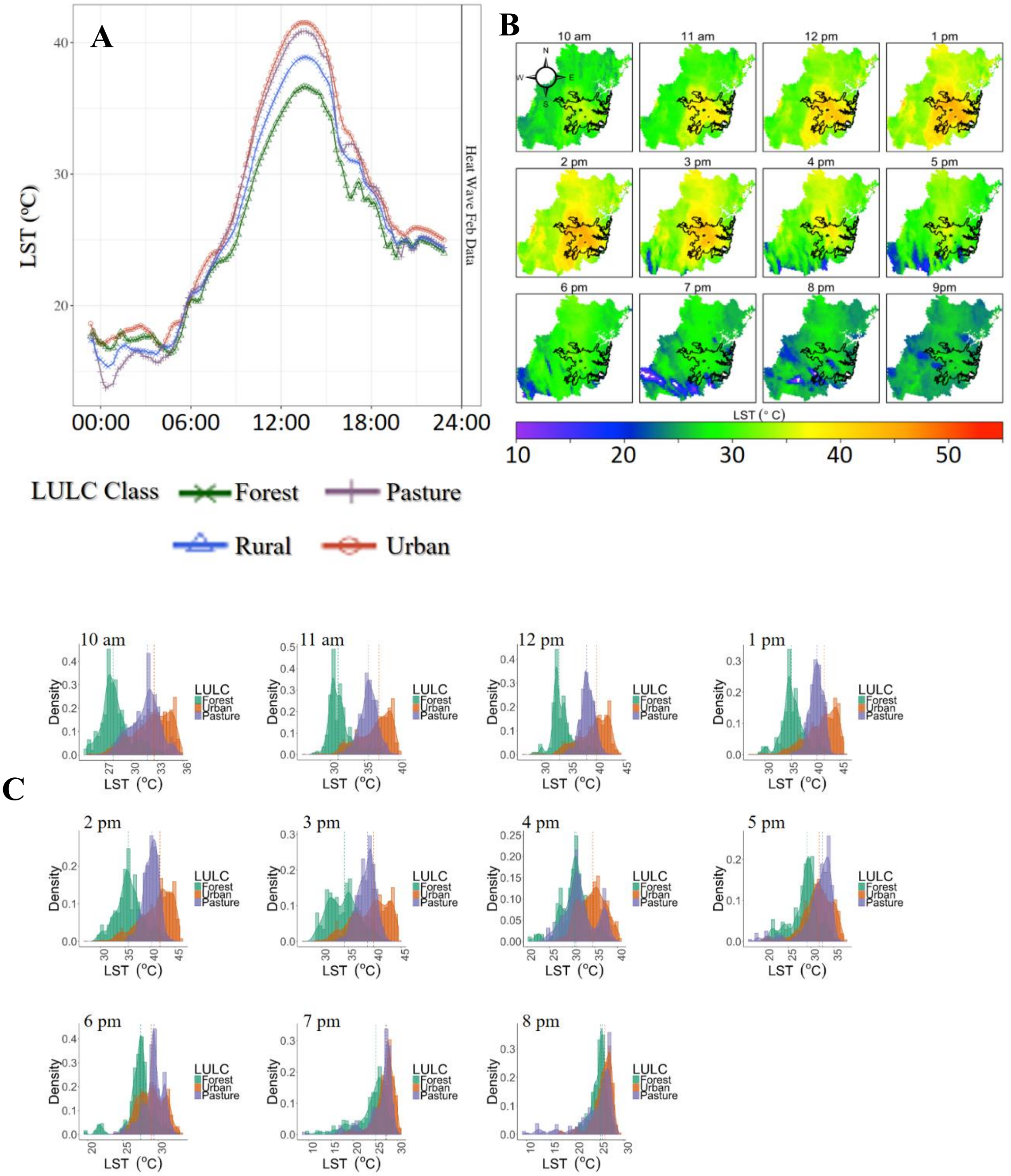

Figure 5.8. (a) February 9, 2017 mean LST variation across Sydney urban and adjacent rural LULC classes (10 min gap); (b) LST spatial variations over Sydney region, the black polygon represents ABS urban boundary as extracted from its Mesh blocks LULC data (ABS, 2016) (hourly gap); (c) Histograms for urban and its two major rural LULC classes that are forest and pasture (hourly gap).

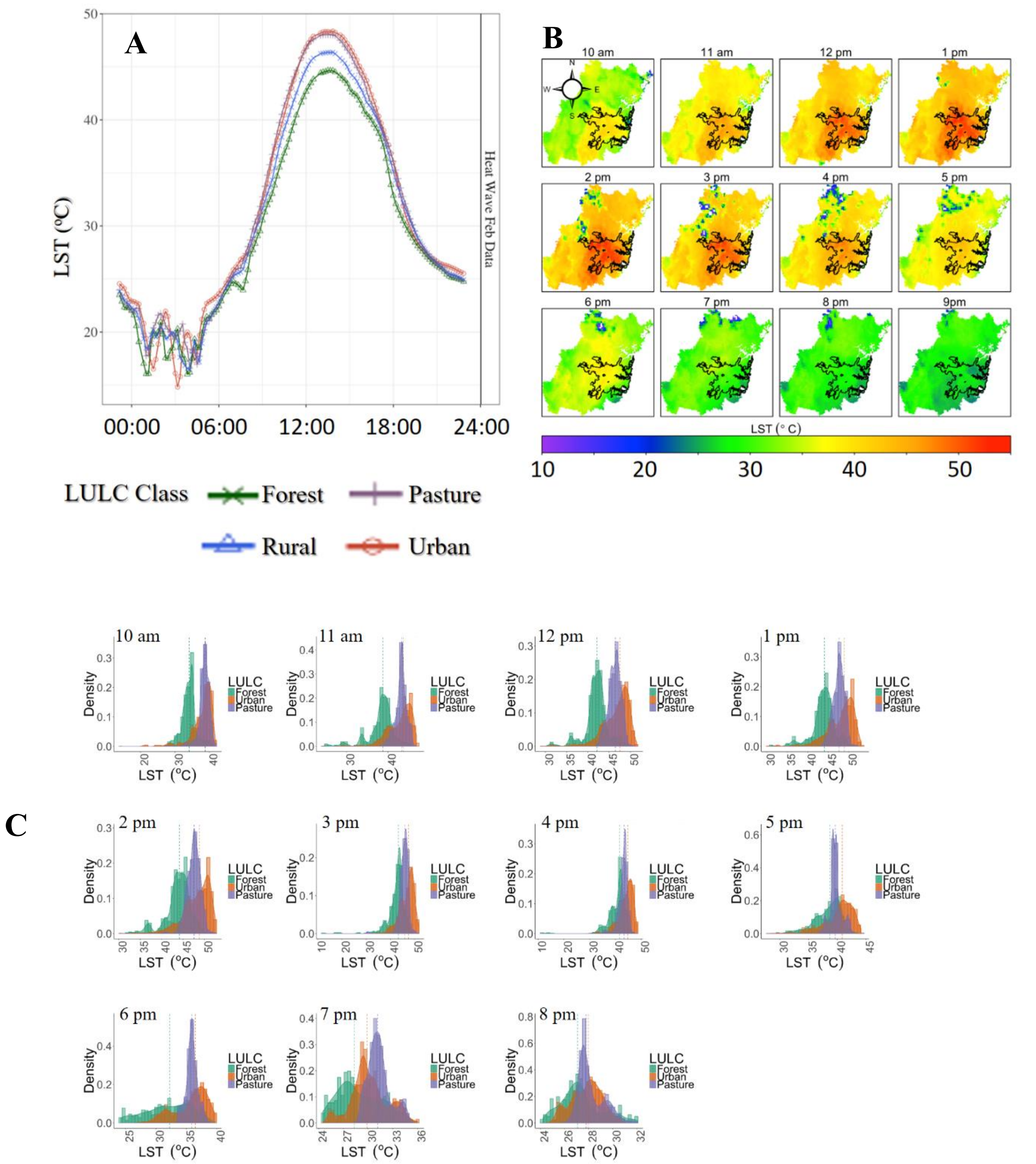

Figure 5.9. (a) February 10, 2017 mean LST variation across Sydney urban and adjacent rural LULC classes (10 min gap); (b) LST spatial variations over Sydney region, the black polygon represents ABS urban boundary as extracted from its Mesh blocks LULC data (ABS, 2016) (hourly gap); (c) Histograms for urban and its two major rural LULC classes that are forest and pasture (hourly gap).

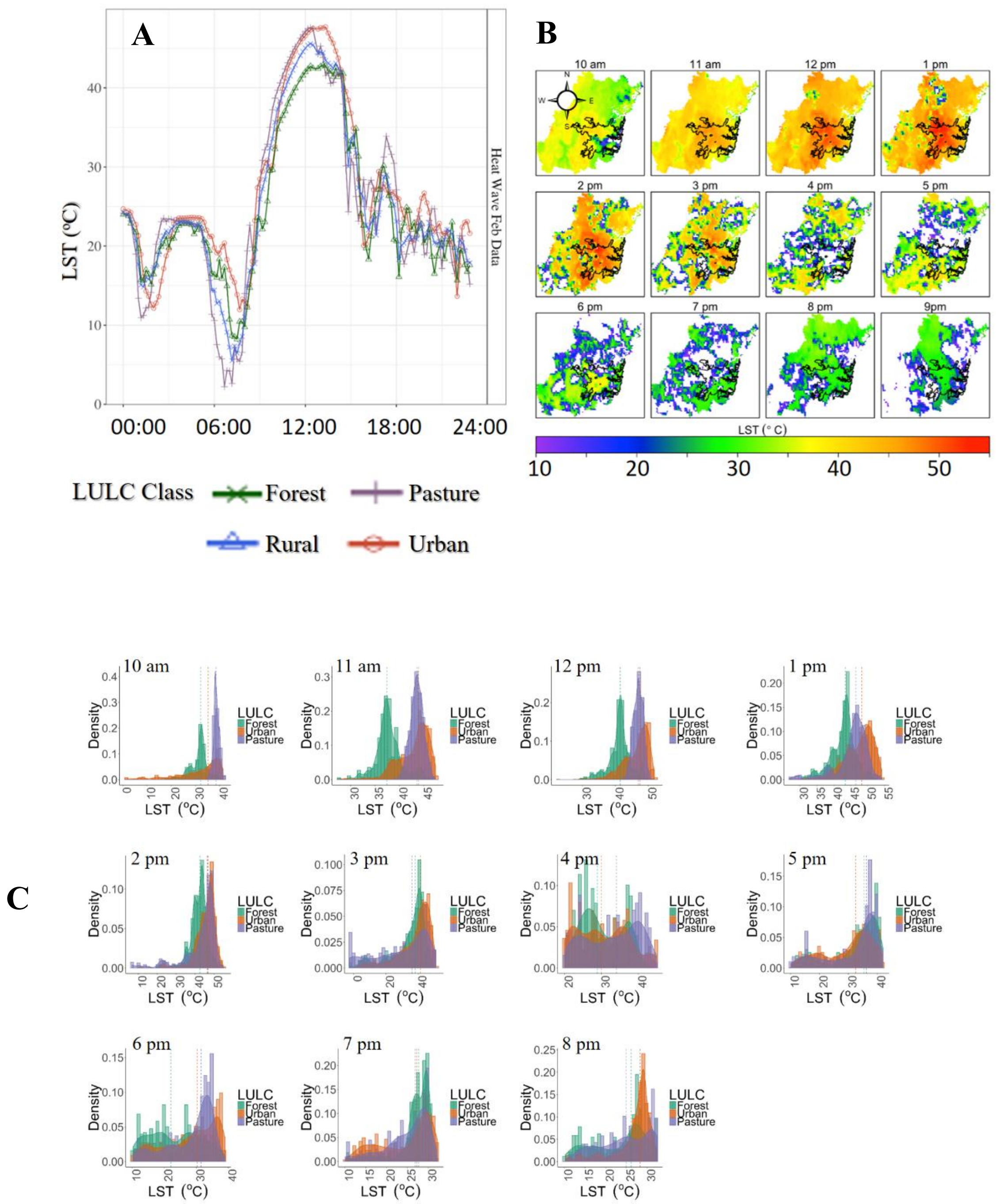

Figure 5.10. (a) February 11, 2017 mean LST variation across Sydney urban and adjacent rural LULC classes (10 min gap); (b) LST spatial variations over Sydney region, the black polygon represents ABS urban boundary as extracted from its Mesh blocks LULC data (ABS, 2016) (hourly gap); (c) Histograms for urban and its two major rural LULC classes that are forest and pasture (hourly gap).

5.3.5 Himawari-8 UHI results (9 to 12February 2017)

Fig.5.11 shows the UHI plot (with 10 mins gap) and maps (with an hourly gap) dated 9th February. Since from previous analysis, we know that forests act as a stable reference and pastures remain an unstable reference when calculating UHI. Fig.5.11(a) clearly shows that the mean of UHI_{forest} reaches as high as 5°C on the selected date. In addition to it, the mean of UHI_{rural} reaches as high as 2.9°C on the same day. Fig.5.11(b) shows pixel-based results for UHI where some pixels reached an intensity of 8°C - 9°C, particularly at daytime (1 pm- 3 pm), 4°C - 5°C at afternoon time (7 pm) and 2°C - 3°C at nighttime (8 pm – 9 pm).

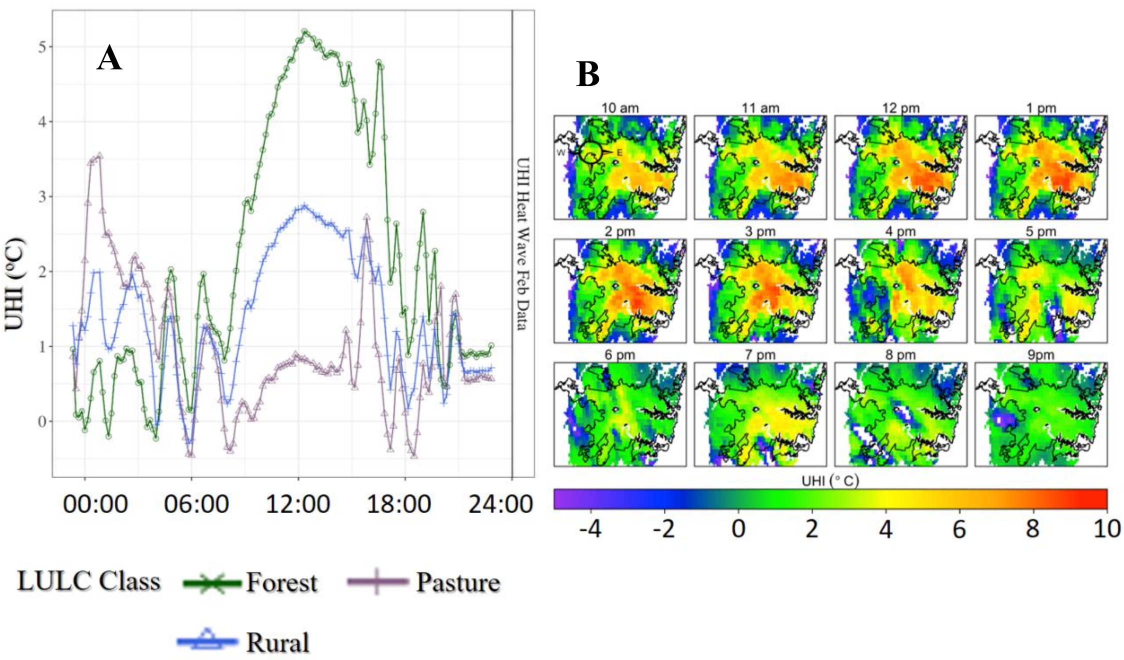

Figure 5.11. UHI dynamics for February 9, 2017 (a) plot for mean UHI over Sydney urban and adjacent rural LULC classes; (b) images for UHI spatial variations over Sydney region, the black polygon represents ABS urban boundary as extracted from its Mesh blocks LULC data (ABS, 2016).

Fig.5.12 also shows similar patterns however with less severe intensity on the selected day. Fig.5.12(a) indicates that UHI_{forest} reaches a mean UHI value of 4°C at daytime and 3°C at nighttime. Fig.5.12(b) further illustrates the hot spots inside the city, which remains dominant throughout the day with few places reaching highest UHI of 8°C in the day (1 pm - 3 pm), 4°C at evening time (6 pm) and 2°C at nighttime (8 pm - 9 pm).

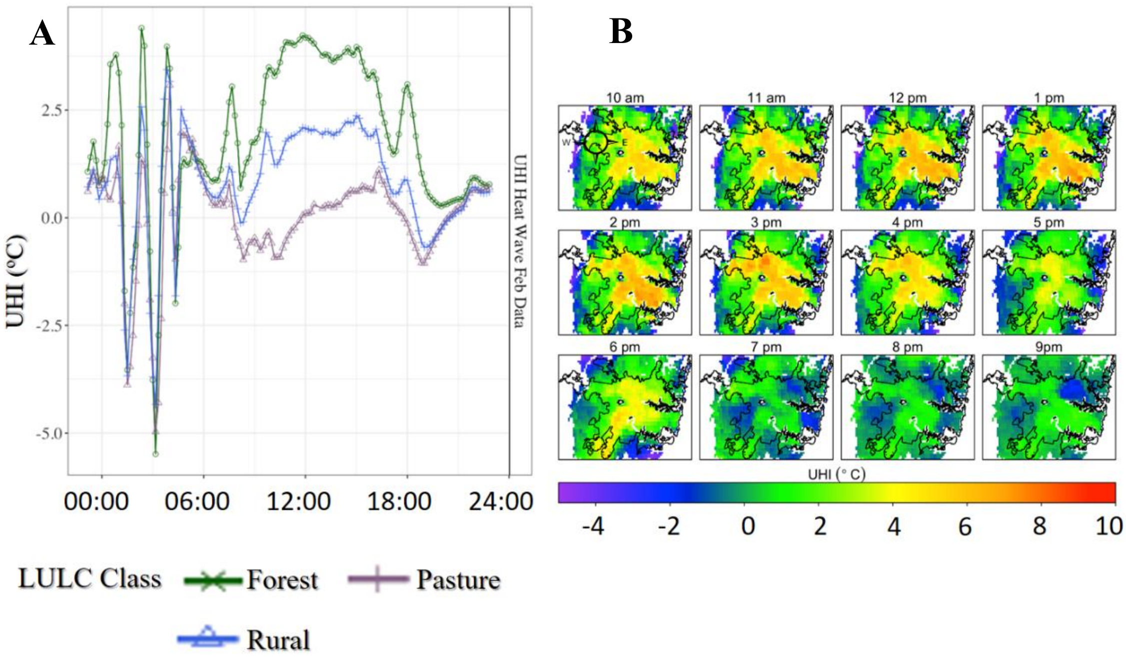

Figure 5.12. Sydney UHI comparisons, derived from Himawari-8, resulting from the use of different rural class references. (a) plot for mean UHI over Sydney urban and adjacent rural LULC classes for February 10, 2017; (b) images for UHI spatial variations over Sydney region, the black polygon represents ABS urban boundary as extracted from its Mesh blocks LULC data (ABS, 2016).

To better understand the UHI during the heat wave and no heat wave situation, we further compared the average UHI in February (2003 – 2016) with UHI during the particular heat wave. The results are presented in the next section.

5.3.6 LST/UHI variations inside the city

From the above analysis, we saw that Sydney was much warmer during the heat wave in its west than in its north or east. Fig.5.13 further supports our study, where plots for 9 February and 10 February show diurnal LST curves of a few suburbs inside the city of Sydney, which are, ‘Blacktown’, Sydney CBD’ and ‘Hornsby’. The results illustrate that ‘Blacktown’ which is a suburb in the west of Sydney, is at relatively warmer temperatures. On the other hand, the results further indicate that the suburb of ‘Sydney CBD’ and ‘Hornsby’, which are located in the east and north respectively, remain relatively cooler during the extreme heat wave event. In addition to it, ‘Blacktwon’ also experiences longer durations of warmer temperatures in the day as compared to ‘Sydney CBD’ and ‘Hornsby’ (table 5.2).

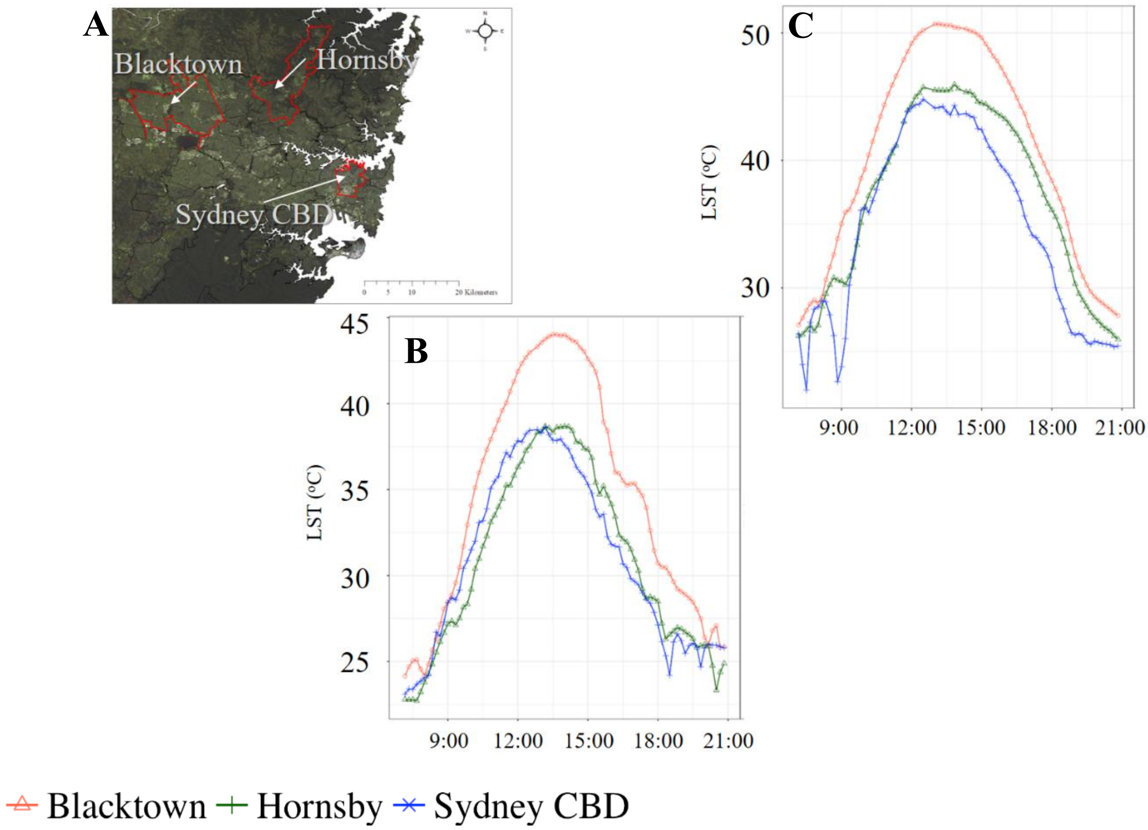

Figure 5.13. (a) Shows selected suburbs inside Sydney city (red colour polygons), which are 'Blacktown', 'Hornsby' and 'Sydney CBD' as seen in Satellite image of Landsat-8 dated 08-09-2015; (b) the Himawari-8 derived LSTs recorded on 9 February 2017 with 10 min interval over selected suburbs; (c) the Himawari-8 derived LSTs recorded on 10 February 2017 with 10 min interval over selected suburbs.

Moreover, these results indicate that 'Blacktown' not only remains at a relatively warmer temperature than other selected suburbs but also experience these warmer temperatures for the longest time of the day since the standard deviation values are relatively higher than other selected suburbs. In addition to, when temperature rises in the region, for example, on 10 February maximum temperatures reach 50°C, then all suburbs experience relatively longer times of warmer temperatures, and again 'Blacktown' remains warmer for the longest time of the day than other suburbs in east or north of the city. Blacktown remains highly built suburb with less vegetation cover, whereas Hornsby is relatively greener than Blacktown and Sydney CBD. The suburb of Sydney CBD remains relatively cooler due to coastal effect.

Table 5.2. Shows the statistical analysis for selected suburbs inside the city

	Blacktown		Hornsby		Sydney CBD	
	9 Feb	10 Feb	9 Feb	10 Feb	9 Feb	10 Feb
Standard deviation	6.68	8.13	5.18	7.0	5.01	7.15
Area under the curve	1707935	2003021	1525888	183349,5	1528022	1722439

Fig.5.14 shows the UHI of selected suburbs inside the city. It can be seen that all suburbs experience highest UHI values, particularly on 10 February when temperatures are worst in the region. These curves further provide evidence of UHI interaction with the heat wave, which not only causing the UHIs to go higher but also making the built-up environment lazy in loosing back the heat to the atmosphere. Eventually, it causes the cities to be at hotter temperature for the longest time of the day inside the city.

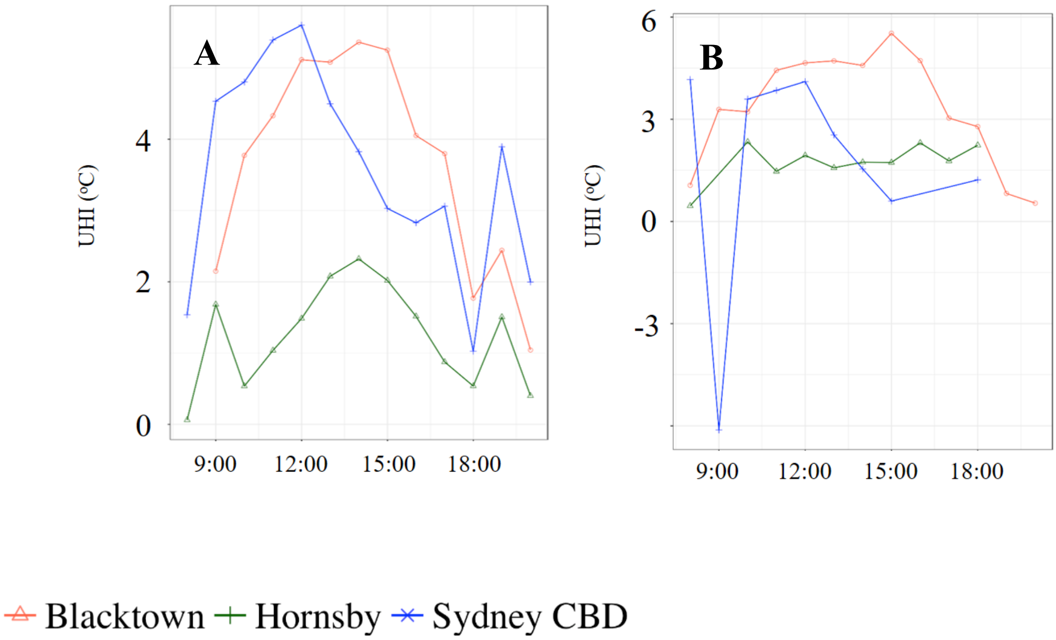

Figure 5.14. Shows UHI curve over selected suburbs inside the city of Sydney (a) on 9 February 2017; (b) 10 February 2017.

5.3.7 Comparing Average February with heat wave LST

Fig.5.15 shows the histogram analysis on urban LST as measured for February (2016) and for 9-12 February in 2017 at daytime (2 pm). We can observe that the heat stress warms the city with an absolute temperature difference of 9°C than on regular February days. The histogram also shows that the absolute difference to be significant (p-value < 0.05).

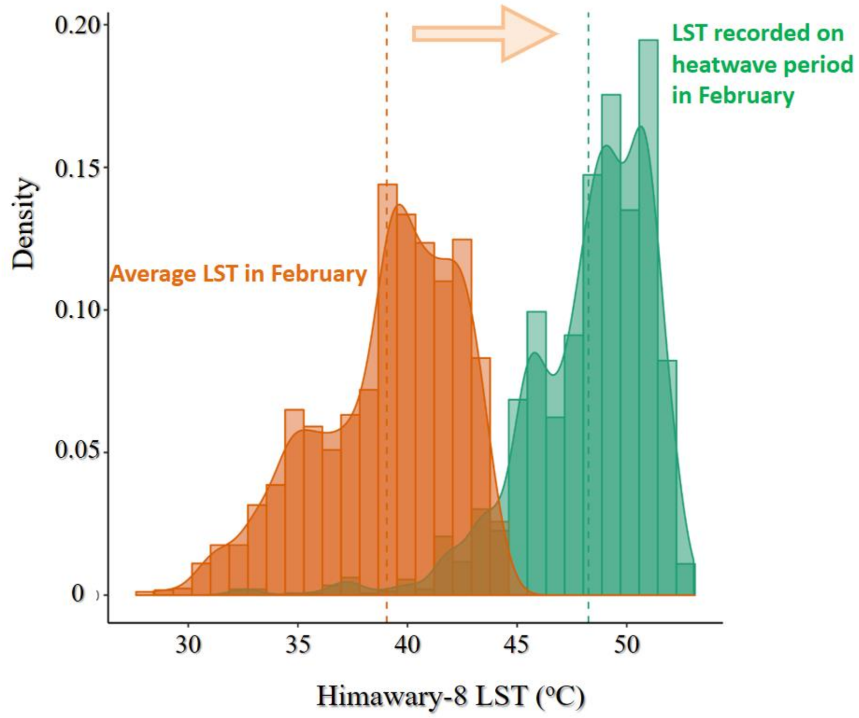

Figure 5.15. Himawari-8 LST values over urban pixels in Sydney, plotted for the average February 2016 (orange colour) and February 9-12 heat wave event (green colour).

5.3.8 Comparing Average February with heat wave UHI

Fig.5.16 shows UHI maps of a heat wave event and of a regular February day (2016), which illustrates the difference of spatial variations across the city during a heat wave and a typical day in February. Furthermore, it indicates that the heat wave causes the UHI to last long as UHI starts diminishing on an average day by 5 pm but on a heat wave day it continues till 6 pm, or an hour more, particularly in the western suburbs of the city. Furthermore, during the heat wave, the footprints of UHI with intensity 7°C expends in the area when compared to an average day.

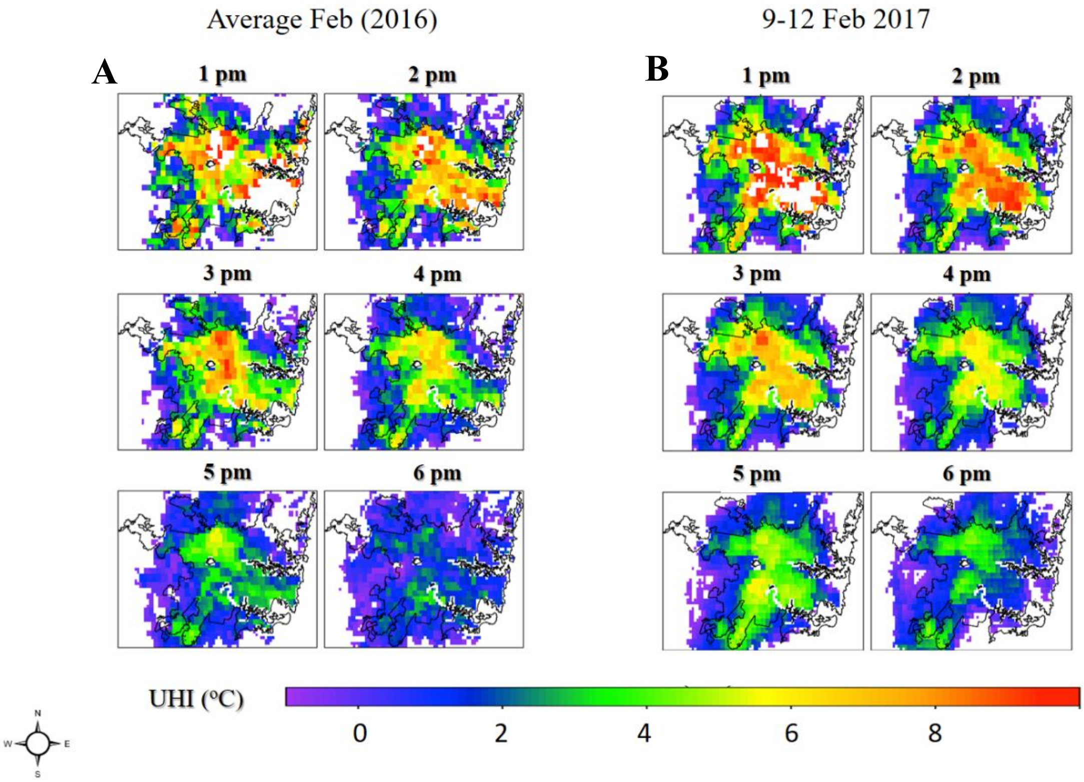

Figure 5.16. Spatial variations in UHI with an hourly gap over Sydney (a) shows the average February 2016; (b) shows heat wave event days (9 – 12 February 2017) as seen in Himawari-08 data.

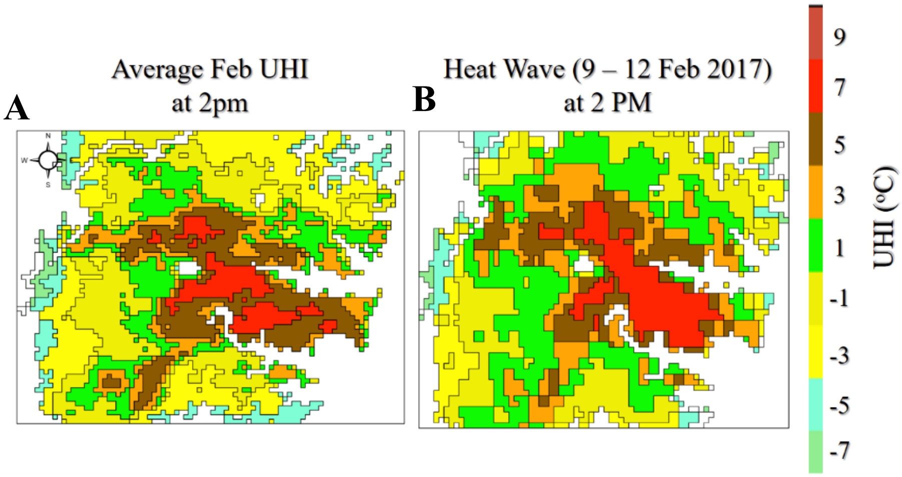

Figure 5.17. Shows contour plots of UHI (a) on an average February 2016 day; (b) heat wave event days (9 – 12 February 2017) at 2 pm (Himawari-08 data).

Fig.5.17 shows the contour plot of UHI daytime (2 pm) for an average February day (2003-2016) and a heat wave day (9-12 February 2017). It can be seen that the area with an intensity of 7°C expends its area by hitting more regions inside the city with a high intensity than on an average day.

5.4 Discussion

This chapter presents a broad study on UHI and heat wave interactions using advanced geospatial data and tools. To investigate the influence of UHI on summer heat waves a case study was carried out for the city of Sydney which was reported to be severely hit by three heat waves in January and February 2017, with record high temperatures from 9 February to 12 February (BOM, 2017). Furthermore, in this chapter, we highlighted the LST and UHI variations across the city at a 10 min/hourly interval over Sydney using recent data of Himawari-08 satellite. The high temporal resolution of Himawari-08 allowed us to look at the heat wave, the existing UHI in the city and its interactions with each other at a much better temporal scale. In the field of urban and peri-urban studies, remote sensing and GIS data are not much explored; this study provides an insight of advanced geospatial datasets in analysing the urban environments with better efficiency and an excellent temporal resolution of 10 mins (Himawari-08).

5.4.1 Himawari-8 LST/UHI (9 to 12-February 2017)

We already know from our previous chapters that forested regions were coolest at daytime in comparison to urban zones, the similar patterns were evident in Himawari-08 satellite 10 min data. During the heat wave event urban zones were seen to reach an average high temperature of more than 45°C whereas the forested regions remained relatively cooler with an average high temperature below 45°C. The pastures being open areas also remained above 45°C on an average. The daily 10 min and hourly intervals further indicated that the during the heat wave particular parts of the city remained warmer for longer times than ones near the coast. Moreover, the city dropped in temperature much later than other adjacent non-built rural regions. Forests were the fastest in losing the heat back to the atmosphere, while urban remained warmer for the relatively prolonged times. We also noted that as the heat stress rose in intensity from 9th February to 10th February, the urban regions became slower in losing the heat back to the atmosphere, as we saw that the length of warm temperatures increased on 10th February when temperatures rose above 45°C. The UHI plots further strengthened our analysis by indicating the intensities to be highest on 9th February than on 10th February. This can well be explained by the fact that since UHI is a difference of temperature between its built and non-built environment, the difference between urban and it's non-urban zones was highest on 9th February however, as the region further warmed, forests started loosing their resilience and also rose in temperature causing the difference and eventually UHI to drop.

5.4.2 Comparing Average February with heat wave

The analysis helped us to understand the influence of climate extremes such as heat waves on existing UHIs in cities at better and efficient scale. Hence we were able to monitor the difference during the heat wave which was causing the UHI to stay longer than regular summer days in February. The analysis further revealed that overall intensity did not change however the UHI footprints were seen to vary in size when hit by heat stress. We also saw that urban LST experienced an absolute temperature difference of 9°C during the heat wave than on regular summer days of February (2016). This analysis showed us that climate extremes could worsen the existing UHIs in the cities, causing it to difficult for urban residents to survive in the wake of projected climate variations. It is highly required to monitor such events and plans our cities better so that we can cope with such extremes. This chapter was a complete work on heat wave and UHI interactions with applications of remote sensing data sets which are easily accessible and feasible to use.

5.4.3 Limitations

The anlaysis was comperhensivc and very much of interest, however, there were few limitations which further need to be resolved. For example we only covered one city for this study and did not include Melbourne, the reason being that Himawari-08 is a geostationary satellite with its static position meant to primarily cover the Japanese region. Whereas, the city of Melbourne is a southern region of eastern Australia, which may cause distortion of pixels in the Himawari-08 captured images. Moreover, the spatial resolution of sensor is 2Km which limited us to conduct regional scale study. In addition, since Himawari-08 is launched in the end of 2015, we were not able to look back at archive data and hence we had to consider 2016 February for comparison analysis. However, the data are still much more benefitial and can be explored further to better map such exteme events at regional scale.

5.5 Conclusion

This chapter presented a comprehensive study on UHI and heat wave event in the city of Sydney in Australia. Furthermore, we presented an efficient way of mapping and monitoring UHI and heatwaves using advanced geospatial data and tools. We conclude from our analysis that UHIs can make the heat waves more deadly and may exaggerate the effects of projected climate change. A better mapping and monitoring strategies are required to make our cities more sustainable for our future generations. From the literature, it is evident that remote sensing data are not much explored in the field of urban environment. However, the data provide much better spatial coverages and temporal resolutions with advancements in technology. It is highly recommended to further explore the data sets in planning for our cities to become more liveable.

5.6 References

Abrahamson, V., Wolf, J., Lorenzoni, I., Fenn, B., Kovats, S., Wilkinson, P., Adger, W.N. and Raine, R., 2008. Perceptions of heatwave risks to health: interview-based study of older people in London and Norwich, UK. Journal of Public Health, 31(1), pp.119-126.

Astrom, D.O., Bertil, F. and Joacim, R., 2011. Heat wave impact on morbidity and mortality in the elderly population: a review of recent studies. Maturitas, 69(2), pp.99-105.

Bonafoni, S., Anniballe, R. & Pichierri, M. 2015, 'Comparison between surface and canopy layer urban heat island using MODIS data', Urban Remote Sensing Event (JURSE), 2015 Joint, IEEE, pp. 1-4.

Bambrick, H.J., Capon, A.G., Barnett, G.B., Beaty, R.M. and Burton, A.J., 2011. Climate change and health in the urban environment: adaptation opportunities in Australian cities. Asia Pacific Journal of Public Health, 23(2_suppl), pp.67S-79S.

Beauro of Meteorology (BOM), < http://www.bom.gov.au/australia/heatwave/about.shtm l>accessed on 01-01-2019.

Dousset, B., Gourmelon, F., Laaidi, K., Zeghnoun, A., Giraudet, E., Bretin, P., Mauri, E. and Vandentorren, S., 2011. Satellite monitoring of summer heat waves in the Paris metropolitan area. International Journal of Climatology, 31(2), pp.313-323.

Gabriel, K.M. and Endlicher, W.R., 2011. Urban and rural mortality rates during heat waves in Berlin and Brandenburg, Germany. Environmental pollution, 159(8-9), pp.2044-2050.

Hanna, E.G., Kjellstrom, T., Bennett, C. and Dear, K., 2011. Climate change and rising heat: population health implications for working people in Australia. Asia Pacific Journal of Public Health, 23(2_suppl), pp.14S-26S.

Huete, A., Didan, K., Miura, T., Rodriguez, E.P., Gao, X. and Ferreira, L.G., 2002. Overview of the radiometric and biophysical performance of the MODIS vegetation indices. Remote sensing of environment, 83(1-2), pp.195-213.

Huete, A., Liu, H., Batchily, K.v. & Van Leeuwen, W. 1997, 'A comparison of vegetation indices over a global set of TM images for EOS-MODIS', Remote sensing of environment, vol. 59, no. 3, pp. 440-51.

Hayhoe, K., Sheridan, S., Kalkstein, L. and Greene, S., 2010. Climate change, heat waves, and mortality projections for Chicago. Journal of Great Lakes Research, 36, pp.65-73.

Kraaijenbrink, P.D.A., Bierkens, M.F.P., Lutz, A.F. and Immerzeel, W.W., 2017. Impact of a global temperature rise of 1.5 degrees Celsius on Asia’s glaciers. Nature, 549(7671), p.257.

Kovats, R.S. and Hajat, S., 2008. Heat stress and public health: a critical review. Annu. Rev. Public Health, 29, pp.41-55.

Kovats, R.S. and Kristie, L.E., 2006. Heatwaves and public health in Europe. European journal of public health, 16(6), pp.592-599.

Meehl, G.A., Tebaldi, C., Teng, H. and Peterson, T.C., 2007. Current and future US weather extremes and El Niño. Geophysical Research Letters, 34(20).

Meehl, G.A., Tebaldi, C., Walton, G., Easterling, D. and McDaniel, L., 2009. Relative increase of record high maximum temperatures compared to record low minimum temperatures in the US. Geophysical Research Letters, 36(23).

Nakai, S., Itoh, T. and Morimoto, T., 1999. Deaths from heat-stroke in Japan: 1968–1994. International journal of biometeorology, 43(3), pp.12

Oke, T.R., 1982. The energetic basis of the urban heat island. Quarterly Journal of the Royal Meteorological Society, 108(455), pp.1-24.

Patz, J.A., Campbell-Lendrum, D., Holloway, T. and Foley, J.A., 2005. Impact of regional climate change on human health. Nature, 438(7066), p.310.

Poumadere, M., Mays, C., Le Mer, S. and Blong, R., 2005. The 2003 heat wave in France: dangerous climate change here and now. Risk Analysis: an International Journal, 25(6), pp.1483-1494.

Scherer, M. and Diffenbaugh, N.S., 2014. Transient twenty-first century changes in daily-scale temperature extremes in the United States. Climate dynamics, 42(5-6), pp.1383-1404.

Seneviratne, S.I., Nicholls, N., Easterling, D., Goodess, C.M., Kanae, S., Kossin, J., Luo, Y., Marengo, J., McInnes, K., Rahimi, M. and Reichstein, M., 2012. Managing the Risks of Extreme Events and Disasters to Advance Climate Change Adaptation: Changes in Climate Extremes and their Impacts on the Natural Physical Environment.

Tan, J., Zheng, Y., Tang, X., Guo, C., Li, L., Song, G., Zhen, X., Yuan, D., Kalkstein, A.J., Li, F. and Chen, H., 2010. The urban heat island and its impact on heat waves and human health in Shanghai. International journal of biometeorology, 54(1), pp.75-84.

Taha, H., 1997. Urban climates and heat islands: albedo, evapotranspiration, and anthropogenic heat. Energy and buildings, 25(2), pp.99-103.

Xiang, J., Bi, P., Pisaniello, D. and Hansen, A., 2014. The impact of heatwaves on workers′ health and safety in Adelaide, South Australia. Environmental research, 133, pp.90-95.

Xie, Z., Huete, A., Ma, X., Restrepo-Coupe, N., Devadas, R., Clarke, K. and Lewis, M., 2016. Landsat and GRACE observations of arid wetland dynamics in a dryland river system under multi-decadal hydroclimatic extremes. Journal of Hydrology, 543, pp.818-831.

Xu, Y., Zhou, B.T., Wu, J., Han, Z.Y., Zhang, Y.X. and Wu, J., 2017. Asian climate change under 1.5–4° C warming targets. Advances in Climate Change Research, 8(2), pp.99-107.

Yunyue, Y., Tarpley, D., Hui, X. & Chen, M. 2010. GOES-R Advanced Baseline Imager (ABI) Algorithm Theoretical Basis Document For Land Surface Temperatue. NOAA NESDIS: Center for Satellite Applications and Research.

Zhang, Y., Nitschke, M. and Bi, P., 2013. Risk factors for direct heat-related hospitalization during the 2009 Adelaide heatwave: a case crossover study. Science of the Total Environment, 442, pp.1-5.

Conclusion and Future Directions

Cities tend to have higher surface/ air temperature relative to nearby rural areas, and this type of phenomena is called the Urban Heat Island (UHI). In this thesis, we characterised UHI at diurnal, weekly, monthly, seasonal, intra and inter-annual scale using recent data and methods in remote sensing and GIS field. We also analysed the possible influence of extreme heatwaves to better understand UHI implications on future climate.

6.1 Summary of Key results and conclusions

The temporal dynamics of the UHI in selected Australian cities has been analysed using hourly, daily, monthly, seasonal and inter-annual data from available remote sensing data over a period of available period of 15 years. The main findings from this study are:

[1] In chapter 2, the analysis brought us to a conclusion that, Sydney and Melbourne have significant absolute/relative daytime and the nighttime temperature difference between its urban and respective rural zones, which indicates the presence of strong significant UHI in both cities. The daytime UHI present in both cities are significant throughout the year with most robust intensity in summer and spring months for Sydney and Melbourne respectively. On the other hand, the nighttime UHI becomes dominant in the summer months for both selected cities. In addition to it, winter months record the lowest UHI values in daytime and nighttime over both selected cities. From this analysis, it is concluded that both Australian cities have different seasons to peak UHI values, particularly in daytime. In addition to it, the daytime intensity are not always relatively larger than nighttime amplitudes, as Melbourne indicated a strong significant nighttime UHI intensity with minimal UHI intensity at daytime particularly in summer months. On the other hand, Sydney was warmer with most strong UHI at daytime in

summer months than at nighttime. The analysis highlighted the diurnal characteristics of LST patterns across urban and its adjacent rural zones and resulting UHI with possible influence of rural thermal properties on UHI intensity. The general conviction that the temperature in green sites can be cooler than non-green sites was confirmed by the analysis on the temperature of parks and residential suburbs inside the city.

[2] In Chapter 3, the analysis on long term trends of UHI and its driving factors highlighted the definite influence and role of dynamics in rural thermal properties on UHI trends over past 15 years (2003 - 2017) in the selected regions. It was concluded that the rural agricultural activities in peri-urban zones had an obvious influence on the UHI intensity and resulting trends in the selected cities. The analysis highlighted the importance of rural thermal properties and their ability to control long term trends and variations in the UHI, particularly at daytime. Nighttime variations were seen to be independent of rural thermal dynamics and their relative influence. Given this, it is a sobering fact that almost none of the heat island studies of the past have provided data on this crucial control rural dynamics on UHI variations.

Moreover, in this chapter, we introduced urban green deficit (UGD) which provided the measure of urban greenness to its adjacent rural lands. Our analysis further showed there was a strong relationship ($R > 0.8$) between UHI and urban green deficit (UGD), whereas the relationship between UHI and delta albedo was not significant ($R < 0.5$). Hence, indicating higher the UGD values, lower the daytime UHI intensity, which means urban green cover less than the rural, will give rise to daytime UHI. However, it is further recommended to integrate the data with ground data for better results. It should also be considered here that, to date, comparative studies of EVI, UHI and albedo are minimal particularly with reference to its influence in rural zones.

[3] Chapter 4 was a short chapter, in which we successfully showed the interactions of vegetation phenology in urban to rural zones, onto inter-annual seasonal variations in UHI amplitude particularly art daytime. Melbourne indicated the strong influence of rural pasture class onto UHI seasonal amplitude. Hence, showing a strong daytime UHI in spring, when the vegetation cover in rural zones was at its peak, causing the urban to rural LST difference to reach its maximum values. Similarly, Sydney indicated that choosing pasture as reference class would result in a cool island in the city, which may not have any specific seasonal behaviour. However, forest class as reference was stable and indicated a consistent pattern over the year with daytime UHI reaching its maximum in summer. We also concluded with dominant influence of forest class in Sydney, which was causing the city to experience a strong UHI and pasture class in Melbourne which was causing the city to reach at its peak UHI amplitudes in spring. In this study, we were able to highlight the reasons behind different seasonal patterns in both cities and the role of adjacent rural zones and respective LULC classes in driving the seasonal attributes in UHI particularly at daytime. Furthermore, we conclude from this chapter that the UHI is affected by the topographic factor, land surface condition and vegetation greenness. The effect of urban areas on the regional climate system occurs through the land surface-atmosphere interactions and that drives the UHI values particularly at daytime.

[4] Chapter 5 highlighted the influence of climate extremes on existing UHIs in the selected cities. It is further believed that the study is very first of its type, to utilise 10 min and hourly LST data for analysing interactions of UHI with the extreme heatwave in the urban zones. We also highlighted in our study, that during the heatwave, as temperature values rose in the region, parts of the city experienced long hours of warmer temperatures, particularly ones in the city's west. The suburbs which were greener and

close to coast were relatively cooler or dropped in temperatures much earlier relative to other parts of the city, particularly ones in its west. The analysis was carried out for selected heatwave event, due to limitations in data availability. It is further recommended to explore more heat wave events and analyse UHI interactions with extreme heatwaves. Moreover, the study was carried out only for Sydney, we did not carry out the study for Melbourne, due to limitations of data availability. However, this study was an excellent example of utilising recent remote sensing datasets in urban studies, which are not explored much in past.

6.2 Future Research Directions

Remote sensing and GIS tools offer better and efficient methods of analysing and investigating UHI amplitudes in cities. However, remote sensing applications in urban climatology are still few due to the complexities of the interactions of thermal infrared and microwave radiations between the atmosphere and urban surfaces. There is still need to integrate both remote sensing and GIS data with ground and in-situ datasets to examine UHI and its implications on future climates.

Also, another viable angle of future studies should focus on mitigation strategies for UHI and explore methods that can reduce the surface temperature in urban zones in the wake of its rural LULC dynamics. Since rural LULC defines the region’s true characteristics. We also recommend researching different parts of the cities using high spatial resolution data from space-borne and airborne sensors. Hence, higher spatial resolution with more temporal sampling and improved better calibrated data would be very useful. Finally, the area needs the development of more research on techniques to analyse implications of LST/UHI in rural areas surrounding the cities such as the effect of vegetation seasonality and increased soil moisture through irrigation canals.

6.3 Final Conclusion

In this thesis I investigated UHI diurnal, seasonal and inter-annual patterns and trends during past 15 years across selected Australian cities using recent remote sensing data and tools. In addition to it, I investigated the influence and interactions of climate extreme heat waves on existing UHI intensity. Doing so I met all objectives and conducted my analysis within a framework of essential and important criteria. I believe this thesis makes an important contribution to urban thermal research particularly utilising remote sensing data and tools.